Investigation And Analysis of Wind Pumping System for Irrigation in Bangladesh

by

Sultan Ahmed

A Thesis
Submitted to the
Department of Mechanical Engineering
in partial fulfillment of the requirements for the degree
of
DOCTOR OF PHILOSOPHY IN MECHANICAL ENGINEERING

BANGLADESH UNIVERSITY OF ENGINEERING AND TECHNOLOGY,
DHAKA
February 2002

The thesis titled "**Investigation and Analysis of Wind-Pumping System for Irrigation in Bangladesh,"** Submitted by **Sultan Ahmmed**, Roll No.Ph.D. 002/10/97F, Session 1994-95-96 has been accepted as satisfactory in partial fulfillment of the requirement for the degree of **Doctor of philosophy in Mechanical Engineering** on 2nd February, 2002.

BOARD OF EXAMINERS

1.	Dr. Md. Quamrul Islam Professor and Dean Department of Mechanical Engineering BUET, Dhaka-1000.	Chairman
2.	Dr. M. A. Rashid Sarkar Professor and Head Department of Mechanical Engineering BUET, Dhaka-1000.	Member (Ex. Officio)
3.	Dr. Md. Abdur Razzaq Akhanda Professor Department of Mechanical Engineering BUET, Dhaka-1000.	Member
4.	Dr. Amalesh Chandra Mandal Professor Department of Mechanical Engineering BUET, Dhaka-1000.	Member
5.	Dr. A. K. M. Sadrul Islam Professor Department of Mechanical Engineering BUET, Dhaka-1000.	Member
6.	Dr. M. Fazli Ilahi Professor & Head Department of Mechanical and Chemical Engineering Islamic University of Technology, Gazipur, Bangladesh	Member
7.	Dr. A. K. M. Iqbal Hussain Professor and Head Energy and Environment Centre Islamic University of Technology, Gazipur, Bangladesh	Member (External)

CANDIDATE'S DECLARATION

It is hereby declared that this thesis or any part of it has not been submitted elsewhere for the award of any degree or diploma.

(SULTAN AHMMED)

ACKNOWLEDGEMENT

I wish to express my sincerest gratitude and indebtedness to Professor Md. Quamrul Islam for his guidance and supervision throughout the entire period of this research work. His initiatives, encouragement, patience and invaluable suggestions are gratefully acknowledged without which this work would have been difficult.

I am grateful to Professor Amalesh Chandra Mandal for his constructive suggestions and advice during several phases of this investigation. Without his kind co-operation and guidance this work could not have been carried out properly.

The advice and inspiration extended by. Professor Md. Abdur Razzaq Akhanda, Professor A. K. M. Sadrul Islam and Professor M. A. Rashid Sarkar are acknowledged with gratitude.

I would like to thank Mr. Nazmul Huda Al Mamun, Asst. Professor for helping me during the research work.

My thanks are due to Mr. Alauddin, Mr. Hanif, Mr.Mizanur Rahman and Mr. Kalam, the technicians of the Fluid Mechanics Laboratory of Mechanical Engineering Department, BUET, for their help in fabricating and assembly different parts and components of the experimental set-up. I would also like to acknowledge the help of Mr. Md. Fakhrul Islam Hazra and Mr. Md. Shahidullah for their co-operation.

Special thank is due to my wife for her patience and encouragement throughout the research period. Without her sincere co-operation and encouragement it would be difficult for the author to complete the work. Special record is also due to my son, master Simab Al kavi and my daughter, Subaita for their sacrifice to complete this work.

Finally, the author wishes to thank the Agriculture Research management project (ARMP), IDA Credit 2815-BD for their financial support given under the award of a scholarship. The author wishes to thanks the authority of Bangladesh Agricultural Research Institute (BARI), Gazipur, Bangladesh for giving me the opportunity for this higher study.

ABSTRACT

An experimental investigation of performance characteristics of horizontal axis wind turbines has been conducted. Wind characteristics of various regions of Bangladesh have been analysed and hence a compatible design of horizontal axis wind turbine applicable to the pump has been performed.

The available wind data collected by the meteorological department of Bangladesh for a period 16 years on 20 stations at different height between 5m to 10m have been converted for the 20m hub-height using power law. From these data monthly average speeds have been calculated. It is observed that for few regions of Bangladesh, there is reasonable wind speed available throughout the year to extract power.

For a prospective regions of Bangladesh a design of wind turbine for water pumping has been performed based on the requirement of water of that region. The design incorporates the generalized procedure for determination of rotor and pump sizes. Thus it can be used for any other region as well.

To present a generalized design for Bangladesh, a nomogram and an empirical relation have been developed for the rotor and the pump sizing for a particular region of Bangladesh.

An extensive experimental investigation of the performance of the designed wind turbine model have been conducted in the wind tunnel. The wind turbines with 2 blades, 3-blades and 4-blades for linearized chord and twist angle have been considered for the experimental investigation. The experimental investigation was performed for each turbine at various blade pitching.

Finally the calculated results of the wind turbine have been compared with the experimental results and in most of the cases good correlation were observed.

TABLE OF CONTENTS

LIST OF SYMBOLS

A	axial interference factor
$a^{/}$	tangential interference factor
A	projected frontal area of turbine, turbine disc area (πR^2)
AR	aspect ratio = H/C
B	number of blades
C	blade chord
C_D	turbine overall drag coefficient = $F_D / \frac{1}{2} \rho A V_\infty^2$
C_{DD}	rotor drag coefficient = $F_D / \frac{1}{2} \rho A V_a^2$
C_l	blade lift coefficient
C_{l_d}	design lift coefficient
C_P	turbine overall power coefficient = $P_0 / \frac{1}{2} \rho A V_\infty^3$
C_Q	turbine overall torque coefficient = $Q / \frac{1}{2} \rho A V_\infty^2 R$
C_T	thrust coefficient
C_t	tangential force coefficient
D	blade drag force
dA	blade element area, C dr
F	Prandtl's loss factor, force on blade airfoil
F_D	turbine drag in streamwise direction
F_{hub}	hub loss factor
F_{tip}	tip loss factor
h	height of turbine, hub height from ground level
M	blade pitching moment
N	number of blades
P	turbine power, power
P_e	amount of power to be extracted
P_{elec}	electrical power
P_{mech}	mechanical power
P_r	rated power
p_∞	atmospheric pressure, free stream pressure
q	dynamic pressure = $\frac{1}{2} \rho W^2$
Q	overall torque
Q_l	local torque
Q_s	blade starting torque
r	radius from turbine axis to local blade element, local blade radius
$\vec{r}$	unit vector
r_{Hub}	hub radius

R	turbine radius at equator, rotor radius
R_e	effective radius
Re	local Reynolds number = WC/υ
T	tension in blade at any point, thrust force, total time
T_0	tension in blade at equator
u	interference factor
U	wind speed through the turbine
V	local velocity, wind velocity
$\overline{V}$	average wind velocity, annual average wind speed
V_{ref}	reference wind velocity
V_{start}	starting wind speed
V_t	tangential wind velocity
V_w	wake velocity in downstream side
V_z	average wind speed at height z
V_Γ	velocity contributed by circulation
W	relative flow velocity
h	height of a particular point from ground level
h_{ref}	height of a reference point from ground level

GREEK ALPHABETS

α	angle of attack, angle of attack for finite wing
α_c	incidence correction angle due to flow curvature
α_d	design angle of attack
α_{ef}	effective angle of attack
α_g	geometric angle of attack
α_i	induced angle of attack
α_l	local angle of attack along plate
α_0	angle of attack appearing in rectilinear flow, angle of attack for infinite wing
α_T	tilt angle
α_v	virtual angle of attack
β	$(\alpha_e - \alpha_i)$, angle between relative flow velocity direction and tangent to blade flight path at blade fixing point, coning angle
β_T	blade twist angle
γ	angle between tangent to blade flight path at blade fixing point and rotational velocity direction, yawing angle
γ_p	blade pitch angle
η	power law exponent
η_{eff}	efficiency of windmill
θ	azimuth angle
θ_K	blade azimuth angle
θ_l	angle in plane of rotation between R and R_l directions
θ_p	pitch angle
λ	tip speed ratio = $R\omega / V_\infty$ = $R\Omega / V_\infty$
λ_d	design tip speed ratio
λ_r	local tip speed ratio
μ	non-dimensional blade radius = r/R
υ	kinematic viscosity
ρ	fluid density, air density
ρ_b	density of blade material
ϕ	Angle of relative wind velocity
ω	angular velocity of turbine in rad/sec, wake rotational velocity
Ω	angular velocity of rotor

CHAPTER 1

INTRODUCTION

1.1 General

Energy is one of the basic inputs in everyday life of human being. Various types of energy, like oil, hydro, coal, natural gas, nuclear etc., are used as fuels for different activities all around the world. Among these conventional fuels, only hydro is renewable in nature and the other sources are major causes of air pollution and greenhouse effect. The conventional fuels may be replaced with renewable energy sources like wind energy, solar (photo-voltaic) systems, solar thermal systems, biomass energy (wood and other plant fuels), geothermal energy, fuel cell, municipal waste etc. The costs of many of these technologies have come down considerably in recent years, particularly wind energy, which is now competitive with conventional power sources in regions with strong winds.

The science of exploitation of wind power is not a new one. For the past few centuries people are extracting energy from the wind in various ways. One means for converting wind energy to a more useful form is through the use of windmills. Recently, due to the fuel crisis, this science is gaining more popularity. Wind energy has become very lucrative now-a-days due to its reliability. According to a projection by American Wind Energy Association (AWEA)-wind turbine installation in the world through the end of 2006 will be 6,950 MW.

There are various types of windmills. The most common one having the blades of airfoil shape is the horizontal axis turbine. Another type is the vertical-axis wind turbine. The primary attraction of the vertical axis wind turbine is the simplicity of its manufacture compared to that of horizontal axis wind turbine. Among the different vertical axis wind turbines, the Savonius rotor is a slow running wind machine and has a relatively lower efficiency. Still it is being used in the developing countries because of its simple design, easy and cheap technology for construction and having a good starting torque at low wind speeds [29,5,37]. Rigorous studies on the performance characteristics of the horizontal axis wind rotor are found in the literatures and these enable the identification of an optimum geometrical configuration for practical design [30,25,4].

1.2 Wind as a Source of Energy

For a long time people are extracting energy mainly from the fossil fuels in almost all the countries. In some of the countries they are also utilizing uranium fuel, which is a source of nuclear energy. With the rising demand of energy and for many other reasons, prices of these fuels are increasing day by day. So people are trying to find the alternate sources of energy to exploit them at the cheapest rate. Wind energy is a kind of energy source which, will never be finished. It is available almost all the times, in all the places and in large quantities all over the world. Again fossil and uranium fuels will be finished once. These are not available in all the countries. Besides these, people are interested to be self-dependent; they do not like to rely on imported fuel, which requires huge amount of foreign currency. On the other hand, to date no effective method has been developed to apply the solar energy. As a result in different parts of the world, people are taking keen interest to develop efficient and economic devices to collect energy from the wind. Recently, the utilization of wind power is increasing highly in many developed as well as under developed countries.

1.3 Global Wind Energy Utilization Scenario

In 1997, wind turbines installed all around the world generated about 13 trillion watt-hour of energy; the installed capacity was 7500 MW. According to AWEA, Europe will continue to dominate worldwide installations over the next 10 years, erecting 14,310 MW of additional wind capacity, or nearly half of the 30,000MW projected for the world. European countries, in particularly Germany, Spain, and the United Kingdom have very strong and consistent domestic market supports in place for at least several years. While those supports are being reduced in many markets, the European wind industry now has enough momentum and investment that rapid growth is expected to continue into the indefinite future.

1.4 Aim of the Present Work

Geographically Bangladesh is situated between 20^0 34' to 26^0 38' North latitudes and 88^0 04' to 92^0 44' E longitudes. It has approximately 724 km long coastal belt, more than 200 km long hilly coastal-line and more than 50 islands in the Bay of Bengal. The strong south/south-westerly monsoon wind coming from the Indian Ocean, after traveling a long distance over the water surface, enter into Asia over the coastal areas of Bangladesh. This wind blows over our country from March to October. The wind velocity is enhanced when strikes the coastal belt of Bangladesh, after traveling a long distance over ocean water surfaces. According to this study its speed ranges from 7 m/s to 8.5 m/s. It can be mentioned here that having the same climates, monsoon trade winds, surface roughness class and terrain types as those of Bangladesh countries like India, Sri-Lanka, Pakistan, Thailand etc., are generating hundreds of MW electricity from their coastal region [40].

In the context of rural energy requirements, water supply for domestic needs and livestock, irrigation and drainage could be considered for potential application of wind pump. In most of the situations wind pump appears to be economical for such applications, if the mean annual wind-speed is in excess of 3.0 m/s. In relation to irrigation and drainage, which are generally seasonal activities, what matters most is not the mean annual wind speed but the wind potential during the season concerned.

Historically, the most widespread application of windpumps has been the livestock water supply and this trend is likely to persist even in the future development of wind water pumping in developing countries. Since even a modest quantity of water could sustain a sizable herd of animals, the value of water in such applications is high and therefore, relatively more expensive traditional wind pumps will still find in their share in this market. The probability of cheaper and lighter designs of the new generation of wind pumps reaching this segment of the market. But there is further constrained by their performance limitations in regard to pumping head and reliability for prolonged unattended operation as is often required in such applications.

The use of wind pumps for drinking water supply may not be as widespread as livestock water supply, but there is potentiality of a large market for this purpose. The economics of wind pumps in this application and other operational conditions are almost similar to those considered in livestock water supply. As water supply for domestic and livestock needs is a constant year round demand, the use of wind pumps for these applications requires persistent year round winds, which may not be a common occurrence in some countries, particularly those along the equatorial belt.

Irrigation is often a seasonal water demand and therefore, operational feasibility of using wind pumps for irrigation is mainly defined by the favourable match between the irrigation water demand and seasonal wind potential in the given region. Traditional wind pumps have rarely been used for irrigation in the past primarily because of water requirements involved and the relatively low economic value of water compared with drinking water supply. Thus, the scope for application of wind pumps for irrigation would be limited by the capital cost of the machine and pumping head. It is precisely in this field that modern light weight wind pump designs could find their place because of the comparatively lower capital cost and their satisfactory performance under low pumping head conditions.

Drainage was one of the most widespread applications of wind power in the Netherlands in the past. In Asia too, wind power was used for drainage purposes, particularly in China and Thailand where the traditional wind power ladder pump was widely used for this purpose. The financial feasibility of the application demands on the value of output obtained from the drained lands [57].

Some developed countries are manufacturing this wind pumping system commercially, their price is high and is not suitable for our weather and socio-economic conditions. The aim of this research was to study wind pumping system and design a simulated wind pumping system, utilizing the wind resources of Bangladesh.

1.5 Objectives:

The study has the following objectives:

1. To analyze the wind velocity in the selected regions of Bangladesh.
2. To select a wind regime for design of the wind pumping system.
3. To design a prototype of horizontal axis rotor suitable for water pumping, using wind data from selected wind regime based on the Strip theory.
4. A model of the horizontal axis rotor was tested in a wind tunnel at different operating conditions.
5. A nomogram was developed based on the calculated data for the different regions of Bangladesh from where the rotor and pump size can be determined.
6. Some empirical relations were developed from turbine-pumping characteristic curves.

1.6 Scope of the Thesis

The prime objectives of the experimental investigation are to observe the aerodynamic effects on the horizontal axis wind model rotor of aerofoil NACA 4418 with 2-blades, 3-blades and 4-blades. This thesis presents a method of development of horizontal axis wind turbine model, with known wind characteristics. Basic aerodynamics and relevant elements associated with wind turbines has been given in the different chapters.

In chapter 1 a short historical development of the wind turbines have been presented. The aims of this work, the contents of the thesis, and review of the existing literatures are also presented in this chapter.

Chapter 2 deals with detailed description of the momentum theory and blade element theory together with the strip theory for horizontal axis wind turbines. Equations of maximum power coefficient for an ideal wind turbine are examined in this chapter. The equations to obtain the blade configurations are also deduced here.

With a view to selecting a prospective wind regime to operate the wind machines, the knowledge about the wind characteristics of that region is necessary; this has been incorporated in the chapter 3. The statistics of the wind data for selection of a suitable wind regime in Bangladesh has been included here. Some idea about the selection of the appropriate site for the wind turbines has been given.

Chapter 4 deals with detailed description of design and fabrication of horizontal axis wind turbine. Design of rotor, selection of tip speed ratio and number of blades, steps for calculation of blade configuration, selection of design parameters, calculations of blade chord, blade twist angles, deviation from the ideal blade form, and choice of blade material have been presented. An iterative procedure to get the optimum blade configuration is also presented in this chapter.

In the chapter 5, a method to calculate the performances of horizontal axis wind turbine has been presented. Theoretical data for the design of a 350 kW wind turbine has been presented. The results obtained by the present method are also compared with the results of existing wind turbines and other numerical data. Comparison of theoretical and experimental results has been presented for 2-blades, 3- blades and 4-blades at the blade setting angles, 0^0, 2^0, 4^0, 6^0 and 8^0.

Chapter 6 deals with detailed description of wind water pumping in Bangladesh for horizontal axis wind turbine. Wind pumping technology, benefits of wind pumping, wind pumping systems with its components, matching of wind turbine and wind pump, energy availability and output, assessment of water requirements, available wind power resources, determination of design month, sizing of wind pump, sizing of storage tank and nomograme are presented in this chapter

Finally, in Chapter 7, general conclusions and recommendations of this work have been presented.

1.7 Historical Background

Wind is an energy source that seems to have had widespread application already in early civilization, perhaps dating back to about 3,000 years. It is believed that Chinese first used wind pumping systems about 2,000-3,000 years ago. Starting from primitive designs of ancient times, the technology of harnessing wind power has been continuously improved to suit the specific needs of the time. By the twelfth century, well-developed designs of windmills were in extensive use in a number of European countries. From the fifteenth century onwards windmills have been widely used in the Netherlands to drain swamps and lakes and reclaim new land.

By the early nineteenth century, following the introduction of steam engines, the use of windmills was in decline in Europe and the concentration on wind pump development shifted to the United States of America and Australia. By the 1880s, the all-steel-America wind pump was developed and since then about six million wind pumps have been built and installed in the United States. Many of these pumps are no longer operational due to competition from other water pumping systems, but it is estimated that approximately one million wind pumps are still being used throughout the world mainly in Argentina, Australia, Denmark, Germany, Holland, Italy and the United States. Besides the expensive all-steel-machines developed in the United States and Europe, there have also been low-cost wind pumping systems in use in other parts of the world. In China, for example, wind-powered ladder pumps have been used for low lift pumping, while in Thailand simple wooden windmills are reported to be used in thousands in the early 1950s for irrigation purposes. Sail clothed Cretan windmills in Greece and Peruvian wind pumps made out of locally available materials are some other example of wind power use in developing countries.

In the aftermath of the "oil crisis", there was world-wide interest in the revival of wind power harnessing and major research programs were initiated in industrialized countries towards the development of modern wind turbines for large-scale electricity generation. Along with these, some institutions, notably the Consultancy Services for Wind Energy in Developing Countries (CWD) in the Netherlands, IT Power Ltd. in the Great Britain and Northern Ireland initiated programs for development and dissemination of new generation of wind pumps for application in rural areas in developing countries. Emphasis of these programs was to develop designs of wind pumps, which were less costly than the traditional multi-bladed wind pump and could be locally manufactured in most developing countries. The designs evolved through these efforts are still being improved, but many of them could be considered mature enough for application under low to medium pumping head conditions. Compared to traditional multi-bladed wind pumps the modern designs seem to lack the reliability and robustness required for prolonged unattended operation in remote locations. But in many situations, the cost effectiveness of these machines could far outweigh the demand for frequent maintenance requirements [57].

1.8 Review of Literature

Arising from the increasing practical importance of wind turbine aerodynamics, there have been, over the past few decades, an enormous increase in research works concerning laboratory simulations, full-scale measurements and more recently, numerical calculations and theoretical predications for flows over a wide variety of wind turbines. Researchers in different countries have contributed greatly to the knowledge of analytical prediction methods of wind turbines, but the major part of the reported works are of fundamental nature involving the flow over horizontal axis wind turbine and vertical axis Darrieus rotor. Most of the researchers have conducted research works on either two semi cylindrical bladed Savonius rotor or S-shaped rotor with various flow parameters. A brief description of some of the papers related to the present work is given below.

Islam et al. [22] investigated the aerodynamic forces acting on a stationary S-shaped rotor and attempt to predict the dynamic performance from these forces. The work was done by measuring the pressure distribution over the surface of the blades. The measurements were carried out in a uniform flow jet produced by an open circuit wind tunnel and at a constant wind speed of 8.9 m/s, which corresponds to a Reynolds number ($Re = U_oD/\nu$) of 1.1×10^5. The results indicate that flow separates over the front and back surfaces of the blades and the point of separation depends on the rotor angle. The pressure difference was observed between the two surfaces of each blade, which in turn, gives drag coefficients. The drag and hence, the torque of each blade varies with rotor angle and becomes maximum at $\alpha=45^\circ$ for the advancing blade and at

α=105° for the returning blade. The net torque is maximum at α=45° and becomes negative in the range of rotor angle between 135° to 165°.

Huda et al. [18] analyzed the performance of S-shaped rotor by placing a flat plate in front of the returning blade. They found that the power coefficient of a S-rotor is dependent on the Reynolds number and the value of Cp (power coefficient) is increased with Reynolds number in the range of the Reynolds number studied and maximum 20% of power coefficient can be increased by using the deflecting plate which occurs at a deflecting angle of 35° for b = 0.5D, where b = distance between plate and rotor center and D = diameter of the rotor.

Bowden, G.J. and McAleese, S.A [6] made some measurements on the Queensland optimum S-shaped rotor to examine the properties of isolated and coupled S-shaped rotor. In particular it is shown that the efficiency of the turbine is around 18%, which is lower than the figure of 23% given by earlier workers. In the experimental setup the open jet air-stream, diameter 0.76m, was used to produce wind speeds in the range 0 to 30 m/s. The turbulence ($\sqrt{u^2}/V_\alpha$) in the jet stream was low. Wind flow measurements were investigated using 'tell-tales' (light pieces of cotton attached to a probe) and a stroboscope. In this way it was possible to detect the direction of the air-flow relative to the angular position of the rotor blades. Many photographs were taken and later used to construct a visual air-flow pattern around the rotor. The linearized hot-wire anemometer, on the other hand, enabled measurements to be made of velocity magnitudes and fluctuations to an upper frequency limit of 5 kHz. It cannot however, be used to measure direction. Hot-wire anemometer linearizer was based on a design of the Institute of Sound and Vibration Research (ISVR), Southampton University, U.K. In general, a storage oscilloscope was used to record the data, particularly from the more structured turbulent regions. However, measurements of turbulence intensity were also made by connecting an rms voltmeter to the output of the hot-wire linearizer. The results of this research were subsequently used to suggest that some form of active coupling between Savonius rotors might be possible. In particular, it has been shown that if two counter-rotating rotor are placed side by side, a natural phase locking occurs between the two turbines.

The most simple prediction method for the calculation of the performance characteristics of a Darrieus wind turbine is the single streamtube mode. It has been introduced first by Dr. Templin [53] in 1974. In this model the whole turbine is assumed to be enclosed within the single streamtube. Dr. Templin first incorporated the concept of the windmill actuator disc theories into the analytical model of a Darrieus wind turbine.

An analytical method using single stream-tube model is presented by Noll and Ham [33] for the performance prediction of a vertical-axis wind turbine with straight blades which are cyclically pitched. They added the effect of strut drag, turbulent wake state and dynamic stall to their analytical method.

An improvement to the above method is the multiple streamtube model introduced by Wilson and Lissaman [56]. In this model the swept volume of the turbine is divided into a series of adjacent, aerodynamically independent streamtubes. Blade element and momentum theories are then employed for each streamtube. In their method they consider the flow as inviscid and incompressible for the calculation of the induced velocity through the streamtube. As a result, there appears only the lift force in the calculation of induced velocity. Wilson et al. considered the theoretical lift for their calculation. This induced velocity varies over the frontal disc area both the vertical and the horizontal directions. Atmospheric wind shear can be included in the multiple streamtube model. Multiple streamtube model is still inadequate in its description of the flow field. Wilson's model can be applied only for a fast running lightly loaded wind turbine.

Strickland [50] in his paper presents a multiple streamtube model for a vertical axis Darrieus turbine. He finds the induced velocity by equating the blade element forces (including airfoil drag) and the change in the momentum along each streamtube. The basic difference between Wilson's and Strickland's model is that Wilson used the lift force (theoretical) only in the calculation of induced velocity while Strickland added the effect of drag force as well for the similar calculation. Wilson's model gives fast convergence while Strickland's model gives slow convergence.

An improved version of multiple streamtube method is presented by Currie [11] for vertical-axis Darrieus wind turbines. In their model the parallel streamtube concept is dispensed with and the expansion of the streamtube is included. It is strictly applicable to low solidity lightly loaded wind turbines with large aspect ratio. It can predict the instantaneous aerodynamic blade forces and the induced velocities better than that by the conventional multiple streamtube model. But prediction of overall power coefficients cannot be made with reasonable accuracy. It usually gives lower power than that obtained experimentally.

Paraschivoiu and Delclaux [36] have made improvements in the double multiple streamtube model. They consider the induced velocity variation as a function of the azimuthal angle for each streamtube. They have added a new formulation for an approximate Troposkien shape by considering the effect of gravitational field and a semi-empirical dynamic stall model.

Paraschivoiu, Fraunie and Beguier [35] introduced in this paper the expansion effects of the streamtubes through the rotor and these are included with the double multiple streamtube model. With the measured and the predicted data they observe that streamtube expansion effects are relatively significant at high tip speed ratios.

Fanacci and Walters [12] presented a two-dimensional vortex model applicable to a straight-bladed wind turbine. In their analysis they considered the angle of attack very small, thereby eliminating the stall effect.

Holme [16] presented a vortex model for a fast running vertical-axis wind turbine having a large number of straight, very narrow blades and a large height-diameter ratio (in order to make a two dimensional flow assumption). Their analysis is valid for a lightly loaded wind turbine only.

Wilson [55] also introduced a two dimensional vortex analysis to predict the performance of a giromill. In his method he did not take into account the stall effect, because the angle of attack is assumed to be small.

Gavalda et al. [14] analyzed the drag and lift coefficient of Savonius wind machine in order to obtain quantitative information about the aerodynamic performance of the savonius rotor. The experiments were carried out in a low turbulence open jet (30 x 50 cm section) outlet. The air speed is adjustable between 0 and 30 m/s. The savonius model is made of two half cylinders of d=7.2 cm in diameter and H=20 cm in height, with adjustable overlap (e). The results of this work showed that for e/d=1/6 (ratio between overlap and cylinder diameter), at which the rotor generates the optimum power, the drag and lift coefficients are little dependent on the operating conditions (Reynolds number, tip speed ratio λ) if λ is near the optimum value $\lambda \approx 1$. There are three findings of this work: (a) the maximum efficiency of the Savonius rotor, in terms of power coefficient, takes place for $\lambda \approx 1$, and that C_P decreases sharply when λ

increases or decreases from this value, (b) for a given Reynolds number, as the tip speed ratio increases from zero, the drag values are maintained practically constant, $C_D \approx 1.15$ in the interval ranging from $\lambda = 0$ to $\lambda = 1.25$. The most interesting zone for power extraction is located near $\lambda \approx 1$, where C_D shows minimum values. For tip speed ratios greater than 1.25, the drag coefficient increases, (c) in a wide interval around $\lambda = 1$ (the most important region of operation of the Savonius rotor) the lift coefficient remains practically constant at $C_L \approx 0.5$.

Sawada, et al. [44] experimentally studied the mechanism of rotation of Savonius rotor which have two semi-cylindrical blades. The force acting on a blade is measured in a water tank for both cases, rotor at rest and is rotated. A flow around the rotor is observed by using aluminum powder floating on the water surface. Although the Savonius rotor is classified as a resistance type, the lift produces a torque in a pretty wide range of blade angles relative to the flow. The researchers concluded that

- The rotor is at rest, the rotor with overlap ratio (ratio between overlap distance and cylinder diameter) a/d = 0.21 produces a positive torque at any rotor angle (α).
- The lift (α= 240°~330°) contributes a lot to the torque occurring when the rotor is rotated. Although, the Savonius rotor is classified as a resistance type, the lift produces a torque in a pretty wide range of angles relative to the flow.
- When the rotor is rotated, the effect of the pressure recovery by the flow through the overlap portion on the lift is little for the rotor of a/d = 0.21. For the rotor of a/d=-0.51, the existence of a flow through the center of the rotor contributes to the production of a negative torque opposing the clockwise rotation.

Aldoss, T. K., et al. [3] analyzed the performance of two Savonius rotor running side by side at different separations using the discrete vortex method. Two configurations were considered. The torque and power coefficients were computed and compared with the available experimental results presented by Aldoss and Najjar in an earlier paper.

Jones, C.N., et al. [26] made comparative tests of the Savonius rotor at constant Reynolds number. They suggested that a plain S-rotor may be as good as or better than the conventional Savonius rotor with an inter-vane gap. A single S-rotor gives a Cp > 0.15 (0.225 uncorrected wind-tunnel value); although duplex rotors have given Cp > 0.18 (0.32 uncorrected value). Comparative particle flow visualization studies within these rotors (Savonius rotor with conventional gap, S-rotor with no gap, and a rotor with separated vanes ('negative' gap) in a water-channel suggest the importance of attached flow round the convex surfaces of the vanes, the doubtful value of the conventional gap, and the importance of vane shape.

Sivasegaram, et al. [47] made an experiemnt in improving the sectional geometry of slow-running vertical-axis wind rotors of the Savonius type has resulted in considerable improvement in rotor performance. They suggested that further improvement in power output from a rotor of given overall dimensions demands the use of power augmenting systems. The influence of important design parameters of the augmenting system and that of wind direction have been investigated and the system configuration giving maximum power augmentation has been determined. They showed that an eighty percent increase in power output could be achieved using a pair of vanes of moderate size.

Islam, et al. [20] investigated Aerodynamic characteristics of a Stationary Savonius rotor of two semi-cylindrical blades. The test was carried out in a uniform flow jet produced by an open circuit wind tunnel. The exit of the wind tunnel consists of a square section nozzle with a side length of 500 m. The rotor was placed at the jet axis and 750 mm downstream of the nozzle exit. This study was carried out at a constant wind speed of U_o = 13.3 m/s i.e., at Reynolds number, Re = 2 x 10^5. The results of this work showed that flow separates over the convex surface of the blades and the separation point moves towards the leading and trailing edges of the advancing and returning blades respectively as the rotor angle increases from 0° to 90°. Beyond α = 90°, flow separates over the convex surface of the returning blade only. They also found that the difference in pressure on the convex and concave surfaces produces drag coefficients, C_n and C_t in the normal and tangential directions of the chord. Drag coefficient C_n and C_t are a function of rotor angle and their resultant reaches maximum value at α = 120° and minimum value at α = 0.

Ahmad, D. [1] reported that water supply is a pre-requisite for successful plant growth. In some developing countries, rural water supply relies mainly on manual pumps, shallow tube wells and diesel powered pumps. Ramana et al. [35] reported that the increasing prices of fuel, depletion of commercial energy sources and frequent failures in power supply, attention is being drawn on utilizing renewable sources of energy for pumping water for irrigation. Wind power is considered as one of the renewable sources of energy for pumping water inspite of the fact that wind is not steady, both in speed and direction. However, wind blow almost everywhere in the world. Several studies were made in India to estimate the wind power and identify areas suitable for utilizing wind energy.

The suitability of wind machines for pumping water for irrigation in any region depends on the wind regime, rainfall distribution, evaporative demand and depth of the water table.

Mahar, S.A. [31] observed that wind speed mostly varied from 3 to 5 m/s during the hour. Taking wind speed of 5 m/s during the hour, 9120 litres of water would be pumped during 24h on a pump stroke of 40.5 mm. A cow and sheep require 68.15 litres and 9.08 litres of water per day, respectively. Therefore 133 head of cows or 1000 sheep could be provided with drinking water per day. The reservoir capacity should be at least 9120 litres.

Mishra et al. [32] investigated that the sufficient wind flux is available in the coastal belt of Orrisa. Wind pump discharge and wind speed has S-curve relationship. Water for irrigation is available in sufficient quantity in all seasons in the localities of Paradeep, Bhubaneswar, Puri and Gopalpur, whreras at Balasore and Cuttack water is available only in the summer and Kharif season. Water pumping rate by windmill pump is economic.

Islam, et al. [22] reported wind speed in some region of Bangladesh is found satisfactory for operating pumps and generating electricity. Following points should be considered for design and operation of the windmills in Bangladesh.

- The windmills should be operated automatically, i.e., the safety system of the windmill will activate when the wind speed exceeds a certain limit.
- The maintenance should be minimum and simple. The rotor should not endanger the people standing on the ground. Environment safety.
- Instead of cloth sails, polythene can be used. If possible, metal blades should be used. Low or medium speed rotors should be preferred for pumping water.
- The windmills should be strong enough so that they cannot be damaged easily. If possible, gearing should be avoided. Locally available materials such as hard wood or bamboo should preferably be used .

Chowdhry, et al. [9] investigated that the low-cost sail-wing windmill was found to work with greater efficiency compared to other types of windmills recently developed in India. The efficiency of the windmill is maximum (23%) at wind speed of 9 km/hr and found to decrease with an increase in wind speed beyond 9 km/hr. The volume of water that can be pumped from the water table at varying depths at wind velocities ranging from 8 to 30 km/hr was also determined.

Panda, et al. [34] studied that the proper assessment of a wind resource is a prerequisite for its successful utilization through appropriate wind energy systems. The southern High planes of the United States is a region with a wind resource for potential water pumping. In this region, wind speed varies between 5.6 and 6.4 m/s at a 10 m height and between 7 and 8 m/s at a 50 m height. The major objectives of this study were to analysis of long term hourly wind-speed data, comparative study of selected windpumps, computation of daily discharge, and estimate of reservoir capacity at different risk levels.

The average and peak discharges of both the mechanical windpumps were almost identical at 30m and 45m operating heads. However, the discharge of the electrical wind pump was more than four times higher than that of its mechanical counterparts at higher wind speeds. Not much difference, except for furling wind speed, was observed in the performance of the electrical windpump at 30m, 45m, and 60m lift conditions. The discharge was significantly higher for 60m lift condition at higher wind speeds. This windpump, therefore, is suitable for pumping ground water under the high wind regime conditions of Southern high Plans.

Burton et al. [8] tested the performance of both leather and elastomeric cup seals. Elastomeric cup seals offer reduced frictional power absorption under pressure load, compared with traditional leather cup seals. Moreover, the performance of the elastomeric seals improves with time as the seals "run in"; however, leather is certainly more tolerant of poor cylinder finish.

Alam, et al. [2] compared the performance of wind pumping systems (WPS) using centrifugal pumps, coupled by either mechanical or electrical drives. For mechanical transmission between centrifugal pump and wind turbine, overall system performance may be improved by running slowly a larger sized centrifugal pump. Matching of this type is likely to be most beneficial for shallow lifts.

Siddig, M. H. [46] studied the feasibility of wind pumping in Zimbabwe. Wind pump was compared to the two conventional pumping methods: diesel and grid powered pumps. The analysis results in a comparative feasibility chart for Zimbabwe and duty is defined as the volume-head product (QH) of water supply per day. It's main features are:

- The wind turbine is the pumping prime mover at average wind speeds exceeding 3 m/s in all of the duty range considered (0-2000 m^4/day)
- In the average wind speed range 2-3 m/s and where the duty exceeds 900 m^4 /day diesel pumping is most feasible.
- The duty-wind speed constraint is seen to dictate, in most conditions, use of a 6 m diameter rotor. Use of the 7m unit would yield higher output at a slightly higher capital. It does also allow extension of use to high-duty low speed conditions. Use of the 3m rotor is limited to low duty high wind speed condition.
- Grid powered pumping is feasible only where grid connection costs are insignificant and, then, within limited duty and wind-speed ranges.

Swift, R. H. [52] had presented the parametric studies for water pumping windmills, with a view to establishing their characteristics, and the manner in their long term efficiency may be maximised. It had shown that the best results may be achieved by using a controlled leakage pump, that is, one with a small diameter hole drilled through the piston, to reduce the starting torque. By virtue of, the reduction in starting torque, a windmill with a given H/R^3 value would be capable of achieving 50% higher maximum long-term efficiency when coupled to a controlled leakage pump, than when equipped with an unmodified piston pump.

Yongfen, W. [58] reported that almost 90% of the small wind turbines now operating in China are found in the Autonomous Region of Inner Mongolia, where they are used predominantly for battery charging. The wind region is not uniform across the region, however, and in many areas the electricity generated is available only for part of the time and involves unfavorable charge cycling, and hence shorter life of the batteries. The high price of the batteries then renders the systems uneconomic. Increasing use if therefore, now being made of solar cell arrays in conjunction with the wind turbines to produce more continuous power throughout the year and reduce the severity of the charging cycle.

Suresh et al. [51] carried out the study includes system design, operational status, performance in the field and to carry out a financial study of deep well windpumps installed under the demonstration program by Ministry of Non-conventional Energy Sources in India. Eight of the twenty-two systems surveyed were found functional and detailed technical evaluation were also carried out. The paper highlights the issues and problems both technical as well as policy wise faced by this sector. Recommendations are made to improve the system performance and better propagation of the technology.

Gasch, et al. [42] derived the equations for the simple near optimum design of wind turbines with mechanically driven centrifugal pumps. According to similarities laws for wind turbines and centrifugal pumps the optimal gear box ratio, the wind speed of optimal total efficiency and the cut-in wind speed can be calculated. The only required data for the turbine series are the power coefficient $C_{p,opt}$ and the tip speed ratio λ_{opt} in the optimal point. The pump series are described by the data of the nominal pump (nominal speed, impeller diameter, as well as shaft power and total head at nominal speed, both as a function of capacity), static head and the diameter ratio of turbine rotor and pump impeller. Results of computer calculations conform the validity of this simple design methods.

Siddig, M. H. [45] suggested the procedures for maximizes system efficiency and secures continuous within the design range and predicts the starting and stopping behaviour of wind-power piston pumps.

Beurskens et al. [5] discussed the discrepancies between the field data and theoretical prediction. In the process of developing low speed water pumping windmill the aerodynamic properties of four different rotors of 1.5 m diameter were tested in an open wind-tunnel.

When the wind tunnel data of the rotor are coupled to the laboratory data of the pump, the ideal net output characteristic of the water pumping windmill can be found. This output curve will be compared with the performance curve, taking all data per m^2 of swept area. After coupling of wind rotor and pump, a series of wind speeds, power speed curves of the rotor and the pump curve are drawn. These curves are corrected for the yawed position of the rotor. The intersections of the curve of the mechanical power requirement for the pump are the operating points of the windmill. Descending to the pump curve gives the corresponding net output of the windmill.

Barton et al. [7] shown that although the rod elasticity causes delay in valve opening, it can nevertheless have the a beneficial effect in moderating excessive rod loading due to late piston valve closure. The option of incorporating additional pump cylinder softness, whilst still maintaining subresonant running is also evaluated.

Rahman [40] measured the wind speed in Patenga, Cox's Bazar, Kuakata, Moheskhali and Noakhali by the computerized anemometers. The wind computer was installed at 20 m height. According to this study annual average wind speeds in the coastal regions of Bangladesh are greater than 6.5 m/s at the height 20 meters. It has been observed that during the day times (8 am to 7pm) wind speed are about 30 to 40 % higher than the average values. The value of the power exponent α has been determined in the above sites and it is 0.139. So, at 40 m height the annual average wind speed is about 7.15 m/s. So, Wind speed at the coastal region of Bangladesh are suitable for both water pumping and electricity generation.

Sarkar et al. [43] collected the hourly wind speed data of the coastal Chittagong for the years 1978-81. From the hourly average wind speed, the hourly and monthly energy outputs were computed for three commercial machines (22 kW, 16 kW and 4 kW) having different cut-in wind speed. The 22kW machine was found to produce higher energy output per m^2 than the other two for our energy region. The hourly and monthly energy variation of the 22 kW machine was studied and the cost per kWh of energy produced by the machine was obtained. Considering the wind speed distribution of Bangladesh, it appears that a wind machine in combination with a conventional diesel back up system will be economically viable for electricity generation in the off-shore islands but not in inland locations.

Hussain, et al. [19] studied the characteristics of wind data for three recent years, recorded at 14 stations of the Bangladesh Meteorological Department. The data have been used to compute the monthly average wind speed and wind energy available for the stations. Average values of monthly wind speed for 1931-1960 have been employed to obtain the energy availability from the energy pattern factor, and the two sets of results have been compared. It has been found that, for the Chittagong station, the frequency distributions have good fits of the weibull type.

Smulders, et al. [48] described selection procedure for coupling and correct sizing of pump and wind turbine. The selection of drive gear ratio is made in terms of wind condition, depth of water lift and the specific speed of the pump.

System performance may be described by assuming that pump power requirements are only dependent upon the cube of shaft speed and not upon flow or head. This simplified approach is compared with a more complete model using polynomials to describe pump characteristics. Some of the less well known rotodynamic pumps are shown to offer particular advantages for low wind water pumping.

Hossain et al. [17] stated that a vertical axis sail-wing rotor having six sails was fabricated using locally available materials and technology. It is coupled with a locally manufactured diaphragm pump to pump water for different total static pressure heads. It is observed that the rotor can be manufactured easily and it can pump reasonable amount of water even at low and variable wind speed. The starting wind speed for the system is found to be about 1.5 m/s (3.35 mph) and the maximum overall combined efficiency was about five percent. Islam, et al. [23] investigated that the appropriate wind turbines might be designed and selected for the purpose to driving irrigation pumps. The performance of Savonius rotor coupled to diaphragm pump is found to be satisfactory. They also mentioned the advantages of this system. These are:

a) Possibility of local production and creation of employment
b) Savings of foreign exchange by using locally available materials
c) Conservation of fuel
d) Promotion of self reliance in villages
e) Does not create environmental pollution

CHAPTER 2

EXISTING THEORIES OF HORIZONTAL AXIS WIND TURBINE

2.1 General

The main purpose of a wind turbine is to extract energy from the wind and then convert it into mechanical energy, which later may be transformed into other forms of energy. The performance calculation of wind turbines is mostly based upon a steady flow, in which the influence of the turbulence of the atmospheric boundary layer is neglected.

For the design and evaluation of wind turbines, the availability of computation tools is essential. Most existing theoretical models are based on the combination of momentum theory and blade element theory. This combined theory is known as modified blade element theory or strip theory. It has been assumed that the strip theory approach will be adequate for performance analysis of wind machines. The basic theoretical development of strip theory is presented here. Effects of wake rotation, tip and hub losses for maximum power are presented as well.

In case of horizontal axis wind turbine, classical strip theory has been found to give adequate results under normal operating conditions near the design tip speed ratio. At both high and low tip speed ratios, however, the wind turbine may operate in flow conditions, which are not easily analyzed by classical theory. Classical theory is inadequate at low tip speed ratios when the airfoils are at high angles of attack. Also at low tip speed ratios the assumption that the axial velocity change at the disc is approximately half the value in the wake does not hold.

2.2 Axial Momentum Theory

The following assumptions are made in establishing the momentum theory.

a) infinite number of blades
b) thrust loading is uniform over the disc
c) non-rotating wake
d) static pressure far ahead and far behind the rotor are equal to the undisturbed ambient static pressure
e) homogeneous flow

2.2.1 Non-rotating wake

The axial momentum theory has been presented by Rankine in 1865 and has been modified by Froude [26]. The basis of the theory is the determination of the forces acting on a rotor to produce the motion of the fluid. The theory has been found useful in predicting ideal efficiency of a rotor and may be applied for wind turbines.

Considering the control volume in Fig. 2.2.1, where the upstream and downstream control volume planes are infinitely far removed from the turbine plane, the conservation of mass may be expressed as:

$$\rho A_1 V_\infty = \rho A U = \rho A_2 V$$

(2.2.1), where,

V_∞ = undisturbed wind velocity

U = wind velocity through the rotor

V = wind velocity far behind the rotor

A = turbine disc area

A_1 = cross-sectional area of incoming wind

A_2 = wake cross-sectional area

The thrust T on the rotor is given by the change of momentum of the flow:

$$T = m(V_\infty - V) = \rho A_1 V_\infty^2 - \rho A_2 V^2 \qquad (2.2.2)$$

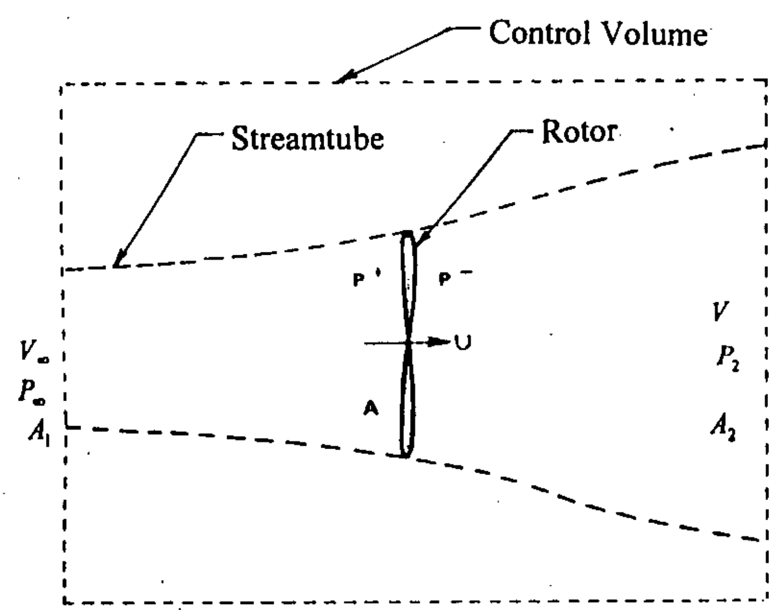

Figure 2.2.1: Control Volume of a Wind Turbine

Introducing equation (2.2.1) leads to the expression

$$T = \rho A U(V_\infty - V) \tag{2.2.3}$$

The thrust on the rotor can also be expressed from the pressure difference over the rotor area as

$$T = A(P^+ - P^-) \tag{2.2.4}$$

where

P^+ = pressure immediately in front of the rotor

P^- = pressure immediately behind the rotor

Now applying Bernoulli's equation:

For upstream of the rotor: $P_\infty + \frac{1}{2}\rho V_\infty^2 = P^+ + \frac{1}{2}\rho U^2$ (2.2.5)

For downstream of the rotor: $P_\infty + \frac{1}{2}\rho V^2 = P^- + \frac{1}{2}\rho U^2$ (2.2.6)

Subtracting equation (2.2.6) from equation (2.2.5), one obtains

$$P^+ - P^- = \frac{1}{2}\rho(V_\infty^2 - V^2) \tag{2.2.7}$$

The expression for the thrust from equation (2.2.4) becomes,

$$T = \frac{1}{2}\rho A(V_\infty^2 - V^2) \tag{2.2.8}$$

Equating the equation (2.2.8) with equation (2.2.3),

$$\frac{1}{2}\rho A(V_\infty^2 - V^2) = \rho A U(V\infty - V)$$

$$\text{or, } U = \frac{V_\infty + V}{2} \tag{2.2.9}$$

The velocity at the rotor U is often defined in terms of an axial interference factor 'a' as,

$$U = V_\infty(1-a) \tag{2.2.10}$$

Balancing equations (2.2.9) and (2.2.10), the wake velocity can be expressed as,

$$V = V_\infty(1-2a) \tag{2.2.11}$$

The change in kinetic energy of the mass flowing through the rotor area is the power absorbed by the rotor:

$$P = m\Delta KE = \frac{1}{2}\rho A U(V_\infty^2 - V^2) \tag{2.2.12}$$

With equations (2.2.10) and (2.2.11), the expressions for power becomes:

$$P = 2\rho A V_\infty^3 a(1-a)^2 \tag{2.2.13}$$

Maximum power occurs when, $\frac{dP}{da} = 0$

Therefore, $\frac{dP}{da} = 2\rho A V_\infty^3 (1 - 4a + 3a^2) = 0$

which leads to an optimum interference factor,

$$a = \frac{1}{3}$$

Putting this value in equation (2.2.13), maximum power becomes,

$$P_{\max} = \frac{16}{27}\left(\frac{1}{2}\rho A V_\infty^3\right) \tag{2.2.14}$$

The factor 16/27 is called the Betz-coefficient [26] and represents theoretical maximum fraction, an ideal rotor can extract from the wind. This fraction is related to the power of an undisturbed flow arriving at an area A, whereas, in reality the volume flow rate through A is not AV_∞ but AU. Hence, the maximum efficiency for maximum power can be written as,

$$\eta_{eff} = \frac{P_{\max}}{\frac{1}{2}\rho A U V_\infty^2} = \frac{16}{27}\frac{V_\infty}{U} = \frac{16}{27}\frac{1}{(1-a)} = \frac{16}{27}\frac{1}{(1-\frac{1}{3})} = \frac{8}{9} \tag{2.2.15}$$

This model does not take into account additional effects of wake rotation. As the initial stream is not rotational, interaction with a rotating windmill will cause the wake to rotate in opposite direction. If there is rotational kinetic energy in the wake in addition to translational kinetic energy, then from the thermodynamic considerations we may expect lower power extraction than in the case of the wake having only translation. In the following article, this wake rotational will be taken into account.

2.2.2 Effect of wake rotation on momentum theory

Considering this effect the assumption is made that at the upstream of the rotor, the flow is entirely axial and the downstream flow rotates with an angular velocity ω but remains irrotational. This angular velocity is considered to be small in comparison to the angular velocity Ω of the wind turbine. This assumption maintains the approximation of axial momentum theory that the pressure in the wake is equal to the free stream pressure.

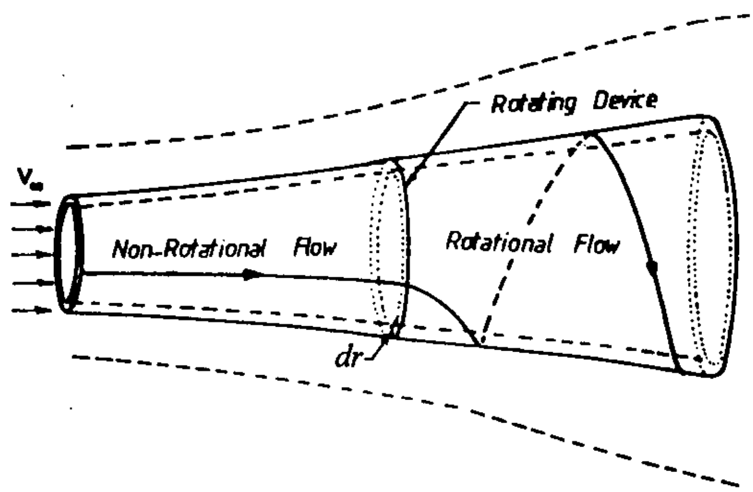

Figure 2.2.2: Streamtube Model Showing the Rotation of Wake

The wake rotation is opposite in direction of the rotor and represents an additional loss of kinetic energy for the wind rotor as shown in figure 2.2.2. Power is equal to the product of the torque Q acting on the rotor and the angular velocity Ω of the rotor. In order to obtain the maximum power it is necessary to have a high angular velocity and low torque because high torque will result in large wake rotational energy. The angular velocity ω of the wake and the angular velocity Ω of the rotor are related by an angular interference factor a′:

$$a' = \frac{\text{angular velocity of the wake}}{\text{twice the angular velocity of the rotor}} = \frac{\omega}{2\Omega} \qquad (2.2.16)$$

The annular ring through which a blade element will pass is illustrated in figure 2.2.3.

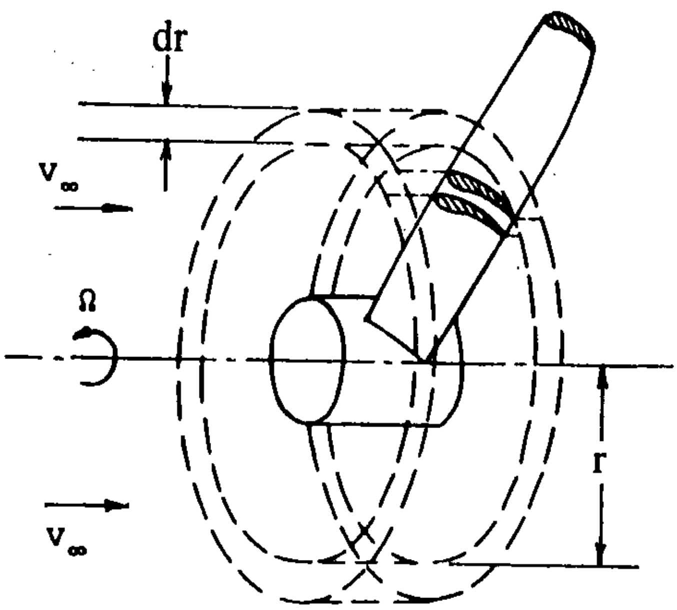

Figure 2.2.3: Blade Element Annular Ring

Using the relation for momentum flux through the ring the axial thrust force dT can be expressed as,

$$dT = dm(V_\infty - V) = \rho dAU(V_\infty - V) \tag{2.2.17}$$

Inserting equations (2.2.10) and (2.2.11)

$$U = V_\infty(1-a) \tag{2.2.10}$$

$$V = V_\infty(1-2a) \tag{2.2.11}$$

and expressing the area of the annular ring dA as,

$$dA = 2\pi r\, dr \tag{2.2.18}$$

The expression for the thrust becomes,

$$dT = 4\pi r \rho V_\infty^2 a(1-a)\, dr \tag{2.2.19}$$

The thrust force may also be calculated from the pressure difference over the blades by applying Bernoulli's equation. Since the relative angular velocity changes from Ω to $(\Omega+\omega)$, while the axial components of the velocity remain unchanged, Bernoulli's equation gives,

$$P^+ - P^- = \frac{1}{2}\rho(\Omega+\omega)^2 r^2 - \frac{1}{2}\rho\Omega^2 r^2$$

$$\text{or,} \quad P^+ - P^- = \rho(\Omega + \frac{1}{2}\omega)\omega r^2$$

The resulting thrust on the annular element is given by,

$$dT = (P^+ - P^-)dA$$

$$\text{or,} \ dT = \rho(\Omega + \frac{1}{2}\omega)\omega r^2 2\pi r\, dr$$

Inserting equation (2.2.16)

$$dT = 4a'(1+a')\frac{1}{2}\rho\Omega^2 r^2 2\pi r\, dr \tag{2.2.20}$$

Balancing equation (2.2.20) and equation (2.2.19), leads to the expression

$$\frac{a(1-a)}{a'(1+a')} = \frac{\Omega^2 r^2}{V_\infty^2} = \lambda_r^2 \tag{2.2.21}$$

where, λ_r is known as the local tip speed ratio which is given by

$$\lambda_r = \frac{r\Omega}{V\infty} \tag{2.2.22}$$

To derive an expression for the torque acting on the rotor the change in angular momentum flux dQ through the annular ring is considered.

$$dQ = dmV_t r$$

$$\text{or,} \ dQ = \omega r\rho dA\, Ur$$

where, V_t is the wake tangential velocity.

Considering equations (2.2.10), (2.2.16) and (2.2.18), the expression for the torque acting on the annular ring is given by,

$$dQ = 4\pi r^3 \rho V_\infty (1-a)a'\Omega\, dr \tag{2.2.23}$$

The generated power through the annular ring is equal to $dP = \Omega\, dQ$, so the total power becomes,

$$P = \int_0^R \Omega\, dQ \tag{2.2.24}$$

Introducing the tip speed ratio λ as,

$$\lambda = \frac{R\Omega}{V_\infty} \tag{2.2.25}$$

Equation for total power from equations (2.2.23) and (2.2.24) becomes,

$$P = \int_0^R 4\pi r^3 \rho V_\infty (1-a)a'\Omega^2 dr$$

This can be written as,

$$P = \frac{1}{2}\rho A V_\infty^3 \frac{8}{\lambda^2}\int_0^\lambda a'(1-a)\lambda_r^3 \, d\lambda_r \tag{2.2.26}$$

where, A is the turbine swept area, which is given by $A = \pi R^2$.

The power coefficient is defined as,

$$C_P = \frac{P}{\frac{1}{2}\rho A V_\infty^3}$$

Inserting equation (2.2.26) power coefficient can be written as,

$$C_P = \frac{8}{\lambda^2}\int_0^\lambda a'(1-a)\lambda_r^3 \, d\lambda_r \tag{2.2.27}$$

Rearranging equation (2.2.21)

$$a' = -\frac{1}{2} + \frac{1}{2}\sqrt{1 + \frac{4}{\lambda_r^2} a(1-a)} \tag{2.2.28}$$

Substituting this value in equation (2.2.27) and taking the derivative equal to zero, the relation between λ_r and a for maximum power becomes,

$$\lambda_r = \frac{(1-a)(4a-1)^2}{(1-3a)} \tag{2.2.29}$$

Introducing equation (2,2,29) into equation (2.2.21) the relationships between a and a' becomes:

$$a' = \frac{1-3a}{4a-1} \tag{2.2.30}$$

This relation will be used later for design purposes.

2.3. Blade Element Theory

With the blade element theory, the forces acting on a differential element of the blade may be calculated. Then integration is carried out over the length of the blade to determine the performance of the entire rotor [26].

Assumptions:

a) There is no interference between adjacent blade elements along each blade.

b) The forces acting on a blade element are solely due to the lift and drag characteristics of the sectional profile of the element.

c) The pressure in the far wake is equal to the free stream pressure.

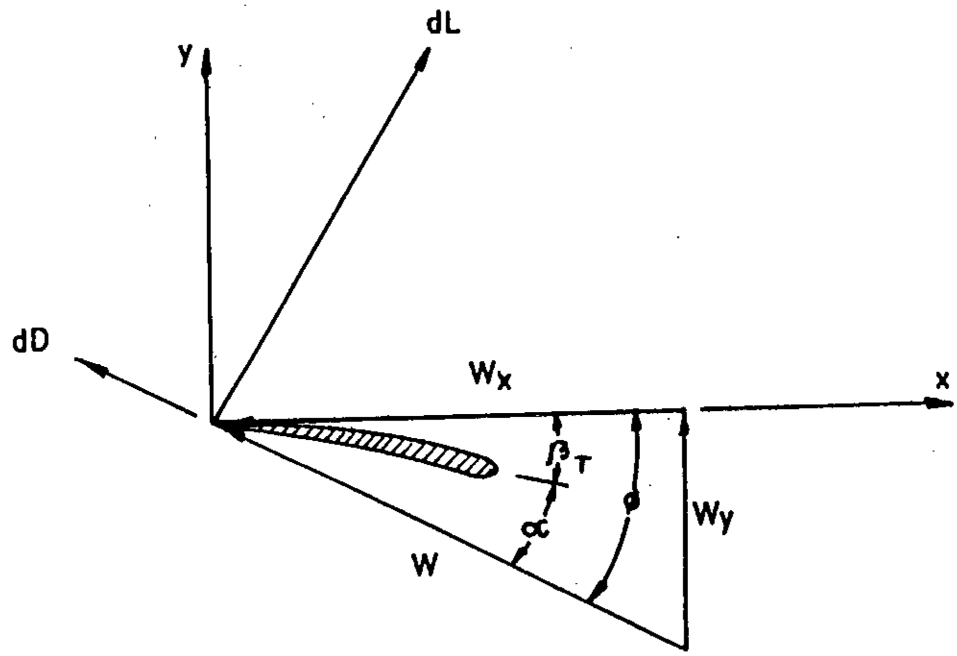

Figure 2.3.1: Velocity Diagram of a Blade Element.

The aerodynamic force components acting of the blade elements are the lift force dL, perpendicular to the resulting velocity vector and the drag force dD acting in the direction of the resulting velocity vector as shown in figure 2.3.1. The following expressions for the sectional lift and drag forces may be introduced:

$$dL = C_L \frac{1}{2} \rho W^2 C\, dr \tag{2.3.1}$$

$$dD = C_D \frac{1}{2} \rho W^2 C\, dr \tag{2.3.2}$$

The thrust and torque experienced by the blade element are

$$dT = dL \cos\phi + dD \sin\phi \tag{2.3.3}$$

$$dQ = (dL \sin\phi - dD \cos\phi) r \tag{2.3.4}$$

Assuming, that the rotor has B blades, the expressions for the thrust and torque becomes,

$$dT = BC \frac{1}{2} \rho W^2 (C_L \cos\phi + C_D \sin\phi)\, dr$$

$$\text{or, } dT = BC \frac{1}{2} \rho W^2 C_L \cos\phi \left(1 + \frac{C_D}{C_L} \tan\phi\right) dr \tag{2.3.5}$$

$$\text{and} \quad dQ = BC \frac{1}{2} \rho W^2 (C_L \sin\phi - C_D \cos\phi) r\, dr$$

$$\text{or, } dQ = BC \frac{1}{2} \rho W^2 C_L \sin\phi \left(1 - \frac{C_D}{C_L} \frac{1}{\tan\phi}\right) r\, dr \tag{2.3.6}$$

According to the Figure 2.3.1 the expression for relative velocity W can be written as

$$W = \frac{(1-a)V_\infty}{\sin\phi} = \frac{(1+a')\Omega r}{\cos\phi} \tag{2.3.7}$$

Introducing the following trigonometric relations based on Figure 2.3.1

$$\tan\phi = \frac{(1-a)V_\infty}{(1+a')\Omega r} = \frac{1-a}{1+a'} \frac{1}{\lambda_r} \tag{2.3.8}$$

$$\text{and } \beta_T = \phi - \alpha \tag{2.3.9}$$

and the local solidity ratio σ as

$$\sigma = \frac{BC}{2\pi r} \tag{2.3.10}$$

The equations of the blade element theory become,

$$dT = (1-a)^2 \frac{\sigma C_L \cos\phi}{\sin^2\phi} \left(1 + \frac{C_D}{C_L} \tan\phi\right) \frac{1}{2} \rho V_\infty^2 2\pi r\, dr \tag{2.3.11}$$

$$dQ = (1+a')^2 \frac{\sigma C_L \sin\phi}{\cos^2\phi} \left(1 - \frac{C_D}{C_L} \frac{1}{\tan\phi}\right) \frac{1}{2} \rho \Omega^2 r^3 2\pi r\, dr \tag{2.3.12}$$

2.4 Strip Theory

From the axial momentum and blade element theories a series of relationships can be developed to determine the performance of a wind turbine.

By equating the thrust, determined from the momentum theory equation (2.2.19) to equation (2.3.11) of blade element theory for an annular element at radius r, we get

$$dT_{momentum} = dT_{blade\ element}$$

$$\text{or, } \frac{a}{1-a} = \frac{\sigma C_L \cos\phi}{4\sin^2\phi}\left(1+\frac{C_D}{C_L}\tan\phi\right) \tag{2.4.1}$$

Equating the angular momentum, determined from the momentum theory equation (2.2.23) with equation (2.3.12) of blade element theory one obtains

$$dQ_{momentum} = dQ_{blade\ element}$$

$$\text{or, } \frac{a'}{1+a'} = \frac{\sigma C_L}{4\cos\phi}\left(1-\frac{C_D}{C_L}\frac{1}{\tan\phi}\right) \tag{2.4.2}$$

Equations (2.4.1) and (2.4.2), which determine the axial and angular interference factors contain drag terms. The drag terms should be omitted in calculation of a and a' on the basis that the retarded air due to drag is confined to thin helical sheets in the wake and have little effects on the induced flow [31, 32]. Omitting the drag terms the induction factors a and a' may be calculated with the following equations.

$$\frac{a}{1-a} = \frac{\sigma C_L \cos\phi}{4\sin^2\phi} \tag{2.4.3}$$

$$\frac{a'}{1+a'} = \frac{\sigma C_L}{4\cos\phi} \tag{2.4.4}$$

Considering the equations (2.4.3) and (2.3.11), the elemental thrust can be written as,

$$dT = 4a(1-a)\left(1+\frac{C_D}{C_L}\tan\phi\right)\frac{1}{2}\rho V_\infty^2 2\pi r\, dr \tag{2.4.5}$$

From equations (2.4.4), (2.3.8) and (2.3.12), the elemental torque can be obtained as,

$$dQ = 4a'(1-a)\left(1-\frac{C_D}{C_L}\frac{1}{\tan\phi}\right)\frac{1}{2}\rho V_\infty \Omega 2\pi r^3\, dr \tag{2.4.6}$$

Elemental power is given by,

$$dp = dQ\,\Omega$$

$$\text{or, } dP = 4a'(1-a)\left(1-\frac{C_D}{C_L}\frac{1}{\tan\phi}\right)\frac{1}{2}\rho V_\infty \Omega^2 2\pi r^3\, dr \tag{2.4.7}$$

Introducing the local tip speed ratio λ_r from equation (2.2.22) with:

$$\lambda_r = \frac{r\Omega}{V_\infty}$$

Equations of total thrust, torque and power become,

$$T = \frac{1}{2}\rho A V_\infty^2 \frac{8}{\lambda^2}\int_0^\lambda a(1-a)\left(1+\frac{C_D}{C_L}\frac{1}{\tan\phi}\right)\lambda_r\, d\lambda_r \tag{2.4.8}$$

$$Q = \frac{1}{2}\rho A V_\infty^2 R \frac{8}{\lambda^3}\int_0^\lambda a'(1-a)\left(1-\frac{C_D}{C_L}\frac{1}{\tan\phi}\right)\lambda_r^3\, d\lambda_r \tag{2.4.9}$$

and

$$P = \frac{1}{2}\rho A V_\infty^3 \frac{8}{\lambda^2}\int_0^\lambda a'(1-a)\left(1-\frac{C_D}{C_L}\frac{1}{\tan\phi}\right)\lambda_r^3\, d\lambda_r \tag{2.4.10}$$

These equations are valid only for a wind turbine having infinite number of blades.

2.5 Tip and Hub Losses

In the preceding sections, the rotor was assumed to be possessed an infinite number of blades with an infinitely small chord. In reality, however, the number of blades is finite. According to the theory discussed previously, the wind imparts a rotation to the rotor, thus dissipating some of its kinetic energy or velocity and creating a pressure difference between one side of the blade and the other. At tip and hub, however, this pressure difference leads to secondary flow effects. The flow becomes three-dimensional and tries to equalize the pressure difference as shown in Figure 2.5.1. This effect is more

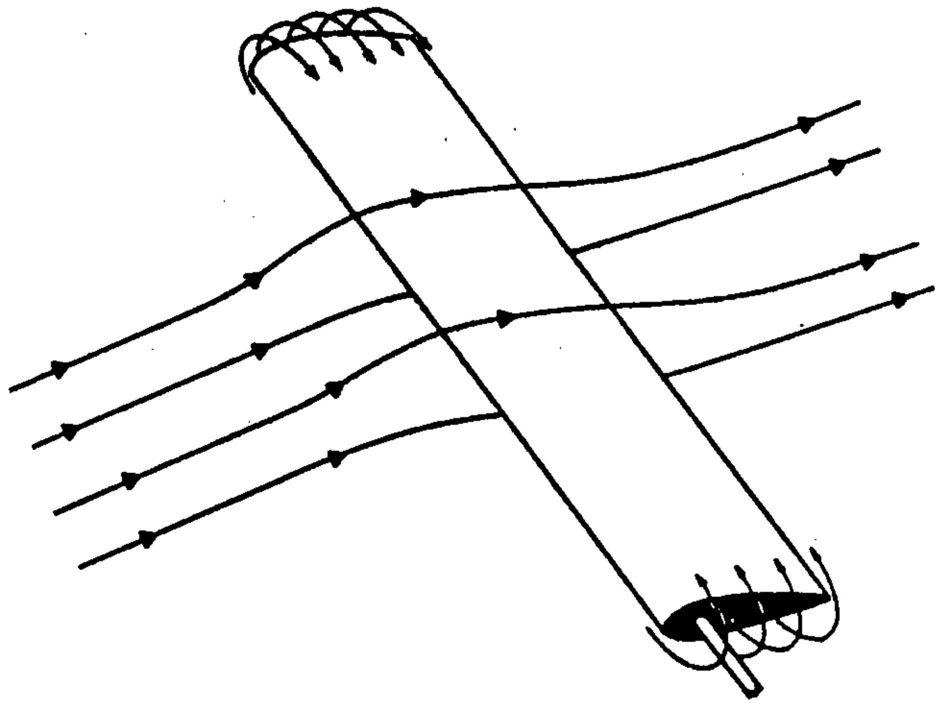

Figure 2.5.1: Tip and Hub Losses Flow Diagram

pronounced as one approaches the tip. It results in a reduction of the torque on the rotor and thus in a reduction of the power output.

The method suggested by Prandtl will be used here. The idea in Prandtl's method is to replace the system of vortices at the tip with a series of parallel planes for which the flow is more easily calculated. It should however be remembered that this approximation was developed for a lightly loaded propeller under optimum conditions which may differ somewhat from the conditions of a wind turbine.

The correction factor suggested by Prandtl is

$$F_{tip} = \frac{2}{\pi} \arccos e^{-f} \qquad \text{where, } f = \frac{B}{2} \frac{R-r}{r \sin\phi}$$

It may also be applied for the hub region and f is then defined as,

$$f = \frac{B}{2} \frac{r - r_{hub}}{r_{hub} \sin\phi}$$

Hence, a correction factor F for total losses is applied as,

$$F = F_{tip} . F_{hub} \tag{2.5.1}$$

The loss factor F may be introduced in several ways for the rotor performance calculation. In the method adopted by Wilson and Lissaman [49], the induction factors a and a' are multiplied with F, and thus the axial and tangential velocities in the rotor plane as seen by the blades are modified. It is further assumed that these corrections only involve the momentum formulas.

Thus the thrust and torque from [equations (2.2.19) and (2.2.23)] momentum theory become,

$$dT = 4\pi r \rho V_\infty^2 aF(1-aF)\,dr \tag{2.5.2}$$

$$dQ = 4\pi r^3 \rho V_\infty a' F(1-aF)\Omega\,dr \tag{2.5.3}$$

The results of the blade element theory remain unchanged.

$$dT = (1-a)^2 \frac{\sigma C_L \cos\phi}{\sin^2\phi}\left(1+\frac{C_D}{C_L}\tan\phi\right)\frac{1}{2}V_\infty^2 2\pi r\,dr \tag{2.3.11}$$

and $$dQ = (1+a')^2 \frac{\sigma C_L \sin\phi}{\cos^2\phi}\left(1-\frac{C_D}{C_L}\frac{1}{\tan\phi}\right)\frac{1}{2}\rho\Omega^2 r^4 2\pi\,dr \tag{2.2.12}$$

Equation (2.3.12) can also be written as [From eq. (2.3.6), (2.3.7) & (2.3.10)],

$$dQ = (1-a)^2 \frac{\sigma C_L}{\sin\phi}\left(1-\frac{C_D}{C_L}\frac{1}{\tan\phi}\right)\frac{1}{2}\rho V_\infty^2 2\pi r^2\,dr \tag{2.5.4}$$

Balancing the equation (2.5.2) with (2.3.11) one finds,

$$aF(1-aF) = \frac{\sigma C_L \cos\phi(1-a)^2}{4\sin^2\phi}\left(1+\frac{C_D}{C_L}\tan\phi\right) \tag{2.5.5}$$

and considering the equations (2.5.3) and (2.5.4),

$$a'F(1-aF) = (1-a)^2 \frac{\sigma C_L}{4\sin\phi}\left(1-\frac{C_D}{C_L}\frac{1}{\tan\phi}\right) \tag{2.5.6}$$

Omitting the drag terms in equations (2.5.5) and (2.5.6) the following expressions yield,

$$aF(1-aF) = \frac{\sigma C_L \cos\phi(1-a)^2}{4\sin^2\phi} \tag{2.5.7}$$

$$a'F(1-aF) = \frac{\sigma C_L (1-a)^2}{4\sin\phi} \tag{2.5.8}$$

From the equations (2.5.7) and (2.5.8), the final expressions for the elemental thrust and torque become,

$$dT = 4aF(1-aF)\left(1+\frac{C_D}{C_L}\tan\phi\right)\rho V_\infty^2 \pi r\, dr \tag{2.5.9}$$

and

$$dQ = 4a' F(1-aF)\left(1-\frac{C_D}{C_L}\tan\phi\right)\rho V_\infty^2 \pi r^2\, dr \tag{2.5.10}$$

2.6 Equations for Thrust, Torque and Power Coefficients

Elemental thrust, torque and power coefficients are defined as,

$$dC_T = \frac{dT}{\frac{1}{2}\rho A V_\infty^2} \tag{2.6.1}$$

$$dC_Q = \frac{dQ}{\frac{1}{2}\rho A V_\infty^2 R} \tag{2.6.2}$$

and $$dC_P = \frac{dP}{\frac{1}{2}\rho A V_\infty^3} = \frac{dQ\,\Omega}{\frac{1}{2}\rho A V_\infty^3}$$

or, $$dC_P = \frac{dQ\,\Omega R}{\frac{1}{2}\rho A V_\infty^2 R V_\infty} = dC_Q\,\lambda \tag{2.6.3}$$

Considering the equations (2.5.9) and (2.6.1), the elemental thrust coefficient can be written as,

$$dC_T = \frac{8}{R^2} aF(1-aF)\left(1+\frac{C_D}{C_L}\tan\phi\right) r\, dr \tag{2.6.4}$$

Again, from equations (2.5.10) and (2.6.2), the elemental torque coefficient is given by,

$$dC_Q = \frac{8}{R^3} a' F(1-aF)\left(1-\frac{C_D}{C_L}\frac{1}{\tan\phi}\right) r^2\, dr \tag{2.6.5}$$

Elemental power coefficient can be obtained from equation (2.6.3) as,

$$dC_P = \frac{8\Omega}{R^2 V_\infty} a' F(1-aF)\left(1-\frac{C_D}{C_L}\frac{1}{\tan\phi}\right) r^2\, dr \tag{2.6.6}$$

Finally, total thrust, torque and power coefficients can be obtained by the following equations:

$$C_T = \frac{8}{R^2}\int_0^R aF(1-aF)\left(1+\frac{C_D}{C_L}\tan\phi\right)r\,dr \tag{2.6.7}$$

$$C_Q = \frac{8}{R^3}\int_0^R a'F(1-aF)\left(1-\frac{C_D}{C_L}\frac{1}{\tan\phi}\right)r^2\,dr \tag{2.6.8}$$

$$C_P = \frac{8}{R^2}\frac{\Omega}{V_\infty}\int_0^R a'F(1-aF)\left(1-\frac{C_D}{C_L}\frac{1}{\tan\phi}\right)r^2\,dr \tag{2.6.9}$$

2.7 Equations for Maximum Power

For maximum power output the relation between a and a' may be expressed by the equation (2.2.29) as:

$$a' = \frac{1-3a}{4a-1}$$

Introducing the equations of induction factors as follows:

$$\frac{a}{1-a} = \frac{\sigma C_L\cos\phi}{4\sin^2\phi} \tag{2.4.3}$$

$$\frac{a}{1+a'} = \frac{\sigma C_L}{4\cos\phi} \tag{2.4.4}$$

From equations (2.2.29), (2.4.3) and (2.4.4), the following expression yields:

$$\sigma C_L = 4(1-\cos\phi) \tag{2.7.1}$$

Considering the local solidity σ as,

$$\sigma = \frac{BC}{2\pi r} \tag{2.3.10}$$

equation (2.7.1) transforms into,

$$C = \frac{8\pi r}{BC_L}(1-\cos\phi) \tag{2.7.2}$$

Local tip speed ratio λ_r is given by,

$$\lambda_r = \frac{r\Omega}{V_\infty} \tag{2.2.22}$$

From equation (2.3.8),

$$\tan\phi = \frac{1-a}{1+a'}\frac{1}{\lambda_r} \qquad (2.3.8)$$

Now replacing the values of (1-a) and (1+a') from equations (2.4.3) and (2.4.4) and putting the value of σC_L from equation (2.7.1), the following relation can be deduced:

$$\lambda_r = \frac{\sin\phi(2\cos\phi - 1)}{(1-\cos\phi)(2\cos\phi + 1)} \qquad (2.7.3)$$

and this can be reduced to

$$\phi = \frac{2}{3} arc\tan\frac{1}{\lambda_r} \qquad (2.7.4)$$

Equation of blade twist angle from the equation (2.3.9) can be written as,

$$\beta_T = \phi - \alpha$$

Equations (2.7.2), (2.2.22), (2.7.4) and (2.3.9) will be used to calculate the blade configurations in chapter 4.

CHAPTER 3

PROSPECT OF WIND ENERGY FOR WATER PUMPING IN BANGLADESH

3.1 Introduction

Winds are available in Bangladesh mainly during the monsoon and around one to two months before and after the monsoon. During the months starting from late October to the middle of February, winds either remain calm or too low to be of any use by a windmill. Except for the above mentioned period of four months, a windmill, if properly designed and located, can supply enough energy.

During the months of June, July and August the peak rainfall occurs in Bangladesh. However, the peak wind speed above average occurs one to two months and in some cases three months before the peak rainfall occurs. So one of the advantages is that the above average winds are available during the hottest and the driest months of March, April and May. During this period, windmills may be used for pumping water for irrigation if it had been previously stored in a reservoir during the monsoon. During the operating seasons, subsoil water from shallow wells can also be pumped up by low lift pumps run by windmills. Wind power can also be incorporated in electricity grid on a substantial basis and could add reliability and consistency to the electricity generated by the Kaptai hydroelectric Power Station during the dry season. This is due to fact that, during the dry season, required water head becomes rather low for total utilization of all the generators. Thus, power generation has to be curtailed during this period. So this power could be compensated with the help of wind power plant.

3.2 Analysis of Wind Characteristics and Site selection

Like other countries of the world Bangladesh has the meteorological department to conduct the survey of wind velocity and wind direction in many parts of the country. They usually keep the record of wind velocity three hourly. The standard practice is to perform the measurements at a height of 5-10m. These data are not sufficient for wind turbine applications. Usually, measurements in the selected site have to be taken at several locations and heights for several months to a year. These detailed measured values can then be compared with the meteorological data to find correlation. But this measurement is very labourious and time consuming, which is out off the capacity of this work.

The Meteorological department of Bangladesh collects 3-hourly wind speed data with the help of vertical axis cup type anemometers. These wind data for the period 1981-1996 of 20 stations were taken and monthly average speeds were computed for all the 20 stations, presented in Table-3.2.1. It can be seen from Table-3.2.1 that the wind speeds at different sites are very low except Patenga, which are not feasible for electricity generation and water pumping. The causes of poor conditions of the meteorological data are [40]:

- Most of the meteorological stations are situated in the places of roughness class 3 as shown in Table-3.2.2. So the wind after loosing 70% energy is measured by the meteorological stations and for this reasons meteorological stations show poor wind speeds.
- Few meteorological stations are located several kilometers away from their respective seacoast and the anemometers do not face the winds coming from the sea directly. So in the areas, directly open to the sea, wind speed will be higher than those in the present locations. Experiments carried out by the International Energy Agency (IEA) and the European Community (EC) countries show that this increase in wind speed may range from 5-100 %.
- Some of the meteorological stations are surrounded by trees, buildings, hills and hillocks etc. The wind speed becomes weak as it faces obstacles on its way and it results the lower value.
- Generally, meteorological stations measure winds at heights of 5 to 10m. But the normal hub-height of modern wind turbines ranges from 30 to 40 meters. So at these heights wind speeds would be better. A thumb rule is that if the height is doubled in the areas of roughness class-3, wind speed is increased by 20% and in the areas of roughness class-0, wind speed increased by 10 %.
- The anemometers of these stations are not calibrated for long times.

The meteorological data provide little information about the fluctuation in the speed and direction of the wind, which are also necessary to predict the performance of turbine appropriately. For a wind turbine, the main source of fluctuating aerodynamic loads is the wind shear, which is once per revolution.

Table-3.2.1: Average Wind Speed (m/s) at 10 Meters Height at Different Locations in Bangladesh

Locations	Months											
	Jan	Feb	Mar	Apr	May	Jun	Jul	Aug	Sep	Oct	Nov	Dec
Barisal	2.38	2.11	2.11	2.92	2.65	2.38	2.22	2.16	2.11	1.73	1.70	1.68
Bogra	1.60	1.80	2.50	3.30	3.40	3.00	2.80	2.50	2.10	1.80	1.50	1.40
Chittagong	2.98	2.36	4.06	4.11	4.52	5.65	5.81	5.60	3.80	2.31	2.78	1.80
Comilla	1.85	2.21	2.11	4.47	3.14	2.62	2.36	2.42	1.49	1.95	1.34	1.39
Cox'sBazar	3.08	3.14	3.70	4.57	3.14	3.39	3.14	3.24	2.62	2.67	2.11	2.67
Dhaka	2.78	2.67	3.60	4.73	5.19	4.68	4.93	4.83	3.60	2.83	2.16	2.42
Dinajpur	2.20	2.00	4.00	2.00	2.40	2.20	2.10	2.00	2.00	2.90	2.00	2.00
Hatiya	2.49	2.16	3.41	3.25	3.95	5.30	4.71	2.16	2.43	2.27	2.51	2.11
Jessore	2.36	2.42	4.06	6.84	6.84	5.14	5.04	4.06	3.55	2.83	2.72	2.62
Khulna	2.43	1.35	2.49	2.50	3.41	3.19	2.71	2.00	2.06	1.62	2.71	1.95
Khepupara	3.44	3.60	3.14	5.81	4.78	3.86	3.39	3.24	2.93	3.03	2.42	2.11
Kutubdia	1.45	1.49	1.90	2.21	2.27	3.00	2.96	2.57	1.73	1.19	0.97	1.06
Mongla	0.88	1.03	1.41	2.06	2.40	2.16	2.03	1.93	1.50	1.04	0.84	0.83
Patenga	5.10	5.20	6.04	6.49	6.94	7.12	7.54	7.00	6.13	5.68	5.50	4.48
Rangamati	1.19	1.35	3.62	2.54	1.73	2.65	1.41	1.84	1.19	1.19	1.14	1.30
Sandip	1.90	2.47	2.62	3.96	2.00	3.14	2.78	2.21	1.90	1.34	1.39	1.39
Sathkhira	3.45	3.61	3.15	5.82	5.01	3.90	3.50	3.30	2.97	3.10	2.90	2.30
Sylhet	1.80	2.40	2.70	2.60	2.00	2.20	2.00	1.70	1.40	1.60	1.55	1.50
Teknaf	3.03	3.29	3.60	3.29	2.72	3.19	3.14	2.36	2.00	1.80	1.29	1.44
Thakurgaon	3.40	4.15	6.50	6.91	7.10	6.60	6.50	5.40	5.20	4.90	4.30	3.90

Table-3.2.2: Types of Terrain, Roughness Classes and Their Energy Contains.

Roughness Class	Terrain Type	Value of α	Energy (%)
0	Water areas, airports, plain lands, etc.	0.17	100
1	Country areas with few bushes, trees and buildings	0.28	70
2	Farmlands with scattered buildings	0.35	60
3	Build-up areas.	0.40	30

Wind velocity changes with height. The rate of increase of velocity with height depends upon the roughness of the terrain. The variation of average wind speed can be determined analytically by using power law expression shown as below [43],

$$\frac{V_Z}{V_{ref}} = \left(\frac{h}{h_{ref}}\right)^{\alpha} \tag{3.2.1}$$

where, V_Z and V_{ref} are the average speeds at h meters and at the reference height of $h_{ref} = 10m$ above the ground respectively and α varies from 0.1 to 0.4 depending on the nature of the terrain. The value of α for the different terrain has been shown in Table-3.2.2 [4]. A value of 0.17 for α may be used, in general, although this is applicable for the open terrain only. The value of α may be chosen as 0.28 for the terrain with trees and houses like the suburb area. But for the city with tall buildings the value of α should be considered as 0.4.

In the present analysis, the average wind speed at 20 m height is determined (Table-3.2.3) from the power law expression as in equation (3.2.1), taking the value of power exponent, $\alpha = 0.28$. The power law description is used for its simplicity.

Attempt would be made to give a detailed idea about various kinds of presentation of the wind data at different sites at 20 m height. This would provide information to make decision whether that site has reasonably potential for the operation of wind machine. Figure 3.2.1 shows the monthly variation of average wind speed for several places in Bangladesh. It can be seen that wind speeds are higher from March to August for all places.

Table-3.2.3: Average Wind Speed (m/s) at 20 Meters Height at Different Locations in Bangladesh

Locations	Months												
	Jan	Feb	Mar	Apr	May	Jun	Jul	Aug	Sept	Oct	Nov	Dec	Mean
Barisal	2.90	2.57	2.57	3.56	3.23	2.90	2.71	2.64	2.57	2.11	2.07	2.05	2.66
Bogra	1.95	2.20	3.05	4.03	4.15	3.66	3.42	3.05	2.56	2.20	1.83	1.71	2.82
Chittagong	3.64	2.88	4.95	5.01	5.51	6.89	7.09	6.83	4.64	2.82	3.39	2.20	4.65
Comilla	2.26	2.70	2.57	5.45	3.83	3.20	2.88	2.95	1.82	2.38	1.63	1.70	2.78
Cox'sBazar	3.76	3.83	4.51	5.58	3.83	4.14	3.83	3.95	3.20	3.26	2.57	3.26	3.81
Dhaka	3.39	3.26	4.39	5.77	6.33	5.71	6.01	5.89	4.39	3.45	2.64	2.95	4.52
Dinajpur	2.68	2.44	4.88	2.44	2.93	2.68	2.56	2.44	2.44	3.54	2.44	2.44	2.83
Hatiya	3.04	2.64	4.16	3.97	4.82	6.47	5.75	2.64	2.96	2.77	3.06	2.57	3.74
Jessore	2.88	2.95	4.95	8.34	8.34	6.27	6.15	4.95	4.33	3.45	3.32	3.20	4.93
Khepupara	4.20	4.39	3.83	7.09	5.83	4.71	4.14	3.95	3.57	3.70	2.95	2.57	4.24
Khulna	2.96	1.65	3.04	3.05	4.16	3.89	3.31	2.44	2.51	1.98	3.31	2.38	2.89
Kutubdia	1.77	1.82	2.32	2.70	2.77	3.65	3.61	3.14	2.11	1.45	1.19	1.29	2.32
Mongla	1.07	1.25	1.72	2.51	2.92	2.63	2.48	2.35	1.83	1.27	1.02	1.01	2.20
Patenga	6.22	6.34	7.37	7.92	8.47	8.69	9.20	8.54	7.48	6.93	6.71	5.91	7.48
Rangamati	1.45	1.65	4.42	3.10	2.11	3.23	1.72	2.24	1.45	1.45	1.39	1.59	2.15
Sandip	2.32	3.01	3.20	4.83	2.44	3.83	3.39	2.70	2.32	1.63	1.70	1.70	2.76
Sathkhira	4.21	4.40	3.84	7.10	6.11	4.76	4.27	4.03	3.62	3.78	3.54	2.81	4.37
Sylhet	2.20	2.93	3.29	3.17	2.44	2.68	2.44	2.07	1.71	1.95	1.89	1.83	2.38
Teknaf	3.70	4.01	4.39	4.01	3.32	3.89	3.83	2.88	2.44	2.20	1.57	1.76	3.17
Thakurgaon	4.15	5.06	7.93	8.43	8.66	8.05	7.93	6.59	6.34	5.98	5.25	4.76	6.59

A wind turbine, if properly designed and located, can supply enough wind energy. The peak rainfall in Bangladesh occurs during the months of June, July and August. But peak wind speeds are available during the hottest and driest months of March, April and May. During this period wind turbine may be used for water pumping for irrigation, if the water is previously stored in a reservoir during the monsoon season. In these operating seasons, subsoil water from shallow wells can be pumped by low lift pump (LLP) run by wind turbine. From September to February the velocities are not at all promising for harnessing power. One point can be noted that there is wide variation of wind velocity in the coastal areas throughout the year. Patenga, Chittagong, Thakurgaon, Jessore, Khepupara and Satkhira are relatively prospective site for extraction of energy.

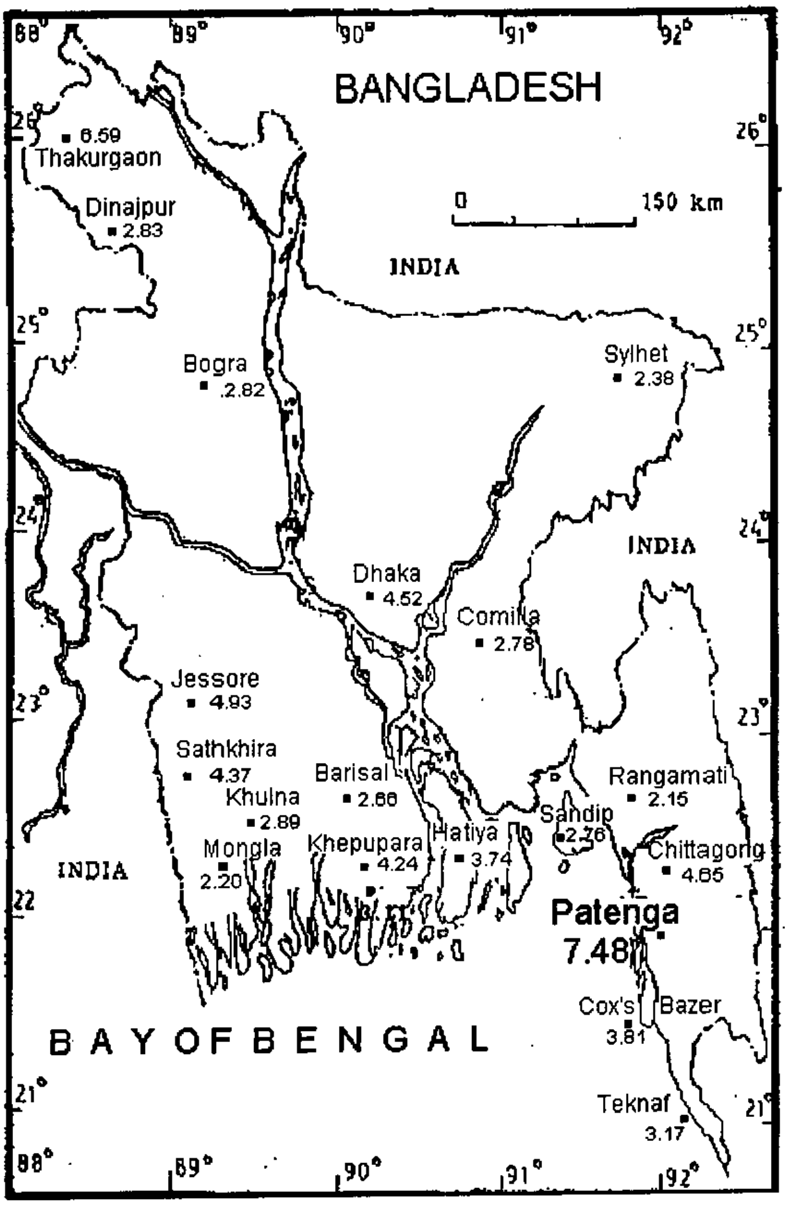

Figure 3.2.2 Map of Bangladesh Showing Annual Average Wind Speed in m/s.

Extractable wind power of an area determines the size and shape of the rotor appropriate to that location. Wind data shown in Table-3.2.4, give an estimation of available wind power. The wind data analyzed here are the average of the data recorded during the period 1981 to 1996 at 20 meters height. In Figure-3.2.2, the annual average wind velocity in different regions of Bangladesh is presented.

The wind power per unit area of approach is proportional to the cube of wind speed [4] and can be expressed as $P/A = 0.6V^3$(watts), where P/A is in W/m^2 and V is in m/s. The available wind power represents the strength of wind and theoretically 59% of this power is extractable but practically only 30-40% can be extracted.

Table-3.2.4: Theoretical Available Power of Different Locations at 20 Meters Height in Bangladesh

Locations	Potential Months For Extracting Wind Power	Average Wind Velocity, V_{av} (m/s)	Theoretical Available Power, $W/m^2=0.6V^3_{av}$
Barisal	April to May	2.66	11.27
Bogra	April to June	2.82	13.40
Chittagong	March to September	4.65	60.49
Comilla	March to September	2.78	12.90
Cox'sBazar	May to August	3.81	33.17
Dhaka	March to October	4.52	55.26
Dinajpur	March to August	2.83	13.55
Hatiya	March to July	3.74	31.29
Jessore	April to September	4.93	71.84
Khepupara	February to September	4.24	45.88
Khulna	April to July	2.89	14.47
Kutubdia	April to August	2.32	7.49
Mongla	May to August	2.20	6.39
Patenga	February to November	7.48	251.11
Rangamati	April to May	2.15	5.97
Sandip	April to July	2.76	12.55
Sathkhira	March to September	4.37	50.16
Sylhet	April to July	2.38	8.13
Teknaf	February to September	3.17	19.06
Thakurgaon	March to August	6.59	172.04

Practically, extractable power by any type of windmill can be written approximately as [4], $P_e = 0.1\ AV^3$ (watt), where A is the total swept area of the rotor blades and V is wind speed (m/s).

Extracted power per square meter of swept area for different months for 20 locations in Bangladesh is shown in Figure 3.2.3. From this figure it can be seen that wind energy can be used in the hottest months i.e., March, April and May for irrigation purposes.

The wind data at other locations also show similar strength of wind energy. The installation of wind power machines at the coastal and island areas will be useful for lifting water and for generation of electricity.

The wind data presented in Table 3.2.3 at 20 m hub-height may be helpful for lifting water, which may solve energy problem in the country to some extent. In most of the areas in Bangladesh, the pumping head is less than 6 m, which is appropriate for using diaphragm pumps and the man-powered pumps. For these pumps, the available wind power in the country can produce good results with a suitable rotor. The use of locally available materials and technology can produce satisfactory wind pumping unit for lifting water.

In coastal areas, island and isolated villages, wind speed is expected to be reasonably sufficient for installing wind plant for electricity. In many areas, the transmission of electricity is either expensive or impossible. The installation of wind plant for generating electricity will be very useful for such areas.

Lack of proper analysis of the wind regime often led to disappointments on the water yields. In Bangladesh, about 30% of total irrigated area is irrigated by hand pumps. So the wind turbine-pumping set may be useful by replacing hand-pumping system for irrigation purposes in rural areas.

In some regions of Bangladesh, the wind speed is satisfactory for operating pumps and for generation of electricity. The wind turbine may also be useful to drive hand pumps used for irrigating agricultural land.

There is a prospective source of wind energy in many places of Bangladesh, namely Patenga, Thakurgaon, Jessore etc. At Patenga, wind speed varies from 5.91 to 9.20 m/s. In Table 3.2.4, it is seen that the average wind speed and theoretical power output per square meter of rotor swept area are 7.48 m/s and 251.11 watts, respectively.

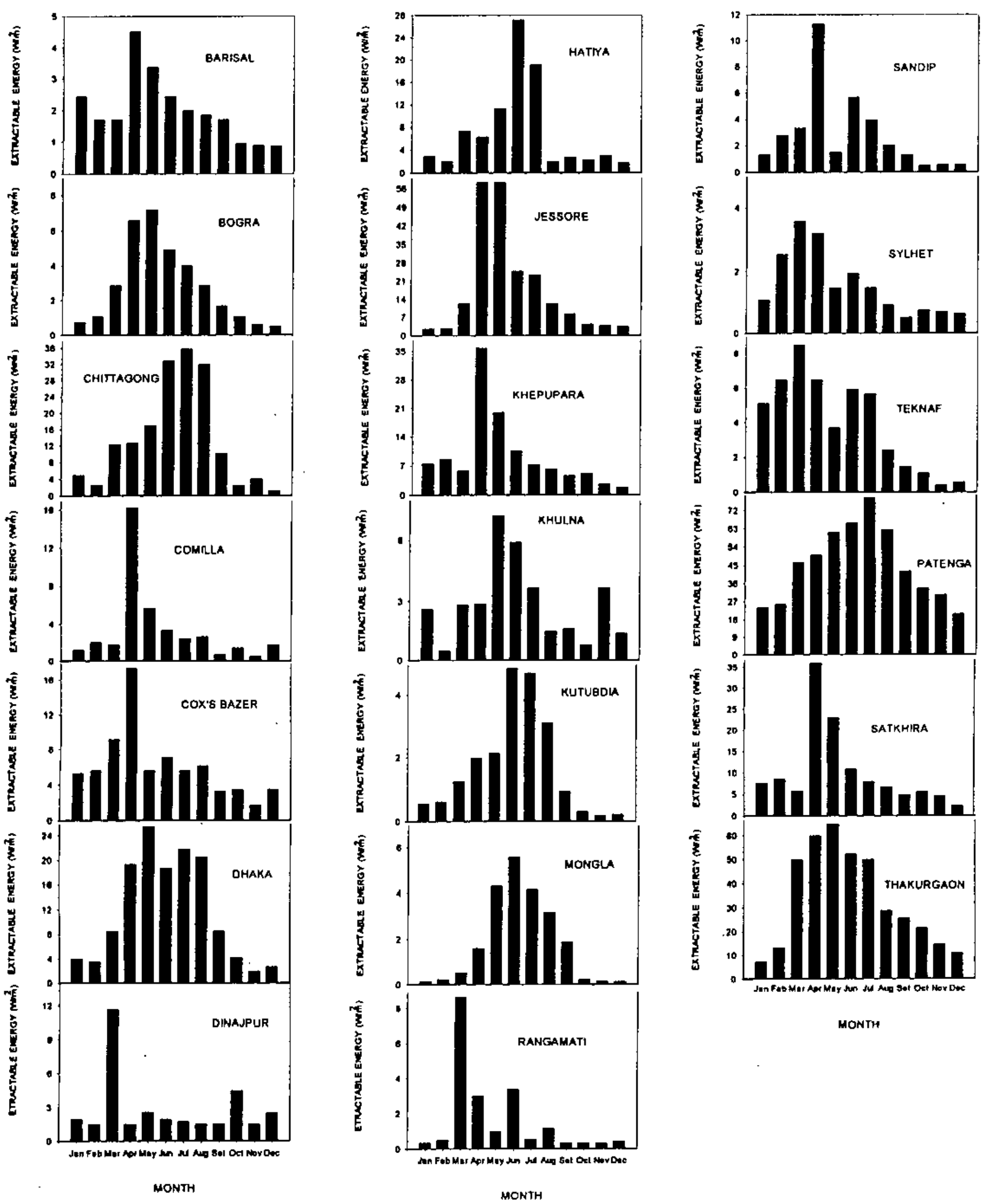

Figure 3.2.3. Monthly Average Extracted Wind Energy at Different Locations

CHAPTER 4

DESIGN AND FABRICATION OF A HORIZONTAL AXIS WIND TURBINE

4.1 Design of the Rotor

The design procedures of a horizontal axis wind turbine in which lift forces on airfoils are the driving forces are described in the following sections. The design of a wind rotor consists of two steps:

- The choice of basic parameters such as the number of blades B, the radius of the rotor R, the type of airfoil and the design tip speed ratio λ_d.
- The calculations of the blade twist angle β_T and the chord C at a number of positions along the blade, in order to produce maximum power at a given tip speed ratio by each section of the blade.

The design procedure is described in the following sections:

4.2 Selection of Design Tip Speed Ratio and Number of Blades

In wind turbine designs, the question arises as to how many blades should be used. In general, as the number of blades increases, so does the cost. Increasing the number of blades results in improved performance and lower torque variations due to wind shear. Furthermore, power output increases but with diminishing return. The choice of λ_d and B is more or less related. For the lower design tip speed ratios a higher number of blades is chosen. This is done because the influence of B on power coefficient C_p is larger at lower tip speed ratio. For higher design tip speed ratio lower number of blades is chosen. Because, higher number of blades for a high design tip speed ratio will lead to very small and thin blades, which results in manufacturing problems. Type of load also limits the choice of the design tip speed ratio. If it is a piston pump or some other slow running load, that in most cases will require a high starting torque, the design speed of the rotor will usually be chosen low. If the load is running fast like a generator or a centrifugal pump, then a high design speed will be selected. The following Table 4.2.1 may be used as the guideline. [30].

Table 4.2.1 Choice of the Design TSR and Selection of Number of Blades

Design tip speed ratio, λ_d	Number of blades, B
1	6 – 20
2	4 – 12
3	3 – 6
4	2 – 4
5–8	2 – 3
8–15	1 – 2

To obtain the optimum configuration the blade is divided into a number of radial stations. Four formulas [15] will be used to describe the information about β_T and C:

Local design speed : $\lambda_r = \lambda_d \dfrac{r}{R}$ (2.1.22)

where, r is the local blade radius and R is the rotor radius and $\lambda_d = R\Omega / V_\infty$ is the tip speed ratio at the design point.

Relation for flow angle : $\lambda_r = \dfrac{\sin\phi(2\cos\phi - 1)}{(1-\cos\phi)(2\cos\phi + 1)}$

or, $\phi = \dfrac{2}{3}\tan^{-1}\dfrac{1}{\lambda_r}$ (2.6.4)

where, ϕ is the angle of relative wind velocity.

Twist angle : $\beta_T = \phi - \alpha$ (2.2.9)

where, α is the angle of attack.

Chord : $C = \dfrac{8\pi r(1-\cos\phi)}{B C_{l_d}}$ (2.6.2)

where, C_{l_d} is the design lift coefficient.

The blade starting torque can be calculated by [5],

$$Q_{S_t} = \frac{1}{2}\rho V_\infty^2 B \int_r^R C(r) C_l [90^0 - \beta_T(r)] r\, dr \quad (4.2.1)$$

where, ρ and V_∞ are the air density and undisturbed wind velocity respectively.

The rotor configuration is determined using the assumption of zero drag and without any tip loss. Each radial element is optimized independently by continuously varying the chord and twist angle to obtain a maximum energy extraction.

4.3 Selection of Airfoil

Power coefficient of the wind turbine is affected by drag coefficient C_d and lift coefficient C_l values of the airfoil sections. For a fast running load a high design tip speed ratio is selected and airfoils with a low C_d / C_l ratio is preferred. But for wind turbines having lower design tip speed ratios the use of more blades compensates the power loss due to drag. So airfoils having higher C_d / C_l ratio are selected to reduce the manufacturing costs.

Drag affects the expected power coefficient via the C_d / C_l ratio. This will influence the size and, even more, the speed ratio of the design. Promising airfoils have minimum C_d / C_l ratio ranges 0.1- 0.01 and the NACA airfoil has the lowest values(Appendix A_1). A large C_d / C_l ratio restricts the design tip speed ratio. At lower tip speed ratios the use of more blades compensates the power loss due to drag. In this collection of maximum power coefficients it is seen that for a range of design speeds $1 \leq \lambda_d \leq 10$ the maximum theoretically attainable power coefficients lie between $0.35 \leq (C_P)_{max} \leq 0.5$.

Due to deviations, however, of the ideal geometry and hub losses for example, these maximums will lie between 0.3 and 0.4. This result shows that the choice of the design tip speed ratio hardly affects the power output.

For different types of airfoils the sensitivity for surface roughness are also different. Using airfoil data of NACA standard roughness in the calculation of wind turbine performance, results losses in peak value of the order of 10- 15% in comparison with the peak value obtained with usual airfoil data for a smooth surface.

4.4 Calculation Steps for Blade Configuration

For calculating the blade geometry the following data must be available beforehand:

Design tip speed ratio, λ_d.

Amount of power to be extracted, P_e.

Design wind velocity, V_d.

Type of airfoil section.

The following steps are to be carried out for getting the blade configurations:

1) A certain number of radial stations for which the chord and blade twist are to be assumed.
2) A tangent from the origin to C_l / C_d graph of airfoil section to locate the minimum value of C_d / C_l are to be drawn. Corresponding to this value find the design angle of attack α_d and design lift coefficient C_{l_d}. This is explained in Appendix A_1.
3) Number of blades B corresponding to the design tip speed ratio λ_d is to be selected.
4) A reasonable value of C_P is to be taken. Estimation of the value of C_P has been explained in Appendix A_4.
5) Calculation of blade radius is done from the equation, $C_P = \dfrac{P_e}{\frac{1}{2}\rho \pi R^2 V_\infty^3}$
6) A fixed value of hub and tip radius ratio, r_{hub} / R is chosen.
7) Calculation of λ_r for each radial station using the equation, $\lambda_r = \lambda_d \, r / R$ is to be done.
8) Determination of ϕ by using the equation, $\phi = \dfrac{2}{3} arc \tan \dfrac{1}{\lambda_r}$ is to be done.
9) The value of chord for each radial station using the equation, $C = \dfrac{8 \pi r}{B C_{l_d}} (1 - \cos\phi)$ is to be found.
10) The value of blade twist is to be calculated using the relation, $\beta_T = \phi - \alpha_d$.

4.5 Selection of Design Parameters

In chapter 3, at Patenga monthly average wind speed varies from 5.91 to 9.20 m/s at 20 meter hub height as shown in Table 3.2.3. In Table 3.2.4, it is seen that the annual average wind speed and theoretical power output per square meter of rotor swept area are 7.48 m/s and 251.11 watts, respectively. It has been observed that during the day times (8 a.m. to 7 p.m.) wind speeds are about 50 % higher than that of during the night times. Although many factors enter in consideration of the Wind Energy Conversion System (WECS), a thumb rule is that a site with an average wind speed of 7- 7.5 m/s will be cost effective with modern wind turbines. So, it can be seen that wind speed in Patenga is suitable for extracting wind energy for water pumping and electricity generation.

In the map of Bangladesh (Figure 3.2.2), the location of Patenga is shown along with the average wind speed (V_α=7.48 m/s). In Bangladesh, the average power needed for a deep tube-well is around 50 kW.

For the design purposes let us consider the airfoil section of NACA 4418 which is generally used for horizontal axis wind turbine blades.

In Appendix A_1, it is given that for airfoil section NACA 44XX, ratio of minimum drag coefficient (C_d) to lift coefficient (C_l) equal to $(C_d/C_l)_{min}$ = 0.01.

Again from Appendix A_2, design lift coefficient, C_{ld} =1.07 and design angle of attack, $\alpha_d = 7^0$

In Appendix A_3, for $(C_d/C_l)_{min}$ = 0.01, maximum power coefficient occurs in the range of design tip speeds ratio, $1 \leq \lambda_d \leq 10$.

For the design purposes, let us consider the design tip speed ratio, $\lambda_d = 6$.

On the basis of $\lambda_d = 6$, from Table 4.2.1, let us consider the number of blades, B = 3.

Considering, $\lambda_d = 6$, B = 3 and $(C_d/C_l)_{min}$ = 0.01, from Appendix A_4, we choose maximum power coefficient, $(C_p)_{max} = 0.5$.

For conservative design, $C_p = (C_p)_{max} \times 0.8 = 0.5 \times 0.8 = 0.4$

From the section 4.4 and step 5, the equation is rewritten as.

$$Rotor\ Radius, R = \sqrt{\frac{2P_e}{\pi \rho V_\alpha^3 C_P}}$$

Now putting the given values, the rotor radius is obtained as 12.50 m. Density of wind is considered as 1.225 kg/m^3. Based on these data, model rotor radius is calculated as 220 mm.

4.6 Calculation of Blade Chord and Blade Setting Angles

For selecting the blade chord and blade setting angles, the design procedure is as follows:

Divide the blade along the radius in 10 cross sections of equal length. Each cross section has a distance r from the rotor center. Local speed ratio 'λ_r', flow angle ' ϕ ', blade setting angle ' β_T' and chord 'C' for each sections are calculated by using the equations stated in the section 4.4, steps 7, 8, 9 and 10. The values are shown in the Table 4.6.1.

Table 4.6.1 Ideal Blade Sections, Local TSR, Angle of Attack, Blade Setting Angle and Chord

Cross section number	R (mm)	λ_r	ϕ^0	α^0	β_T^0	C (mm)
1	22	0.6	39.36	7	32.36	39.07
2	44	1.2	26.54	7	19.54	33.30
3	66	1.8	19.37	7	12.37	28.25
4	88	2.4	15.08	7	8.08	23.73
5	110	3.0	12.29	7	5.30	19.74
6	132	3.6	10.35	7	3.35	16.82
7	154	4.2	8.93	7	1.93	14.62
8	176	4.8	7.85	7	0.85	12.91
9	198	5.4	6.99	7	-0.01	11.56
10	220	6.0	6.31	7	-0.69	10.43

4.7 Deviations from the Ideal Blade Form

In the previous section it has been discussed how to calculate the ideal blades form. The chords as well as the blade twist vary in a non-linear manner along the blade. Such blades are usually difficult to manufacture and may not have structural integrity. In order to reduce these problems it is possible to linearize the chords and the twist angles. This results in a small loss of power. If the linearization is done properly the loss becomes only a few percent. In considering such linearization, it must be realized that the outer half of the blades extract about 75% of the power that is extracted by the rotor blades from the wind. Because the blade swept area varies with the square of the radius and the efficiency of the blades is less at smaller radii, where the tip speed ratio λ_r is small. On the other hand, at the tip of the blade the efficiency is low due to the tip losses. For the reasons mentioned above it is advised to linearize the chord C and the blade setting angles β_T between r = 0.5R and r = 0.9R [25]. The equations for linearized chord and twist can be written in the following way,

$$C = C_1 r + C_2 \tag{4.7.1}$$

$$\beta_T = C_3 r + C_4 \tag{4.7.2}$$

where, C_1, C_2, C_3 and C_4 are the constants. With the value of C and β_T at 0.5R and 0.9R from the ideal blade form the values of C_1, C_2, C_3 and C_4 can be obtained. The ultimate expressions for chord and twist of linearized blade can be written as,

$$C = 2.5(C_{90} - C_{50})\frac{r}{R} + 2.25C_{50} - 1.25C_{90} \tag{4.7.3}$$

$$\beta_T = 2.5(\beta_{90} - \beta_{50})\frac{r}{R} + 2.25\beta_{50} - 1.25\beta_{90} \tag{4.7.4}$$

where,

C_{50} = chord of the ideal blade form at 0.5R

C_{90} = chord of the ideal blade form at 0.9R

β_{50} = twist angle of the ideal blade form at 0.5R

β_{90} = twist angle of the ideal blade form at 0.9R

A further simplification of the blade shape consists of omitting the twist altogether. Introduction of a rotor blade without twist results in a power loss penalty of about 6 to 10% [54]. This might be acceptable for a single production unit but loses its attraction in case of mass production. When the main purpose is the design of a cheap wind turbine, an untwisted blade with a constant chord seems to be a good choice with only limited power losses.

Ideal blade form was linearized by using the equations (4.7.1), (4.7.2), (4.7.3) and (4.7.4) and shown in Table 4.7.1. Figure 4.7.1 and Figure 4.7.2 show the distribution of chord and blade twist angles for two types of blades. From these figures it is found that the changes in chords and twist angles are very small at the outer half of the blade.

Large variations with the linear chord and twist distributions are found only at the lower radius of the blade.

Table 4.7.1 Linearized Blade Cross Sections, Local TSR, Blade Setting Angle and Chord

Cross section number	r (mm)	λ_r	ϕ^0	α^0	$\beta_T^{\,0}$	C (mm)
1	22	0.6	17.58	7	10.58	28.00
2	44	1.2	16.26	7	9.26	26.01
3	66	1.8	14.94	7	7.94	24.03
4	88	2.4	13.62	7	6.62	22.05
5	110	3.0	12.30	7	5.30	19.74
6	132	3.6	10.98	7	3.98	18.09
7	154	4.2	9.66	7	2.66	16.11
8	176	4.8	8.34	7	1.34	14.13
9	198	5.4	7	7	0	11.56
10	220	6.0	7	7	0	10.17

Thus, the Design values for the model are as follows:

Blade airfoil type	: NACA 4418
Rotor radius	: 220 mm
Root chord length	: 28 mm
Tip chord length	: 10.17 mm
Root twist angle	: 10.58^0
Tip twist angle	: 0^0
Hub radius	: 22 mm
Number of Blades	: 2, 3 and 4 were used

Experiments were carried out with three rotors having 2, 3 and 4 blades. The schematic diagram of the rotor is shown in Figure 4.7.3.

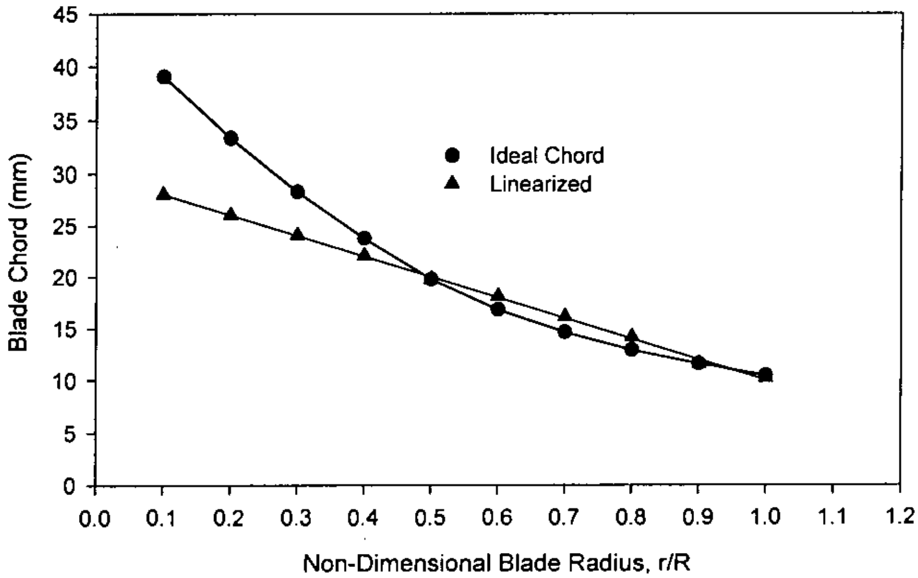

Figure 4.7.1 Optimum and Linearized Balde Chord Distribution

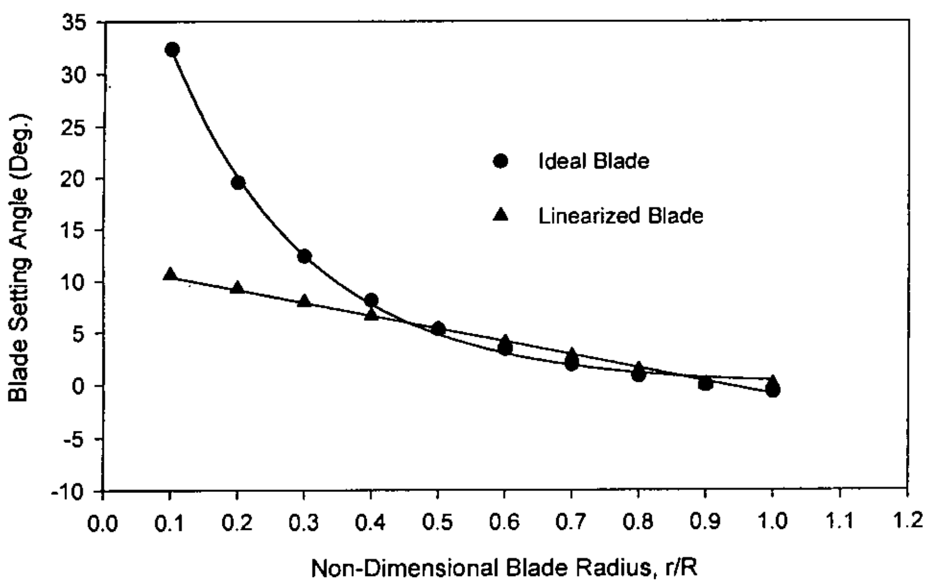

Figure 4.7.2 Optimum and Linearized Balde Twist Distribution

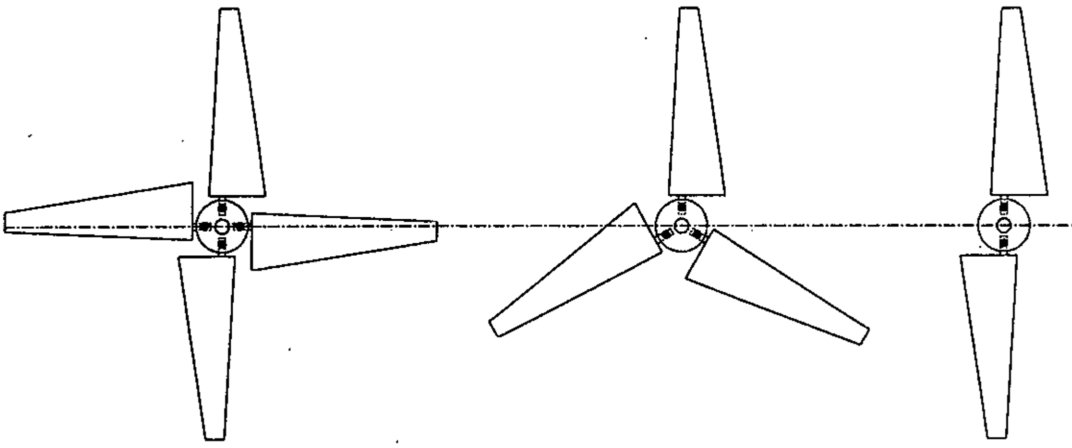

Figure 4.7.3 Schematic Diagram of the Rotors

4.8 Choice of Rotor Blade Material

Different blade materials can be used for rotor construction. Some have been tested by Peter Garman [13]:

(i) solid aluminium alloy;

(ii) laminated hardwood sheathed with glass fiber reinforced plastic (GRP);

(iii) steel spar with polyurethane foam filled GRP fairing;

(iv) untreated hardwood;

(v) ferrocement (a) untreated, (b) painted, (c) sheathed with Al alloy sheet;

(vi) steel spar, timber fairing sheathed with Al alloy sheet.

Blade surface finish is critical from the performance point of view and any deterioration causes drastic shaft power reduction. So drag produced by the blade surface friction is very important [13]. In this consideration, Al-alloy maintains its surface highly finished and hence, high level of performance can be maintained. For this reason, Al-blades are used to fabricate the model.

CHAPTER 5

EXPERIMENTAL SET-UP AND PERFORMANCE ANALYSIS

5.1 The Wind Tunnel

The rotor model has been tested in the wind tunnel in order to predict the performance of actual wind turbine. The experimental results obtained from the wind tunnel test were compared with the theoretical results.

The open circuit subsonic wind tunnel was 6.55 m long with a test section of (490mmx490mm) cross-section. The wind tunnel with a model wind turbine having 4-blades has been depicts in Figure 5.1.1. The successive sections of the wind tunnel comprised of a converging entry, a perspex section, a rectangular section, a fan section (two rotary axial flow fans), a butterfly valve section, a silencer with honey comb section, a diverging section, a converging section and an exit flow straightener section. The central longitudinal axis of the wind tunnel was maintained at a constant height from the floor. The converging mouth entry was incorporated into the system for easy entry of air into the tunnel and maintain uniform flow into the duct free from outside disturbances. The induced flow through the wind tunnel was produced by a two-stage rotating axial flow fan of capacity 30,000 cfm at the head of 152.4 mm of water and 1475 rpm. A butterfly valve, actuated by a screw thread mechanism, was placed behind the fan and was used to control the flow. A silencer was fitted at the end of the flow controlling section in order to reduce the noise of the system. The diverging and converging section of the wind tunnel was 460mm long and made of 16 SWG black sheets. The angle of divergence and convergence was 7°, which was done with a view to minimizing expansion and contraction loss and to reduce the possibility of flow separation. Other three outlet square (610mm each) sections were used to make the flow straight and uniform.

5.2 Experimental Procedure

The experiment was carried out in the open circuit subsonic wind tunnel with an outlet test section of (490 mm x 490 mm) cross-section as shown in Figure 5.1.1. The central longitudinal axis of the wind tunnel was maintained at a constant height of 990 mm from the floor. Average wind tunnel air velocity was measured directly by an electrical anemometer, which was placed in front of the rotor at different locations and average velocity was measured directly. Non-contact electrical tachometer was used to measure the speed of the model wind turbine at different loadings.

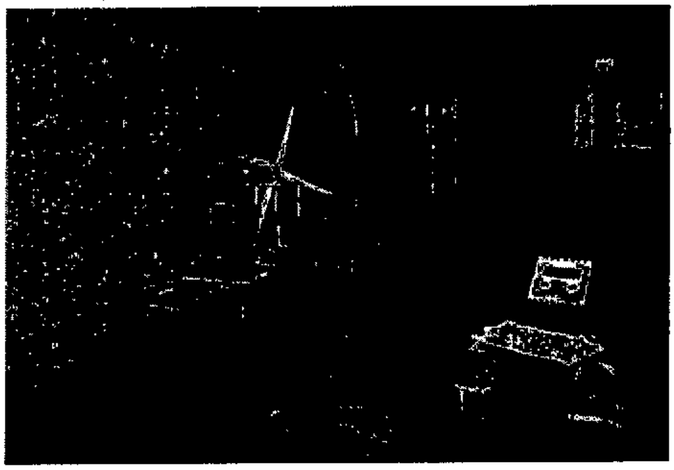

Figure 5.1.1 Wind Tunnel with a Model Wind Turbine having 4-Blades

The hub has been design to provide with zero coning angle and permitted changing of blade pitch setting several degrees above and below the nominal setting angle. The hub and the blades were made from plastic and aluminium, respectively.

The model rotor assembly was mounted on a movable frame structure (580 mm x 410 mm x 990 mm) and was placed in front of the wind tunnel. The height of the frame structure was equal to that of the wind tunnel bottom in order to avoid blockage of airflow from the wind tunnel.

Prior to the commencement of the test, a strain gauge was calibrated by dead weight method. The calibration factors obtained from the loading tests were used to convert the transducer reading into engineering unit. The strain gauge was fixed on the bottom side of a stainless steel plate in order to respond on bending moment as shown in Figure 5.2.1.

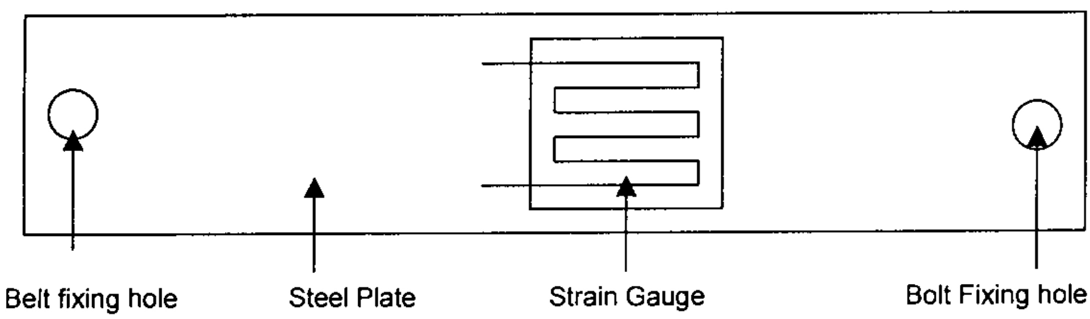

Figure 5.2.1 Steel plate with Strain Gauge, Model-TML, YL 10

One end of the plate was fixed on the top of the frame by nut and bolts and a cotton belt passing over the pulley was fastened at the free end. A small pan was hanged at the other end of the cotton belt. Two wires from the strain gauge were connected to the transducer and the outputs were recorded.

5.3 Performance Analysis

5.3.1 Comparison of the results with theoretical and earlier experimental data

Comparison of earlier experimental and theoretical results with present theoretical results has been done for MOD-1 wind turbine. Schematic diagram of the MOD-1 wind turbine is presented in the Figure 5.3.1. The performance of MOD-1 wind turbine in terms of C_p versus λ is shown in Figures 5.3.2 to 5.3.5. The MOD-1 is a two bladed 61 meters diameter wind turbine, which uses a NACA 44XX profile for its blade. Rated power of 2000 kW is produced at the tip speed ratio of 10. From these figures it can be seen that there is a closer correlation among the values predicted by the present method and those calculated by references [38] and [24], although the present calculation and reference [24] are done by using NACA 4418 airfoil data. Here the 'Present Method' means computer program used for the theoretical comparison.

5.3.2 Theoretical Results of Designed 50 kW wind turbine

The effect of pitch angle on calculated power, thrust and torque coefficients versus tip speed ratio can be seen in Figures 5.3.6 to 5.3.8. Increasing pitch angle reduces the maximum availability at low tip speed ratios. Figures 5.3.6 can also be used to illustrate some generalizations concerning wind machine. At low tip speed ratios, the power coefficient is strongly influenced by the maximum lift coefficient. The angle ϕ is large at low tip speed ratios and much of the rotor, particularly the inboard stations, can be stalled when operating below design speed. At tip speed ratios above the peak power coefficient, effect of drag becomes dominant. A high drag coefficient will result in a rapid decrease in power and at some large tip speed ratios the net power output will become zero. The power curve is sensitive mainly to blade pitch angle in the stalling region. To avoid too much drop off of the power after stalling point a blade pitch angle of 2^0 and 4^0 are seem to be more convenient than the performance at 0^0 pitch angle. Increase of the pitch angle shows the shifting of maximum power coefficients to the smaller values of tip speed ratios. From Figure 5.3.7 it is found that rotor thrust coefficient increases continuously with tip speed

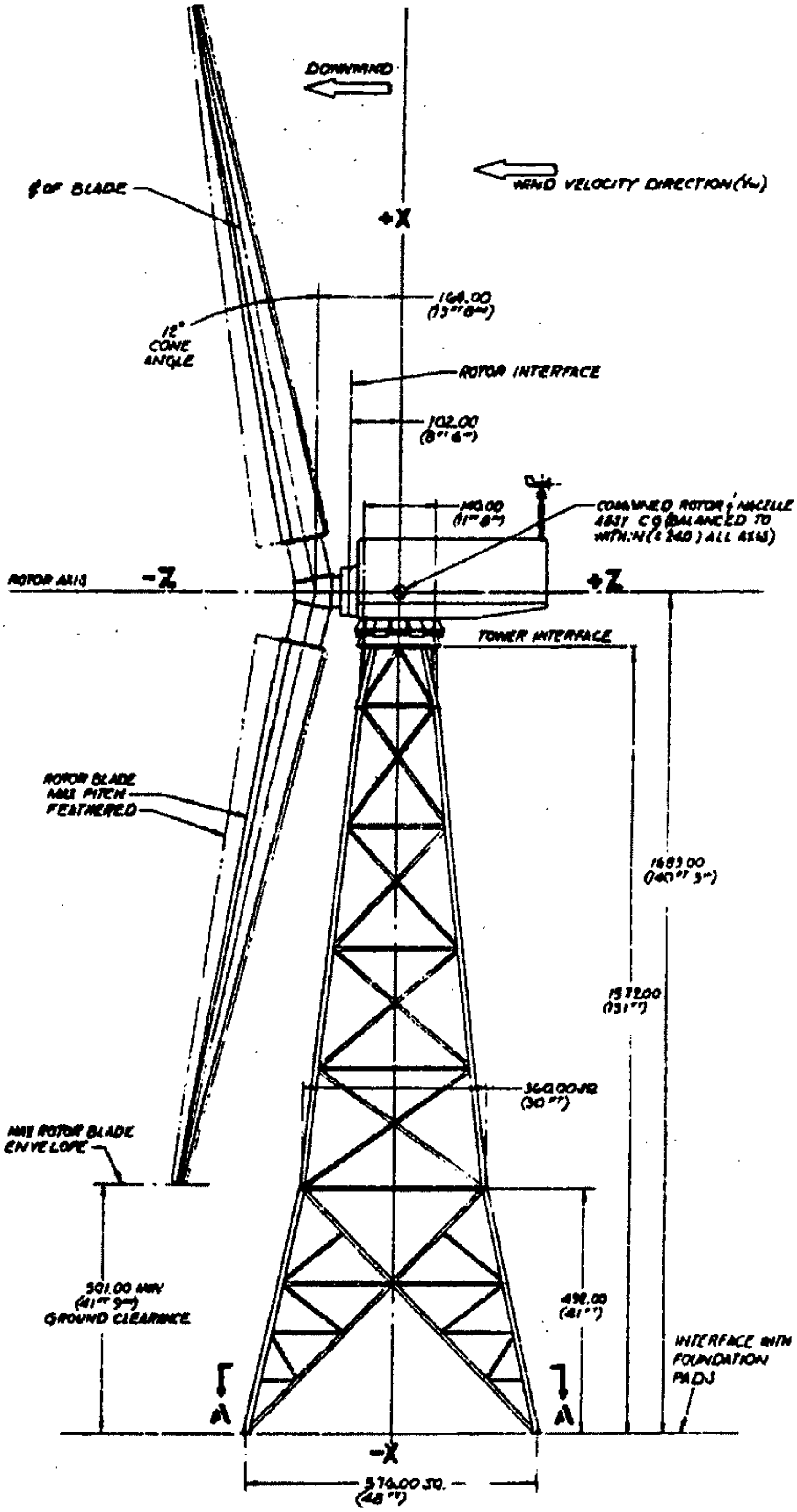

Figure 5.3.1 MOD-1 2000 kW Wind Turbine

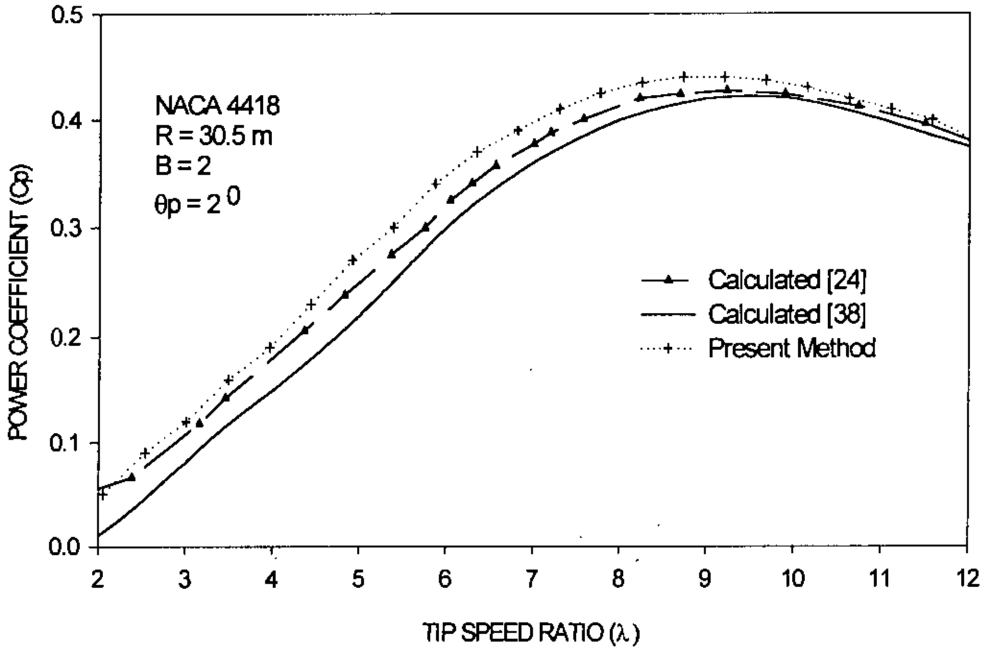

Figure 5.3.2 Performance Curves of MOD-1 Wind Turbine

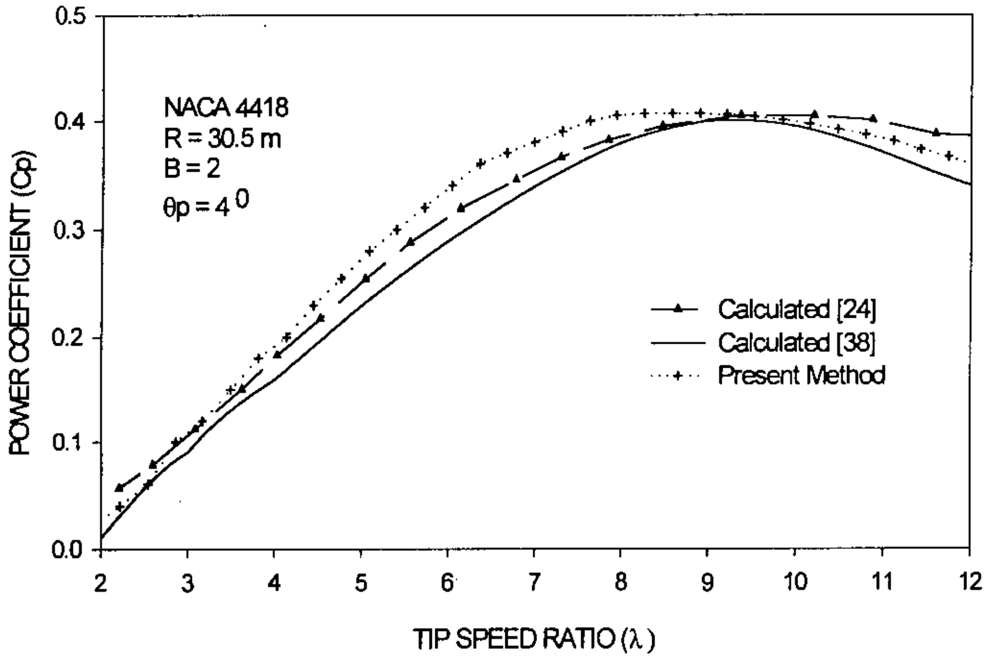

Figure 5.3.3 Performance Curves of MOD-1 Wind Turbine

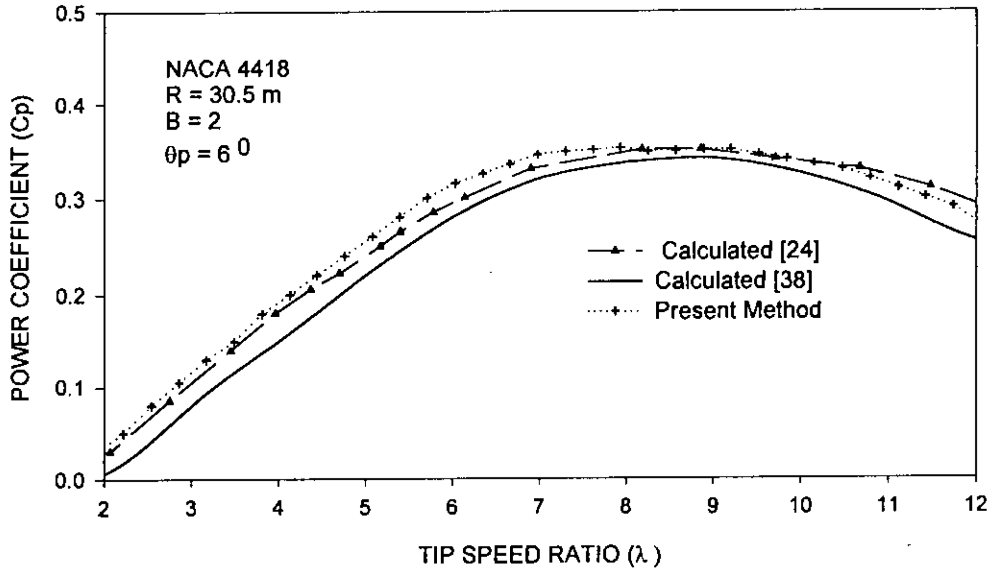

Figure 5.3.4 Performance Curves of MOD-1 Wind Turbine

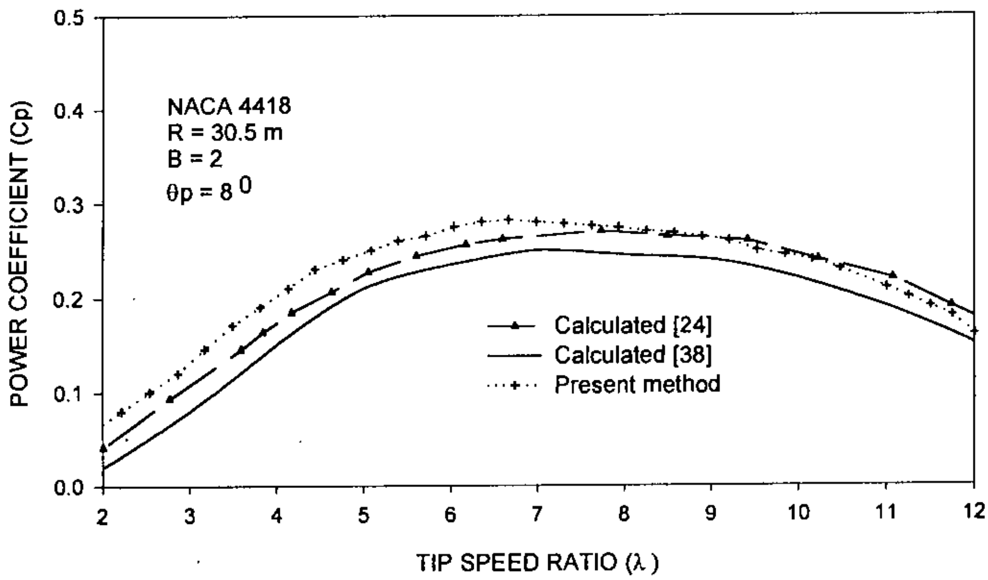

Figure 5.3.5 Performance Curves of MOD-1 Wind Turbine

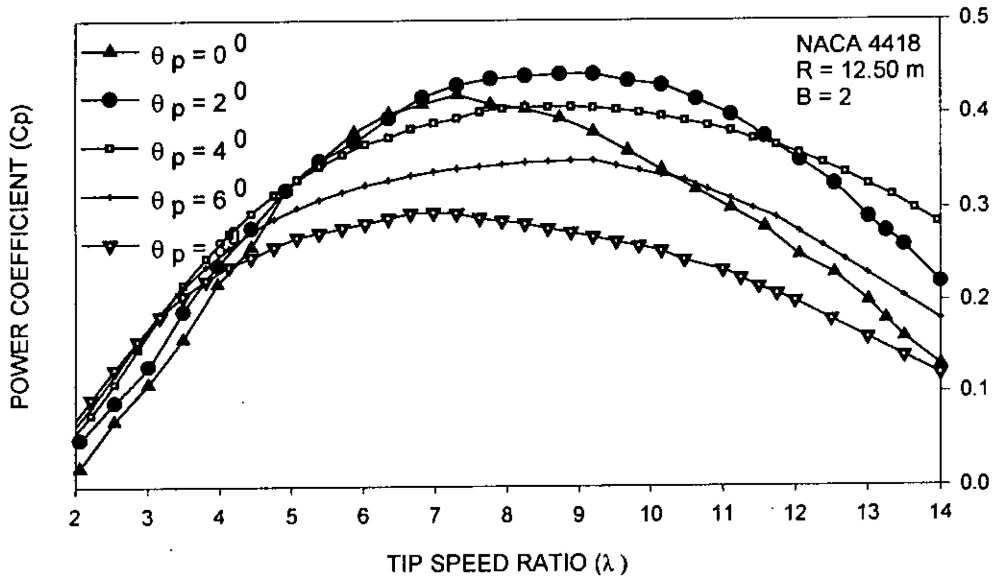

Figure 5.3.6 Effect of Pitching on Power Coefficient (C_p) of 50 kW Wind Turbine

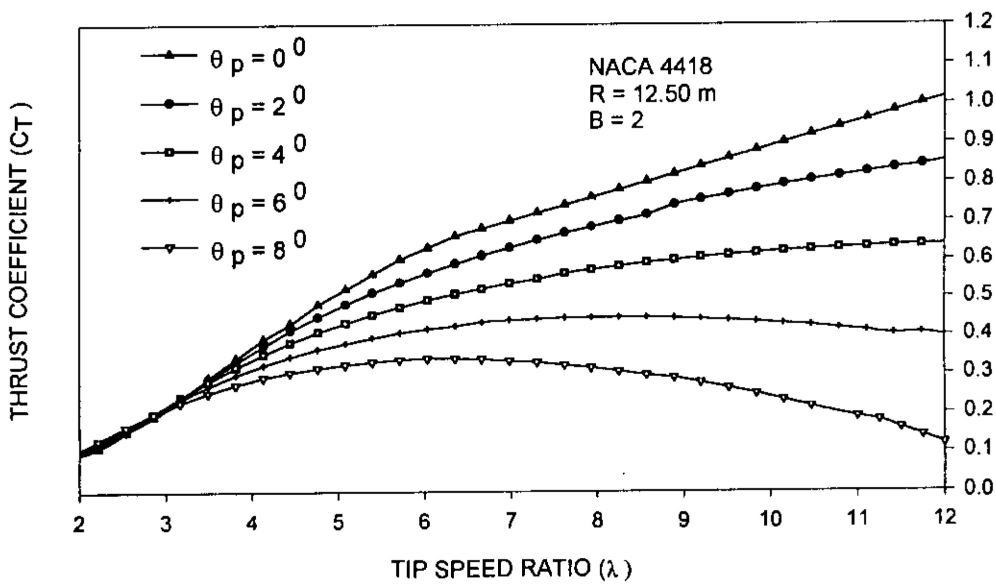

Figure 5.3.7 Effect of Pitching on Thrust Coefficient(C_T) of 50 kW Wind Turbine

ratio and that the values greater than unity can be achieved. At high tip speed ratios it is possible to achieve velocities through the turbine that are less than half the free stream velocity. This implies that the velocity in the fully developed wake has reversed direction and flows back towards the turbine. The flow reversal induces a vortex flow in the wake, which violates a basic assumption for the blade element theory. The theoretical performance prediction in this condition by the present method is not acceptable. With the increase of blade pitch angle the values of induced velocity factor close to or lower than 0.5, which means a more reliable solution.

The variation of torque coefficient with tip speed ratio is shown in Figure 5.3.8. With the increase of blade pitch angle the maximum value of torque coefficient moves toward the lower values tip speed ratio. By changing the blade pitch angle means that the resulting angle of attack is reduced and lift coefficient is shifted from stalling region. The pitch of the blade provides higher torque coefficient at lower tip speed ratios.

Figure 5.3.9 is a plot of power versus wind velocity for constant power and Figure 5.3.10 shows the pitch angle variation versus the wind velocity for maintaining different constant powers. Among the four curves, one is for rated power, one is for 20% lower and other two are 20% and 40% higher values of the rated power.

Radial distribution of power, thrust and torque are shown in Figures 5.3.11 to 5.3.13. It is noted that about 75 % of power, the outer 50% radius produces thrust and torque. This is because the blade swept area varies with the square of the radius and also the efficiency of the blades is less at small radius, where the speed ratio λ_r is small. On the other hand, due to the tip losses there is a decrease of power, thrust and torque near the tip of the blade.

5.3.3 Comparison of theoretical and experimental results for model wind turbine

Experimental results have been compared to different wind turbine models consisting of 2-blades, 3-blades and 4-blades respectively, and are shown in Figures 5.3.14 to 5.3.16.

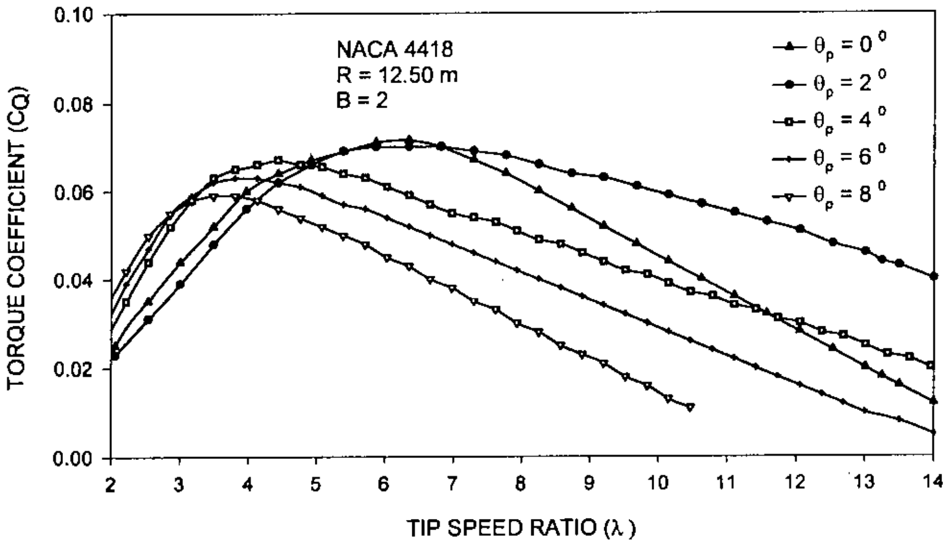

Figure 5.3.8 Effect of Pitching on Torque Coefficient (C_Q) of 50 kW Wind Turbine

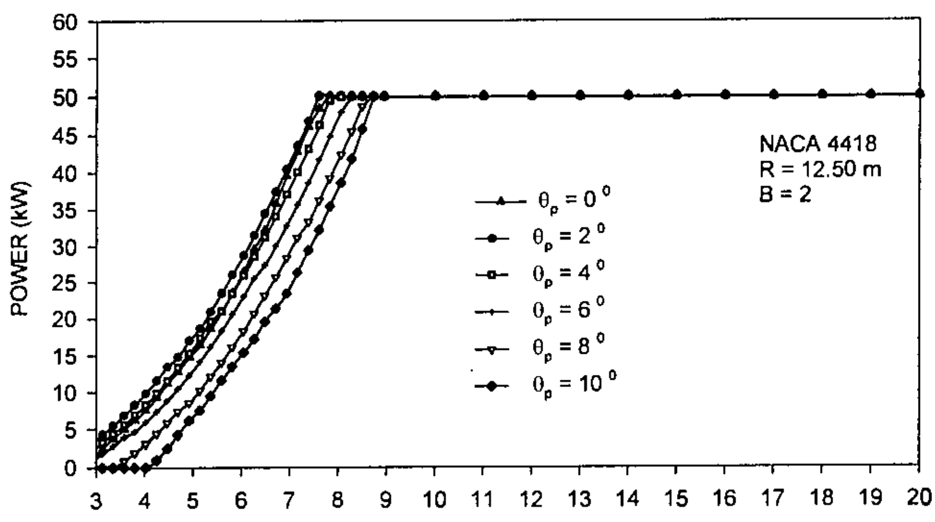

Figure 5.3.9 Power Versus Wind Velocity for Constant Power (50 kW)

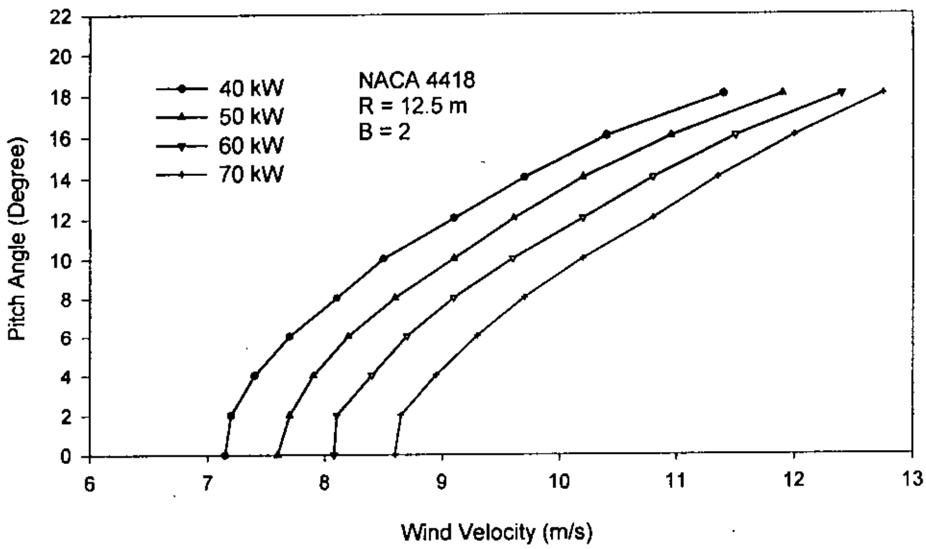

Figure 5.3.10 Pitch Regulation for Constant Power

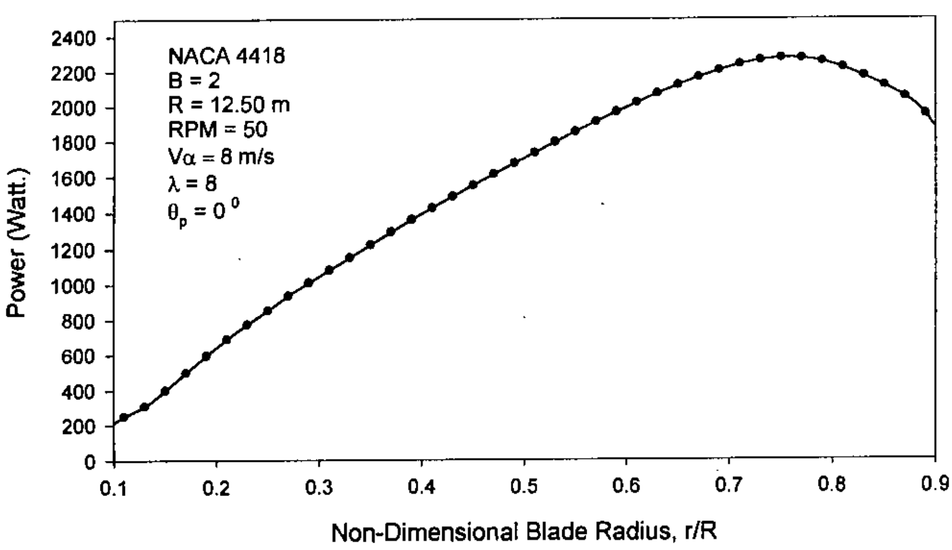

Figure 5.3.11 Radial Variation of Extracted Power

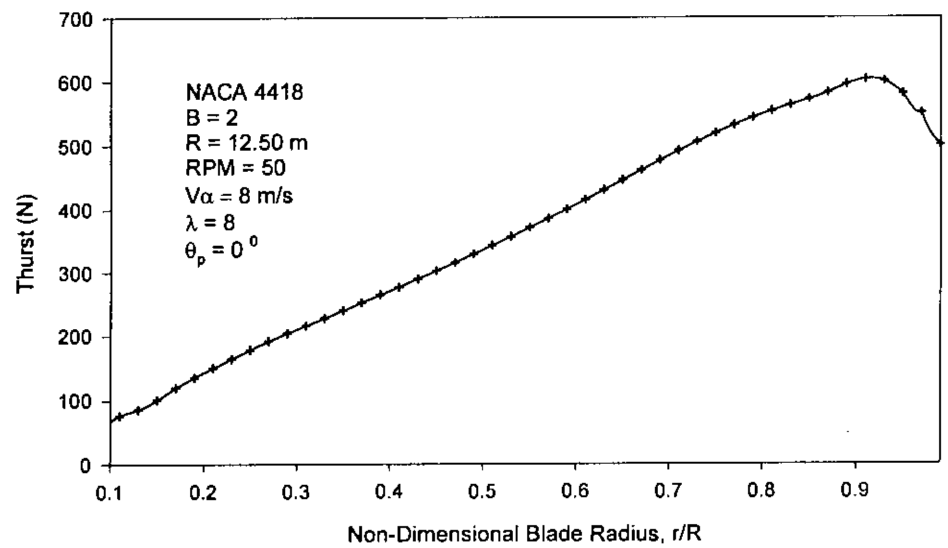

Figure 5.3.12 Radial Variation of Thrust Force

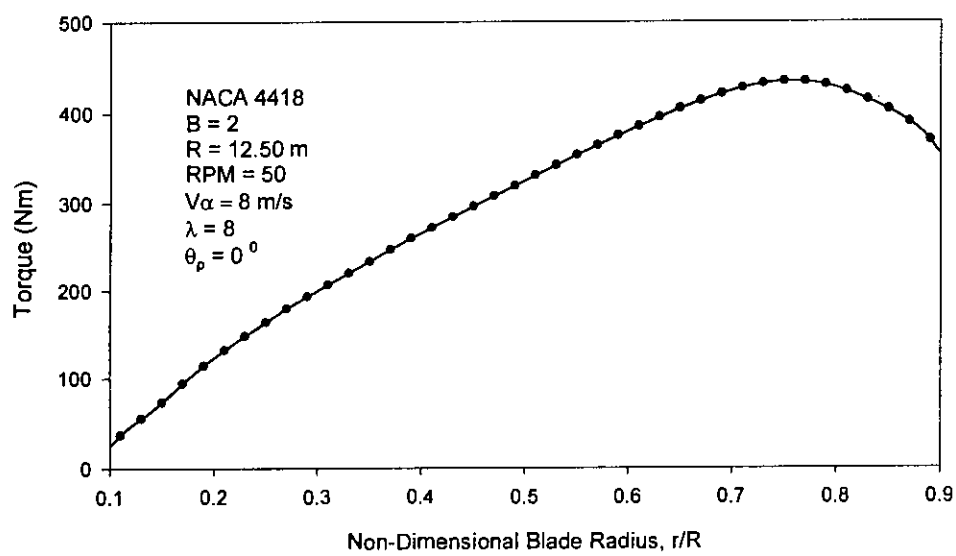

Figure 5.3.13 Radial Variation of Torque

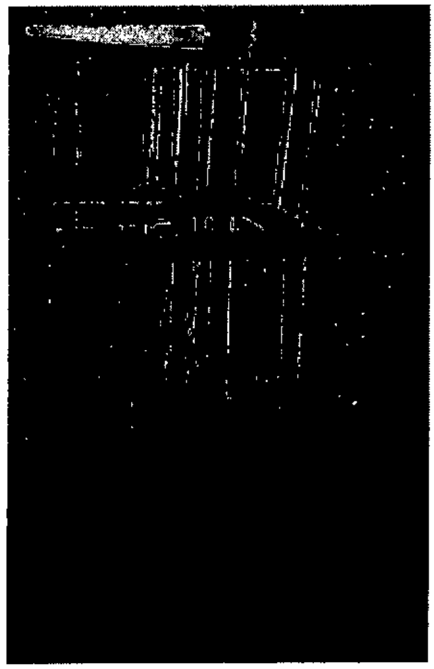

Figure 5.3.14 Two-Blades Wind Turbine Model

The wind turbine model performance in terms of C_p versus λ and C_Q versus λ are shown in Figures 5.3.17 to 5.3.18 for 2-blades. Rated power of 50 kW for actual turbine is produced at the tip speed ratio of about 6 and maximum power coefficient is obtained at 2^0 blade pitch angle. Figures 5.3.19 to 5.3.28, which show performances at different pitch angle, it is seen that there is a closer correlation between the values predicted by the present method and those obtained from the wind turbine model experiments.

The performance of wind turbine model in terms of C_p versus λ and C_Q versus λ having three blades are shown in Figures 5.3.29 to 5.3.30. Maximum power coefficient is obtained at 2^0 blade pitch angles at rated power and the tip speed ratio is about 6. From Figures 5.3.31 to 5.3.40, it is seen that there are good agreement between the values predicted by the present method and those calculated by the wind turbine model.

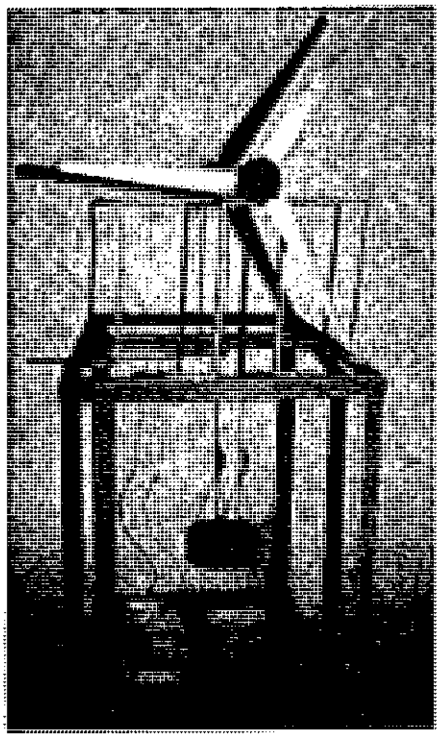

Figure 5.3.15 Three-Blades Wind Turbine Model

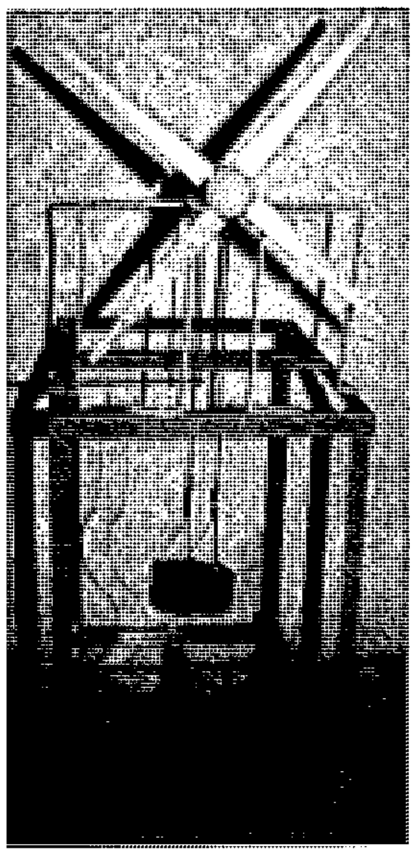

Figure 5.3.16 Four-Blades Wind Turbine Model

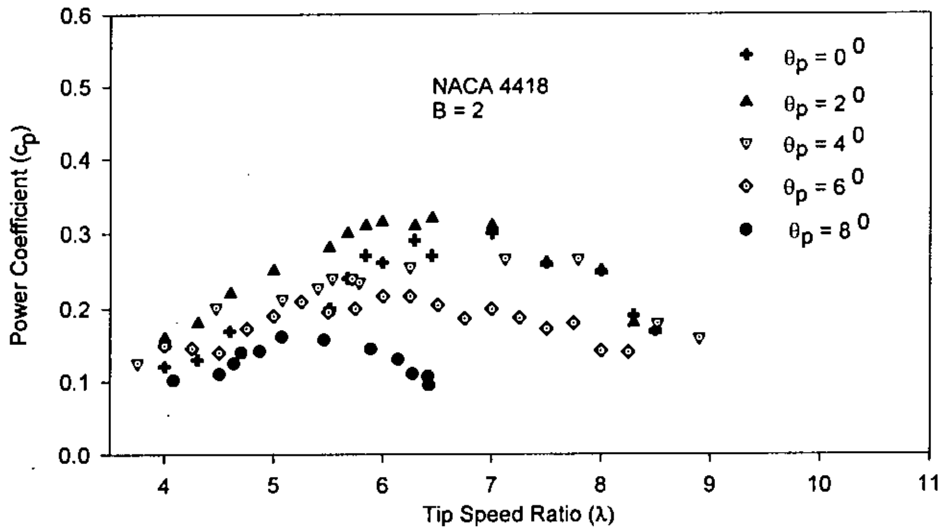

Figure 5.3.17 Power Coefficient (C_p) VS Tip Speed Ratio (λ)

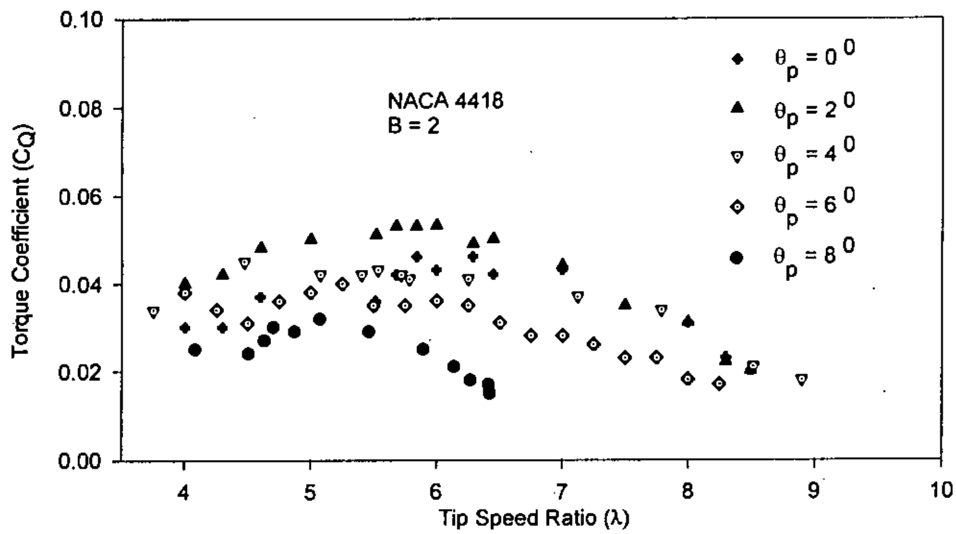

Figure 5. 3.18 Torque Coefficient (C_Q) VS Tip Speed Ratio (λ)

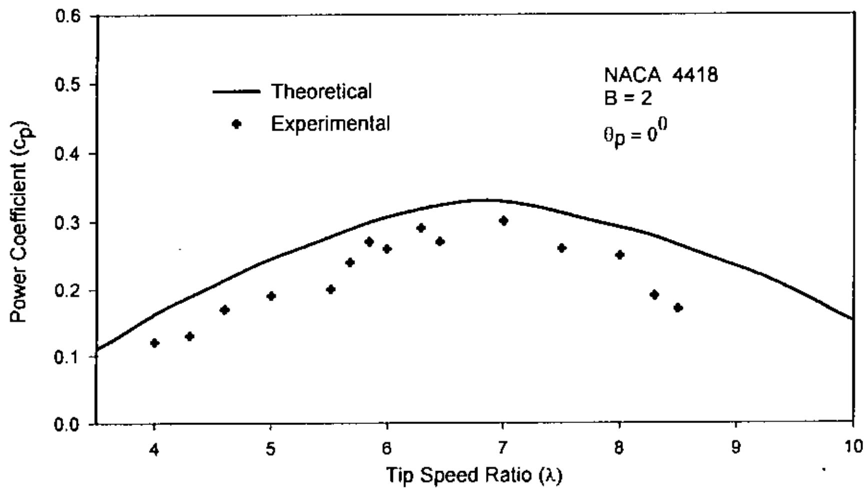

Figure 5.3.19 Power Coefficient (C_p) VS Tip Speed Ratio (λ)

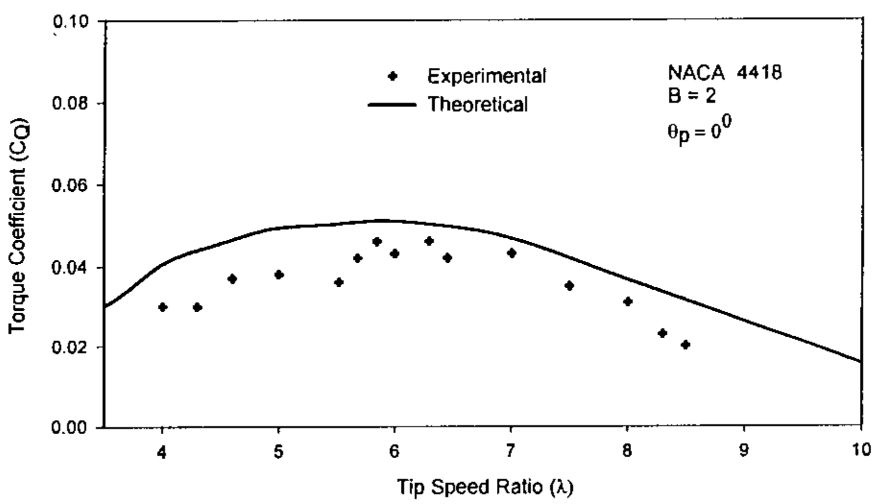

Figure 5.3.20 Torque Coefficient (C_Q) VS Tip Speed Ratio (λ)

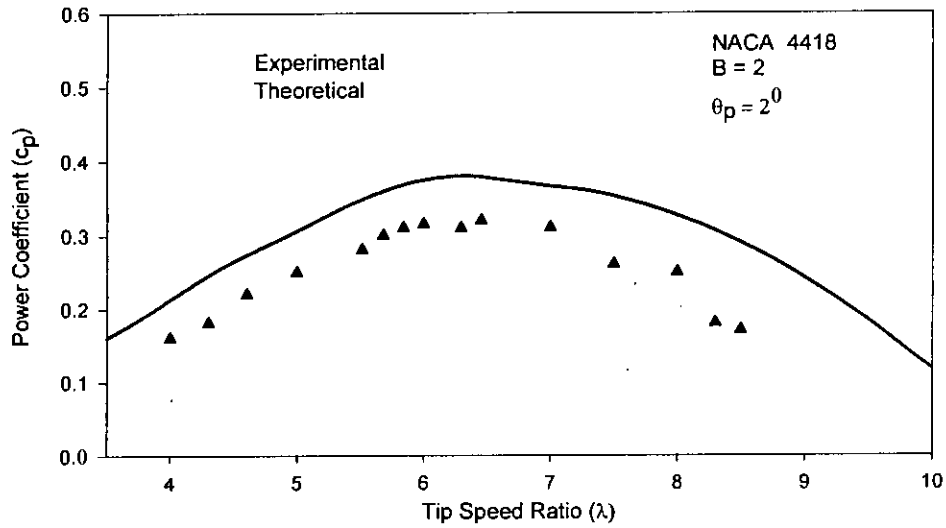

Figure 5.3.21 Power Coefficient (C_p) VS Tip Speed Ratio (λ)

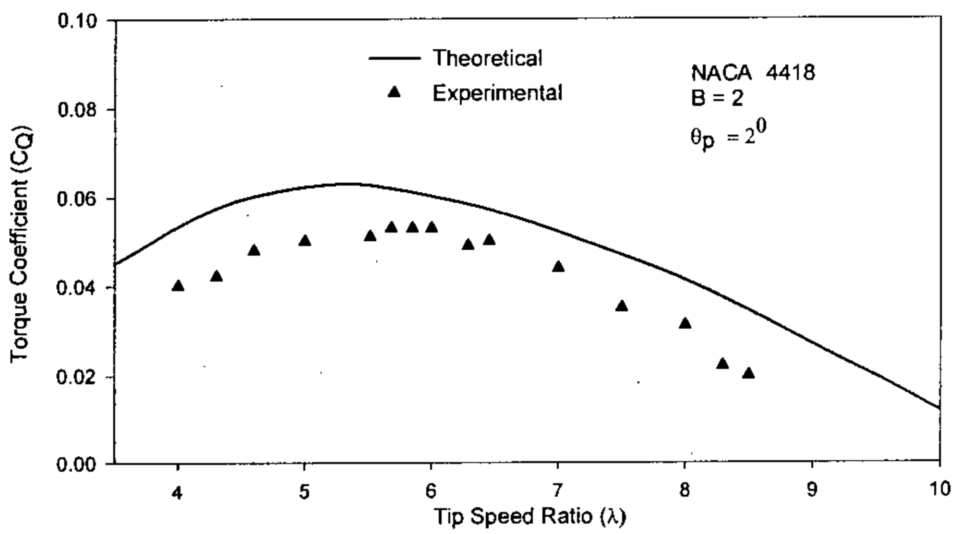

Figure 5.3.22 Torque Coefficient (C_Q) VS Tip Speed Ratio (λ)

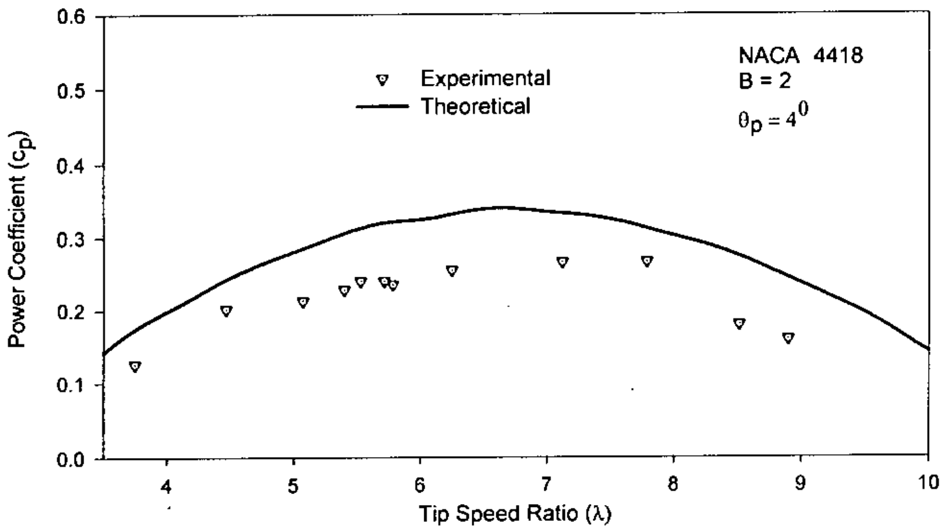

Figure 5.3.23 Power Coefficient (C_p) VS Tip Speed Ratio (λ)

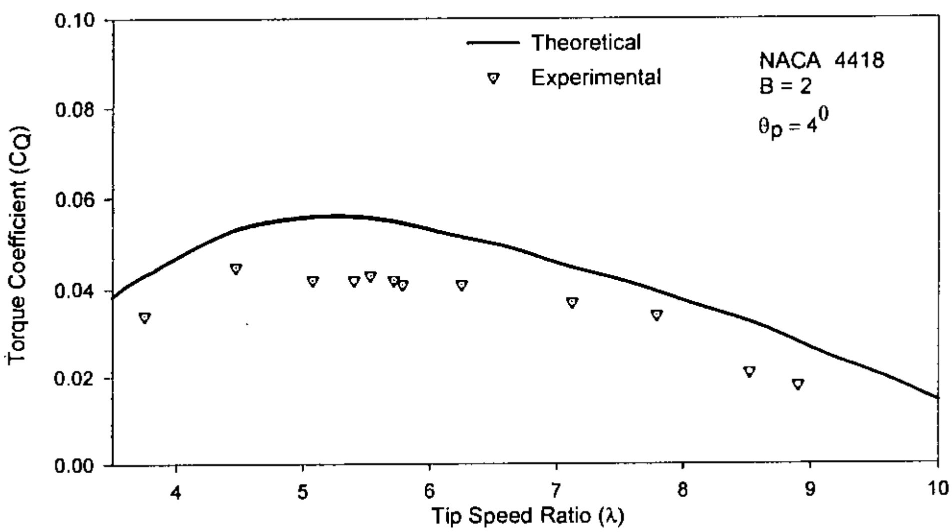

Figure 5.3.24 Torque Coefficient (C_Q) VS Tip Speed Ratio (λ)

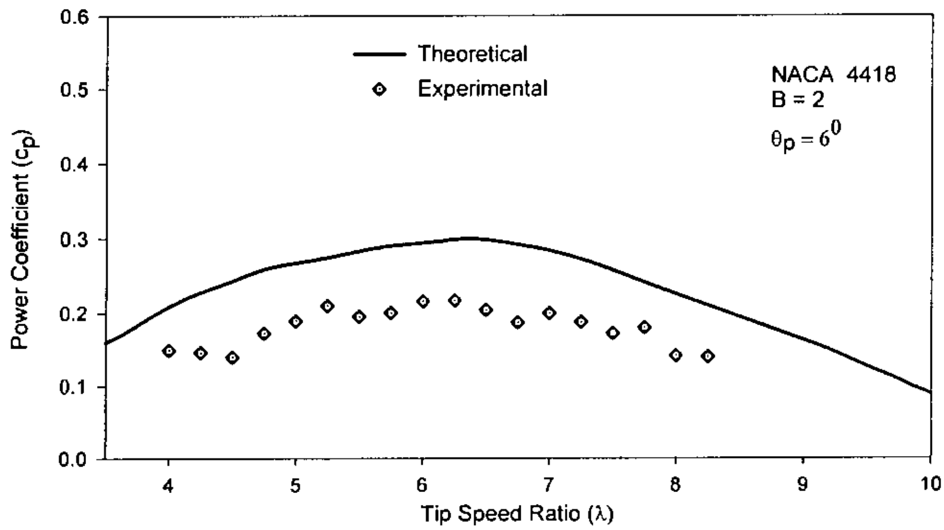

Figure 5.3.25 Power Coefficient (C_p) VS Tip Speed Ratio (λ)

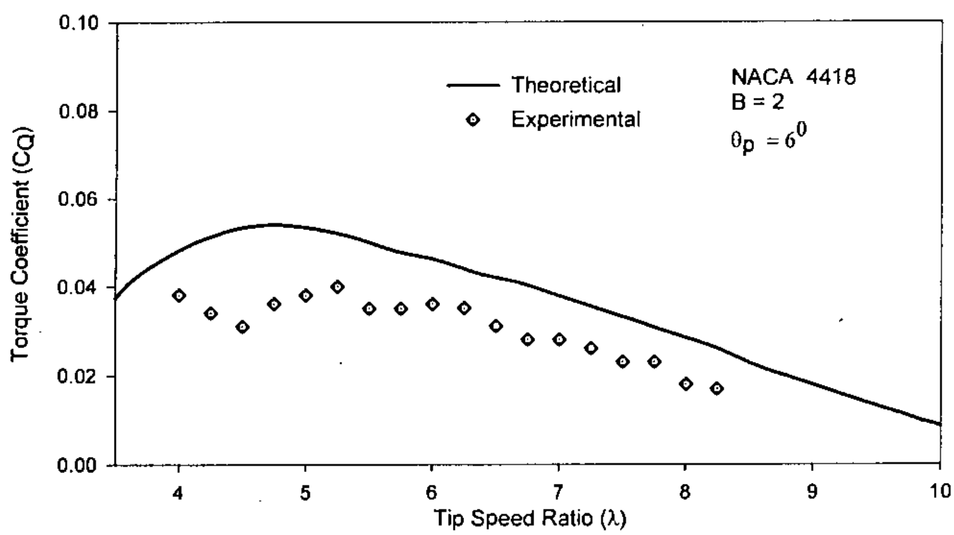

Figure 5.3.26 Torque Coefficient (C_Q) VS Tip Speed Ratio (λ)

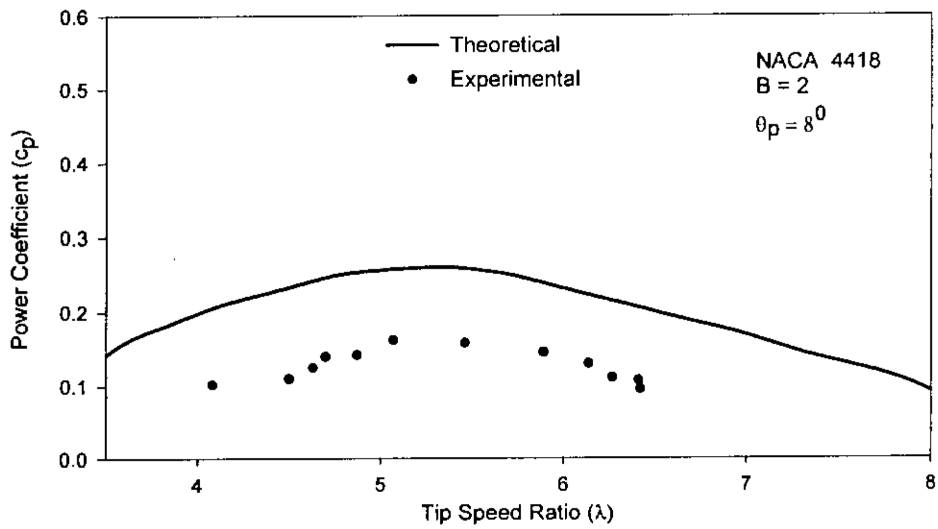

Figure 5.3.27 Power Coefficient (C_p) VS Tip Speed Ratio (λ)

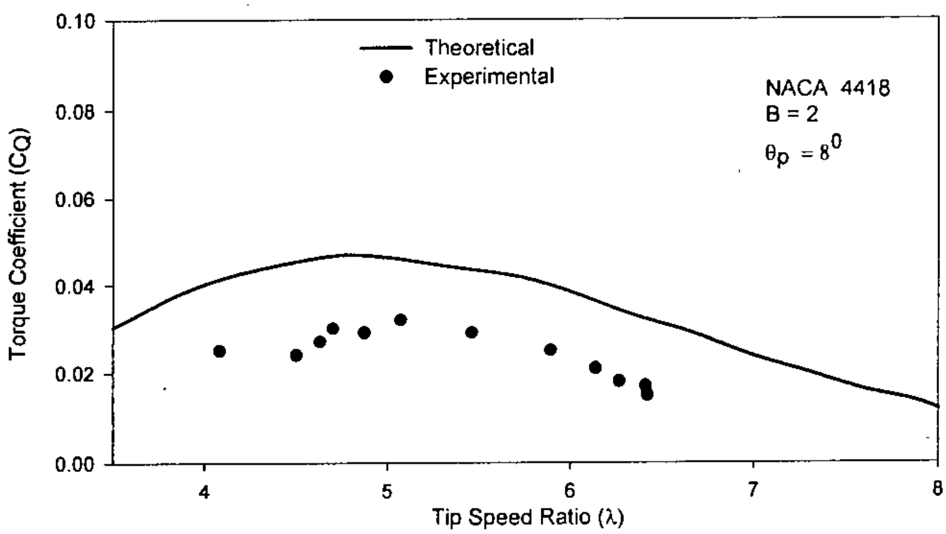

Figure 5.3.28 Torque Coefficient (C_Q) VS Tip Speed Ratio (λ)

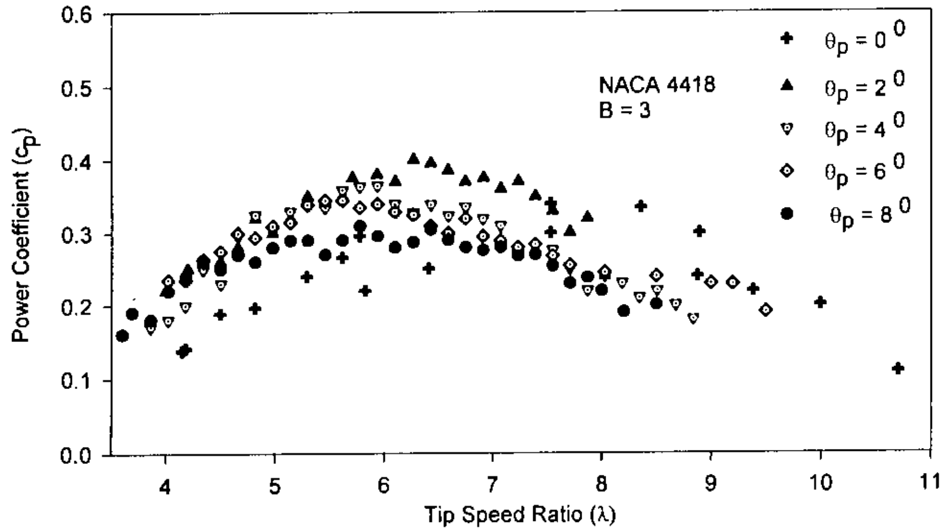

Figure 5.3.29 Power Coefficient (C_p) VS Tip Speed Ratio (λ)

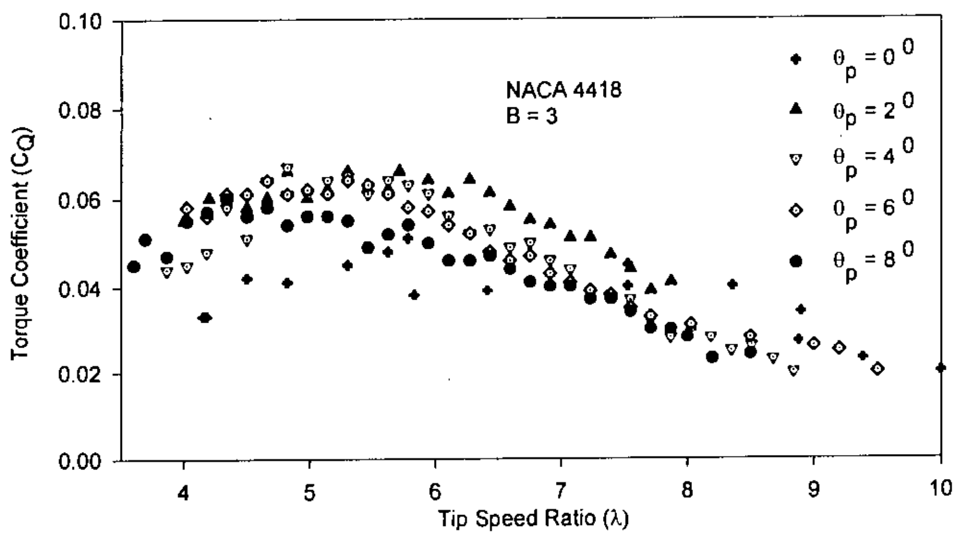

Figure 5.3.30 Torque Coefficient (C_Q) VS Tip Speed Ratio (λ)

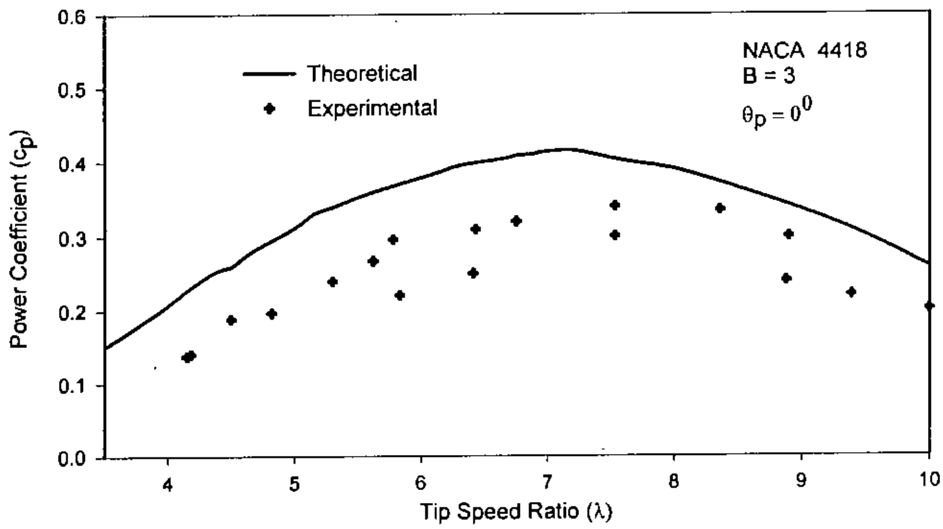

Figure 5.3.31 Power Coefficient (C_p) VS Tip Speed Ratio (λ)

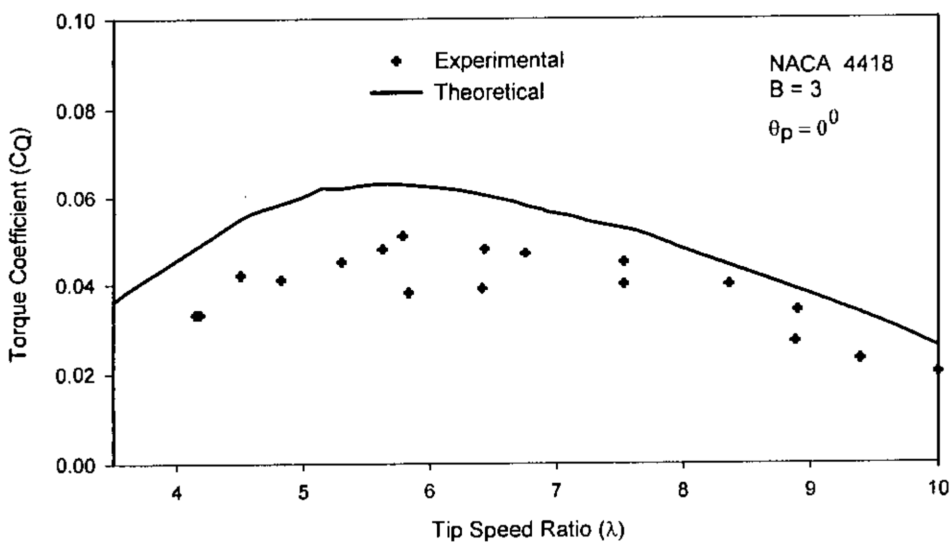

Figure 5.3.32 Torque Coefficient (C_Q) VS Tip Speed Ratio (λ)

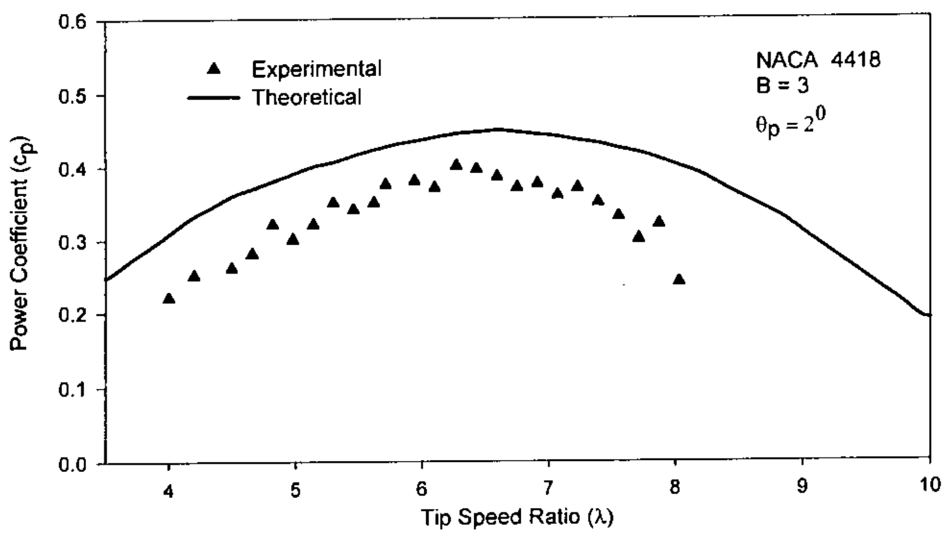

Figure 5.3.33 Power Coefficient (C_p) VS Tip Speed Ratio (λ)

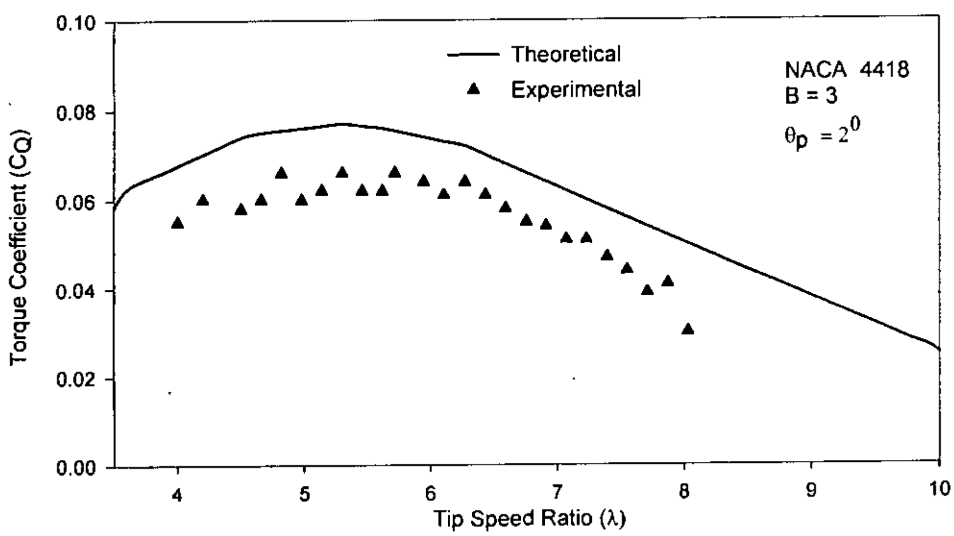

Figure 5.3.34 Torque Coefficient (C_Q) VS Tip Speed Ratio (λ)

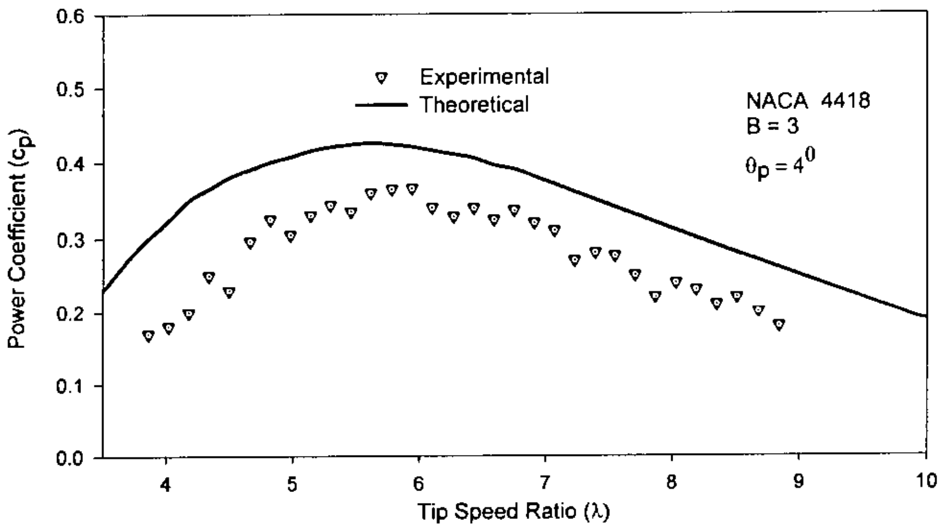

Figure 5.3.35 Power Coefficient (C_p) VS Tip Speed Ratio (λ)

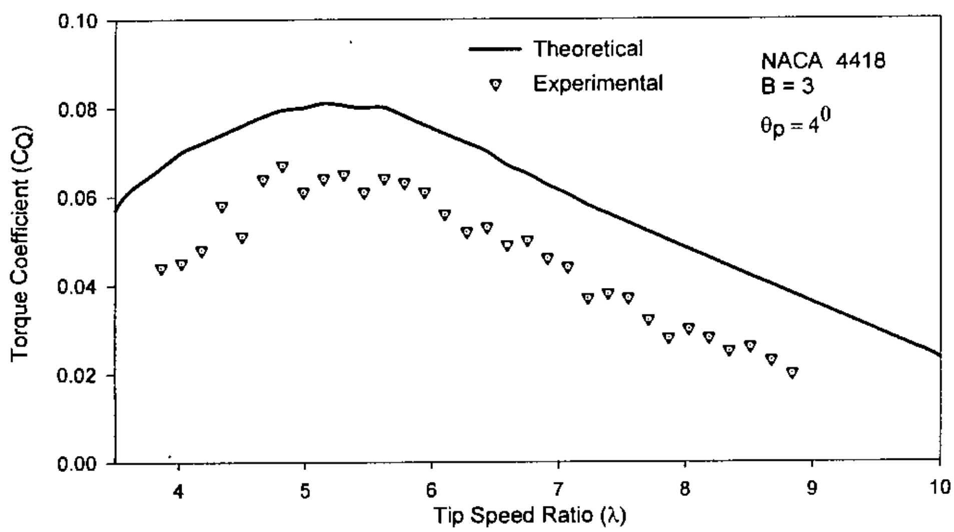

Figure 5.3.36 Torque Coefficient (C_Q) VS Tip Speed Ratio (λ)

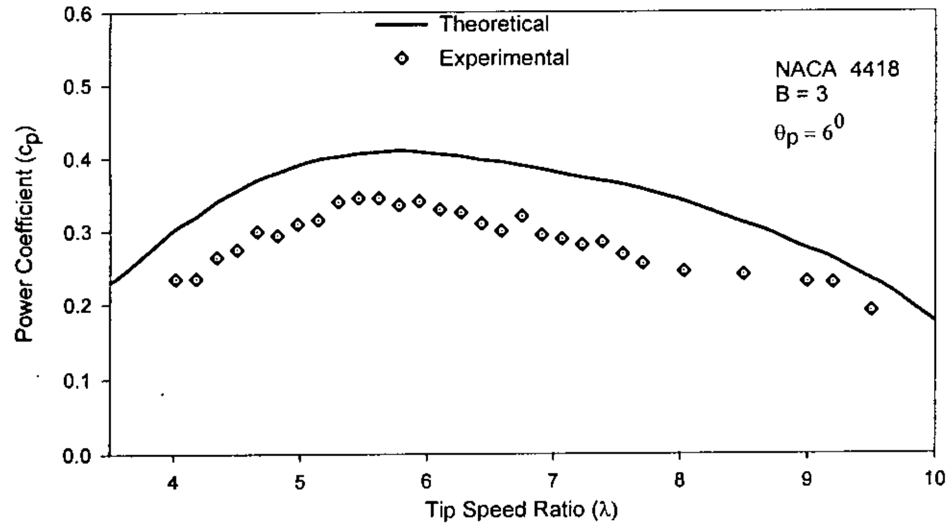

Figure 5.3.37 Power Coefficient (C_p) VS Tip Speed Ratio (λ)

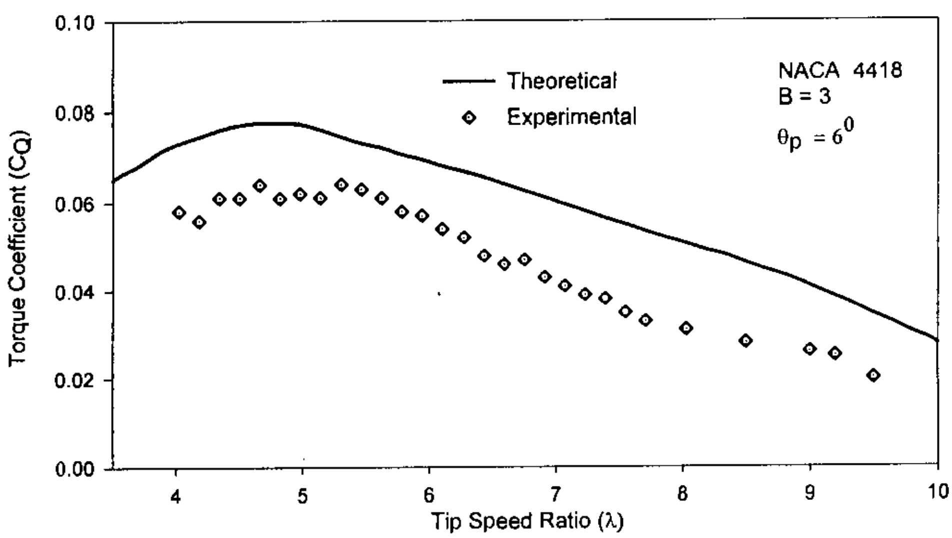

Figure 5.3.38 Torque Coefficient (C_Q) VS Tip Speed Ratio (λ)

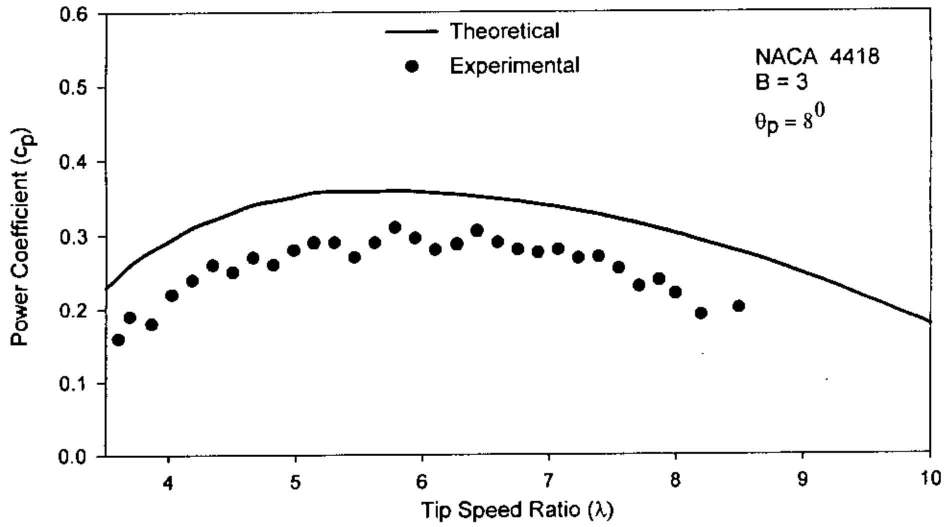

Figure 5.3.39 Power Coefficient (C_P) VS Tip Speed Ratio (λ)

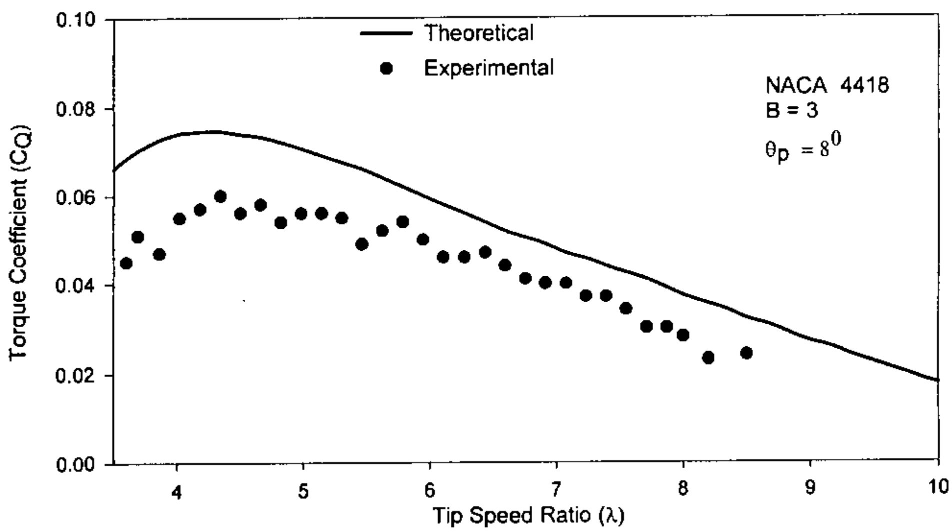

Figure 5.3.40 Torque Coefficient (C_Q) VS Tip Speed Ratio (λ)

The performance of wind turbine model having four blades has been shown in Figures 5.3.41 and 5.3.42 in terms of C_p versus λ and C_Q versus λ. At the tip speed ratio of around 6, maximum power coefficient is obtained. From Figures 5.3.43 to 5.3.52, it is seen that there is a closer correlation between the values predicted by the present method and those calculated by the wind turbine model. Here the 'Present Method' means computer program used for the theoretical comparison.

5.3.4 Effect of number of blades on the performance of model wind turbine

In considering a wind turbine design, the question arises how many blades should be used. In general, as the number of blades increases so does the cost. The advantages of increasing the number of blades are improved performance and lower torque variations due to wind shear. The number of blades also affects the maximum power coefficient. This is caused due to tip losses that occur at the tips of the blades. These losses depend on the number of blades and tip speed ratios. For lower tip speed ratios, in general, higher number of blades is chosen. This is done because the influence of number of blades on power coefficient is larger at lower tip speed ratios. For higher design tip speed ratios higher number of blades will lead to very small and thin blades which results in manufacturing problems and a negative influence on the lift and drag properties of the blades.

To illustrate the effect of the number blades the power coefficient for 2, 3 and 4 blades were calculated using NACA 4418 airfoil section. The diameter of the scale down upwind rotor is 484 mm. The variations of results for changing number of blades in terms of C_p versus λ and C_Q versus λ are shown in figures 5.3.53 to 5.3.62. It is noticed that a general difference in peak power coefficients between 2 and 3 blades is significant but the differences in peak power coefficients between 3 and 4 blades is small. However, the maximum power coefficient is affected by changing the number of blades. Increase of number of blades shows that the region of higher power coefficients move to the region of smaller values of tip speed ratios. So as in the case of slow running load where the design tip speed ratio is generally low, increase number of blades provide higher starting torque.

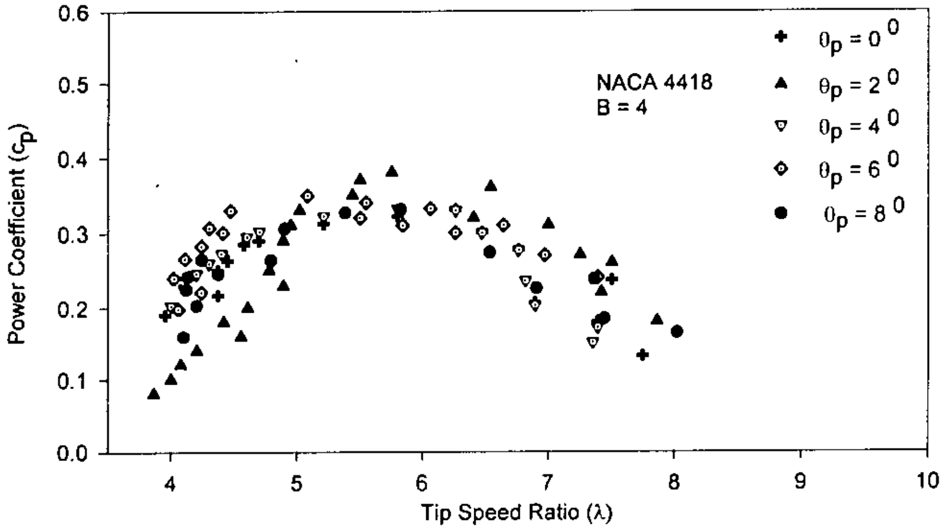

Figure 5.3.41 Power Coefficient (C_p) VS Tip Speed Ratio (λ)

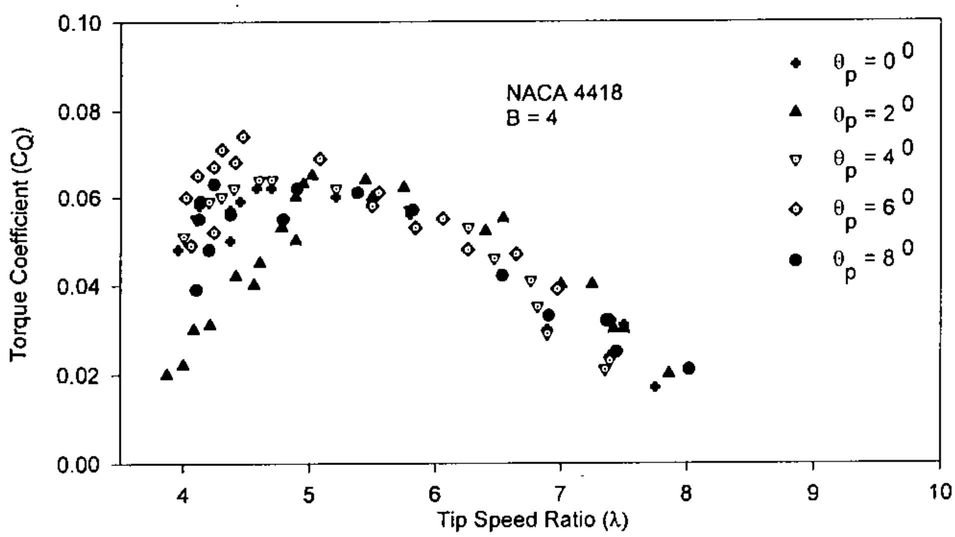

Figure 5.3.42 Torque Coefficient (C_Q) VS Tip Speed Ratio (λ)

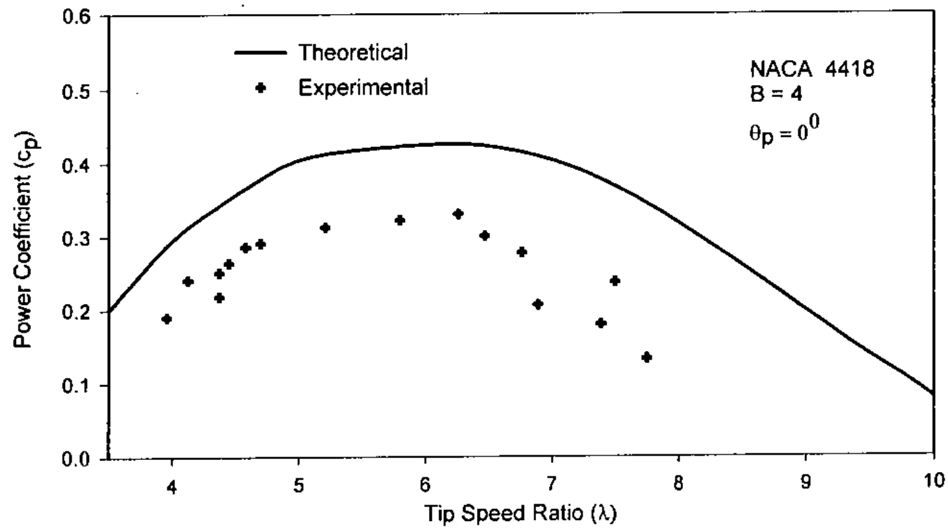

Figure 5.3.43 Power Coefficient (C_p) VS Tip Speed Ratio (λ)

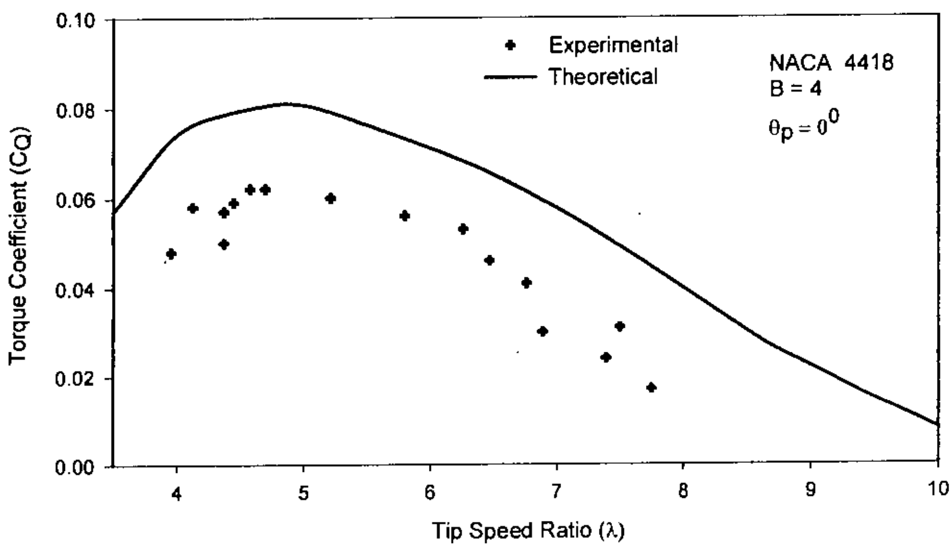

Figure 5.3.44 Torque Coefficient (C_Q) VS Tip Speed Ratio (λ)

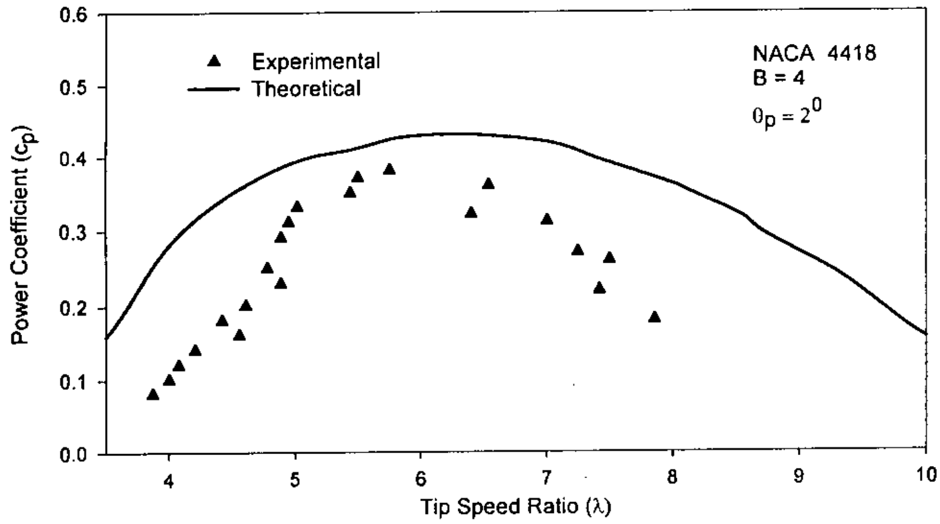

Figure 5.3.45 Power Coefficient (C_p) VS Tip Speed Ratio (λ)

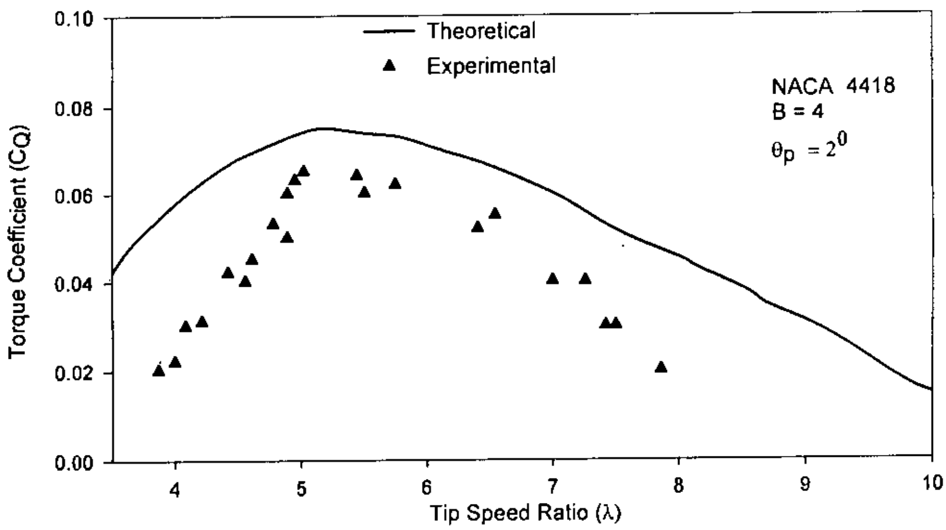

Figure 5.3.46 Torque Coefficient (C_Q) VS Tip Speed Ratio (λ)

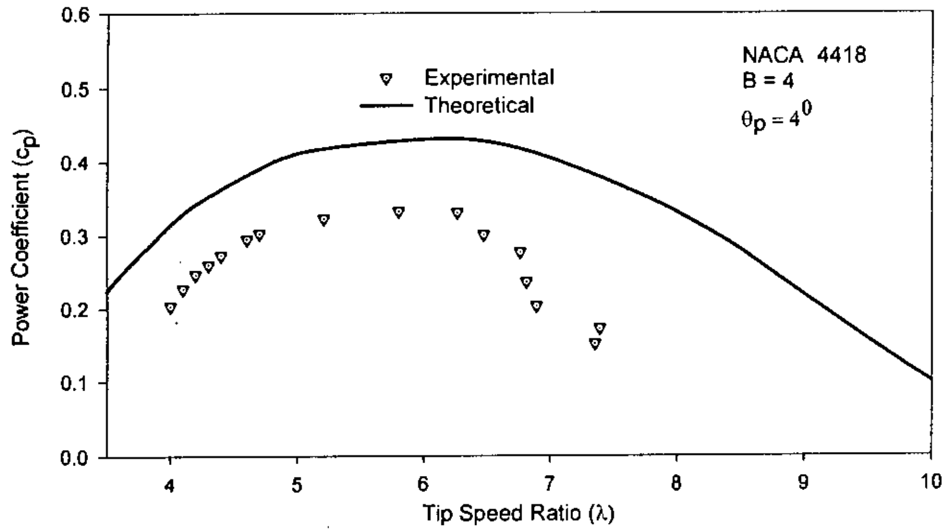

Figure 5.3.47 Power Coefficient (C_p) VS Tip Speed Ratio (λ)

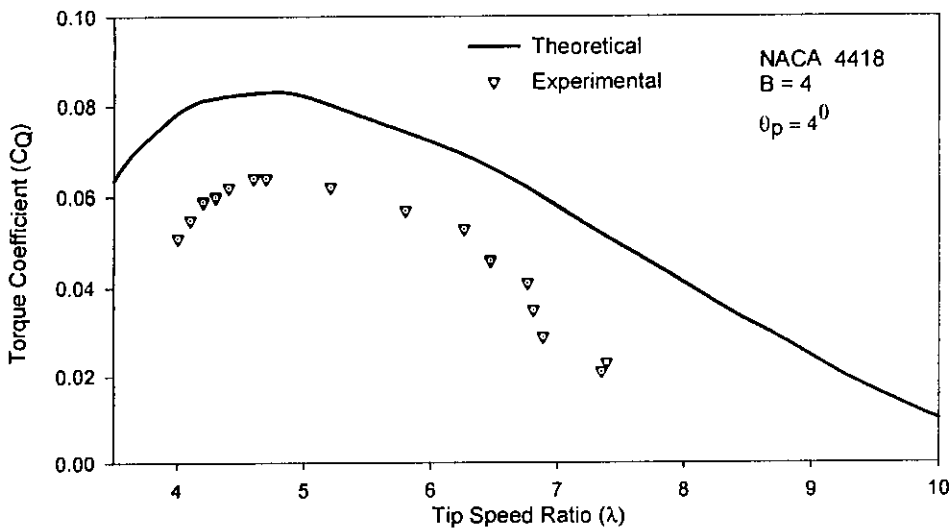

Figure 5.3.48 Torque Coefficient (C_Q) VS Tip Speed Ratio (λ)

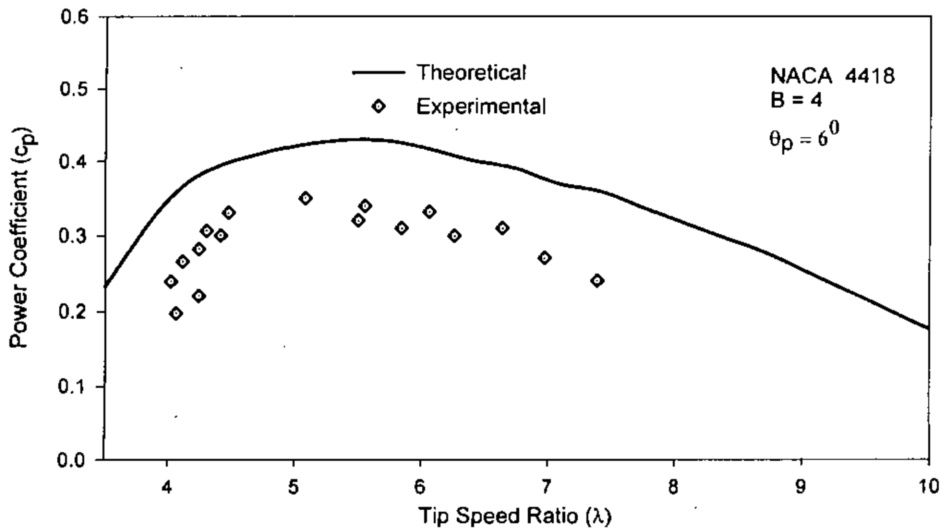

Figure 5.3.49 Power Coefficient (C_p) VS Tip Speed Ratio (λ)

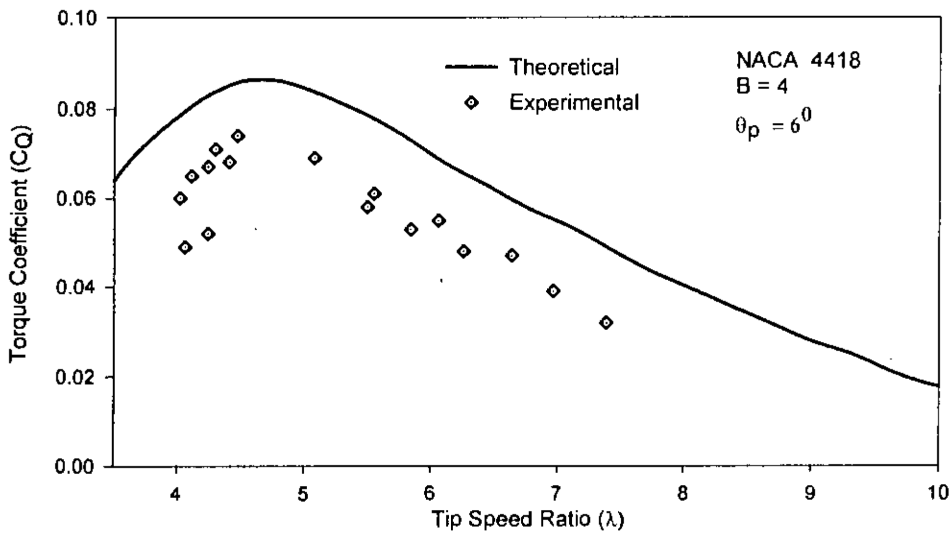

Figure 5.3.50 Torque Coefficient (C_Q) VS Tip Speed Ratio (λ)

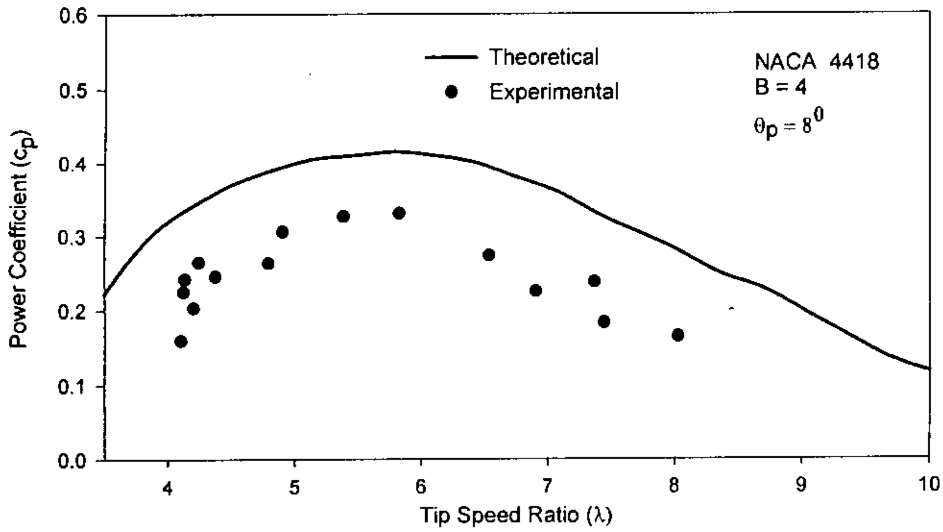

Figure 5.3.51 Power Coefficient (C_p) VS Tip Speed Ratio (λ)

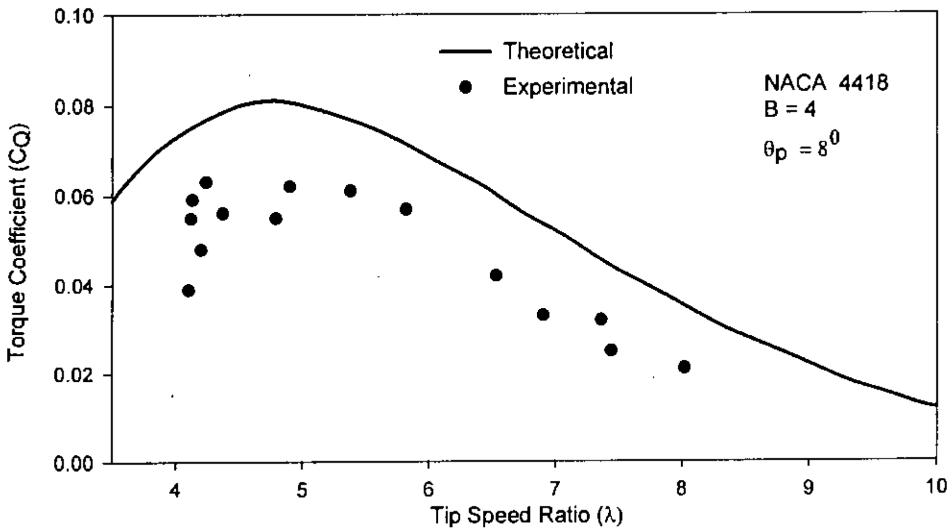

Figure 5.3.52 Torque Coefficient (C_Q) VS Tip Speed Ratio (λ)

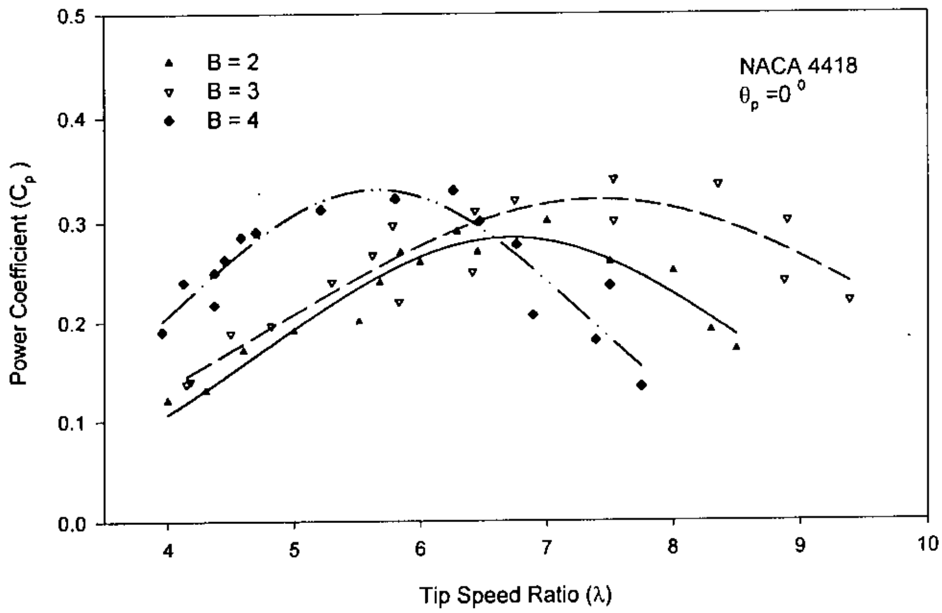

Figure 5.3.53 Power Coefficient (C_p) VS Tip Speed Ratio(λ)

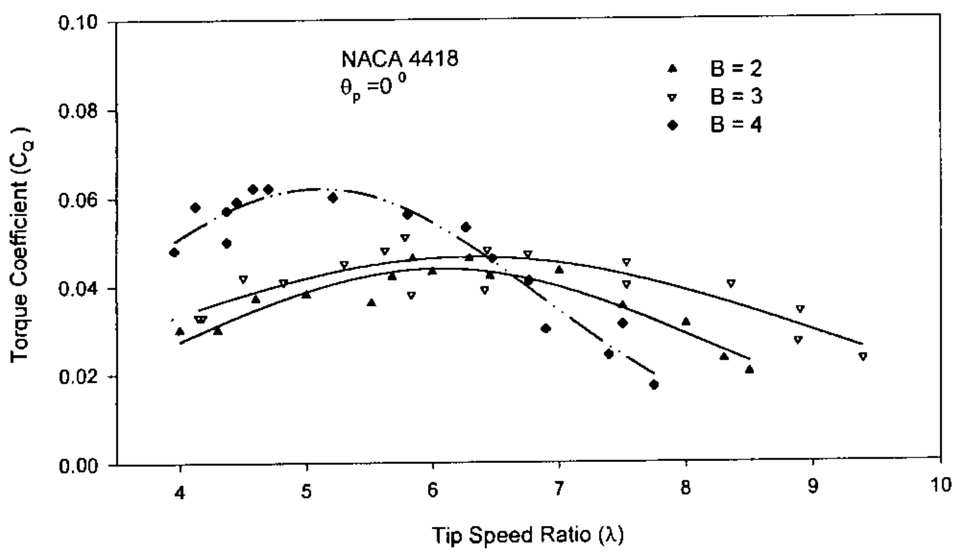

Figure 5.3.54 Torque Coefficient (C_Q) VS Tip Speed Ratio(λ)

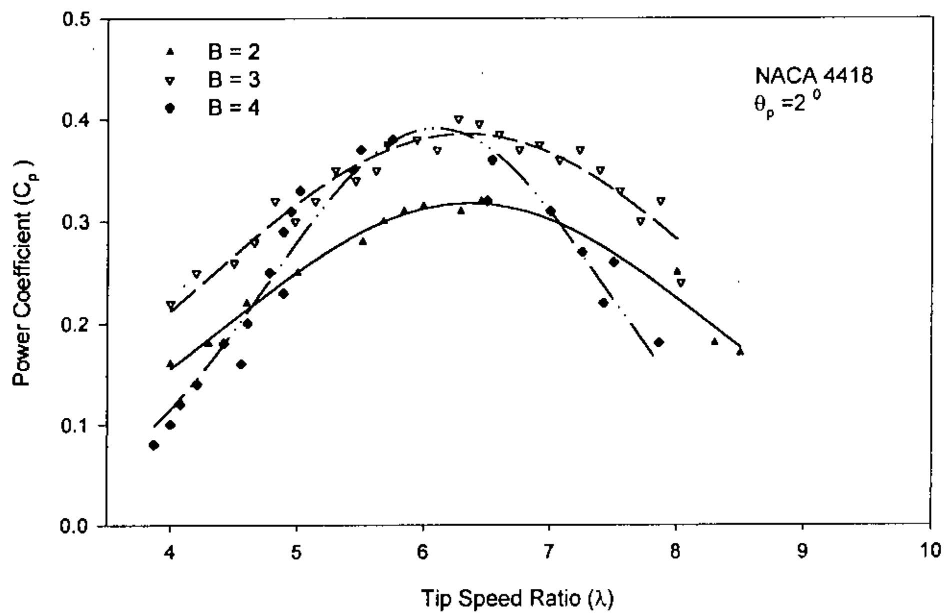

Figure 5.3.55 Power Coefficient (C_p) VS Tip Speed Ratio(λ)

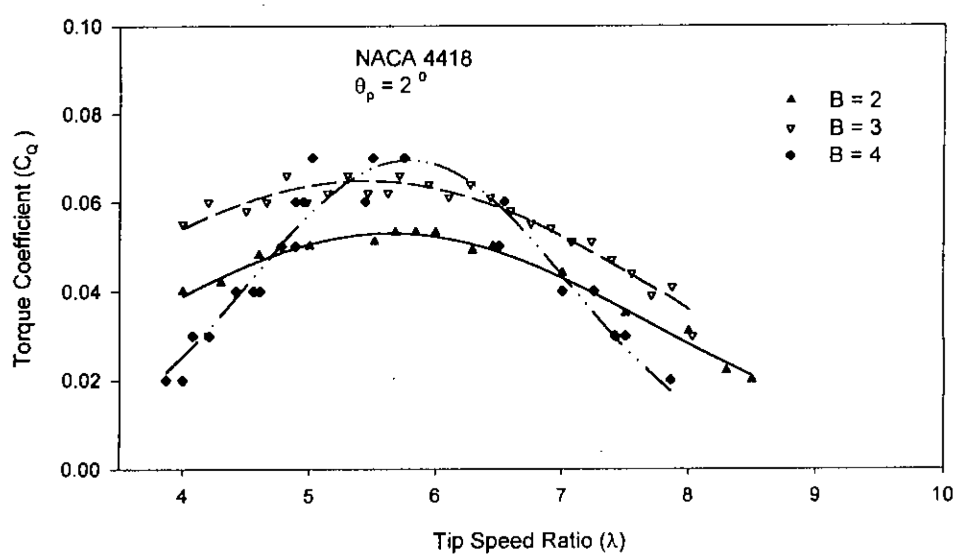

Figure 5.3.56 Torque Coefficient (C_Q) VS Tip Speed Ratio(λ)

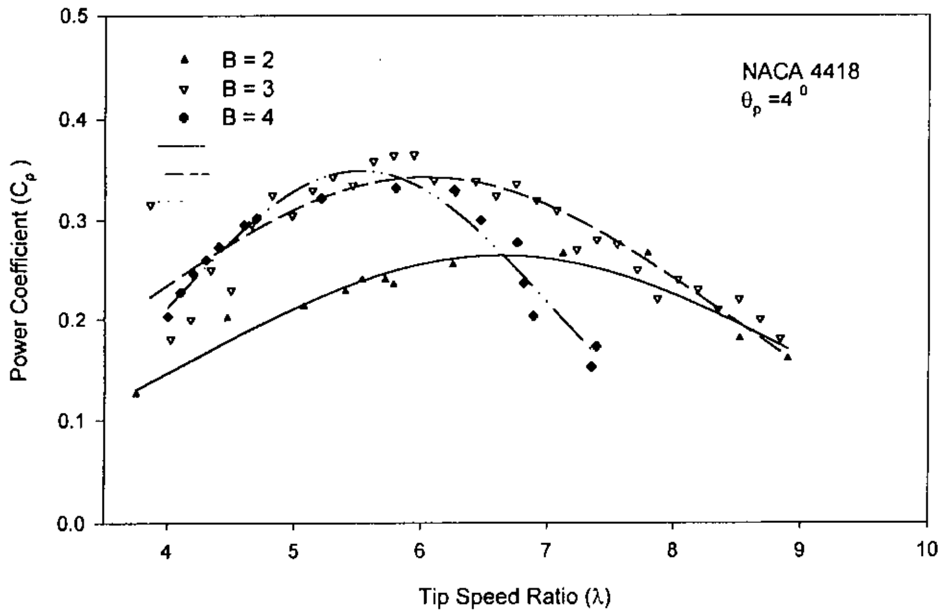

Figure 5.3.57 Power Coefficient (C_p) VS Tip Speed Ratio(λ)

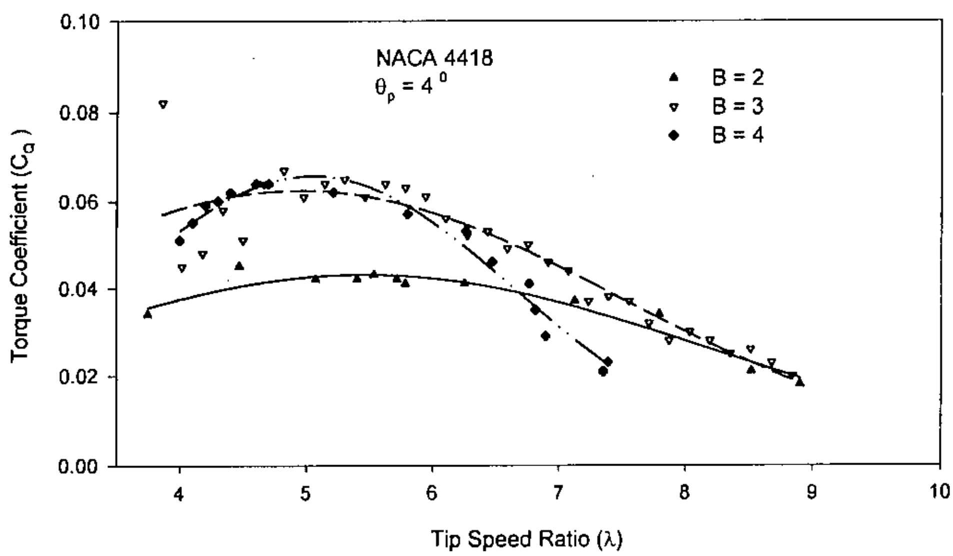

Figure 5.3.58 Torque Coefficient (C_Q) VS Tip Speed Ratio(λ)

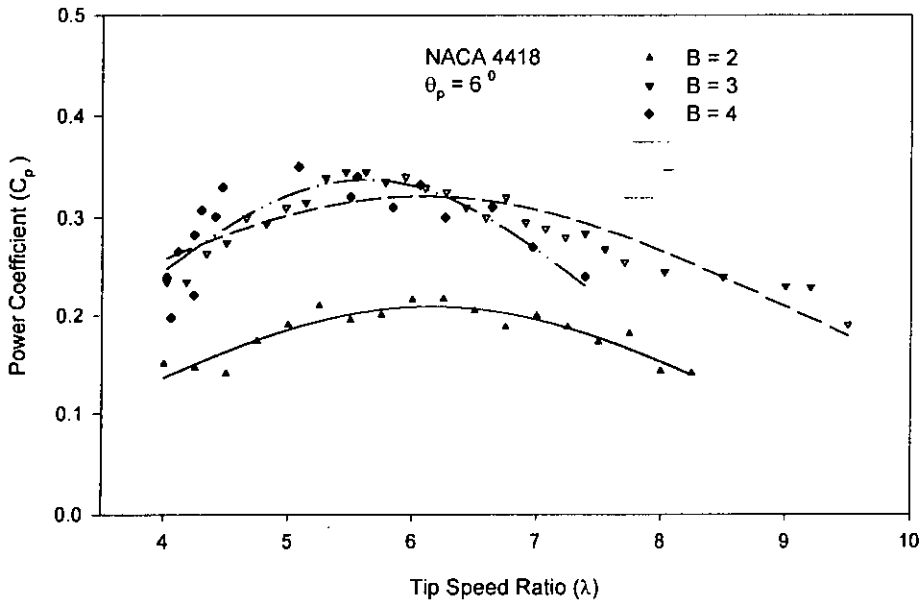

Figure 5.3.59 Power Coefficient (C_p) VS Tip Speed Ratio(λ)

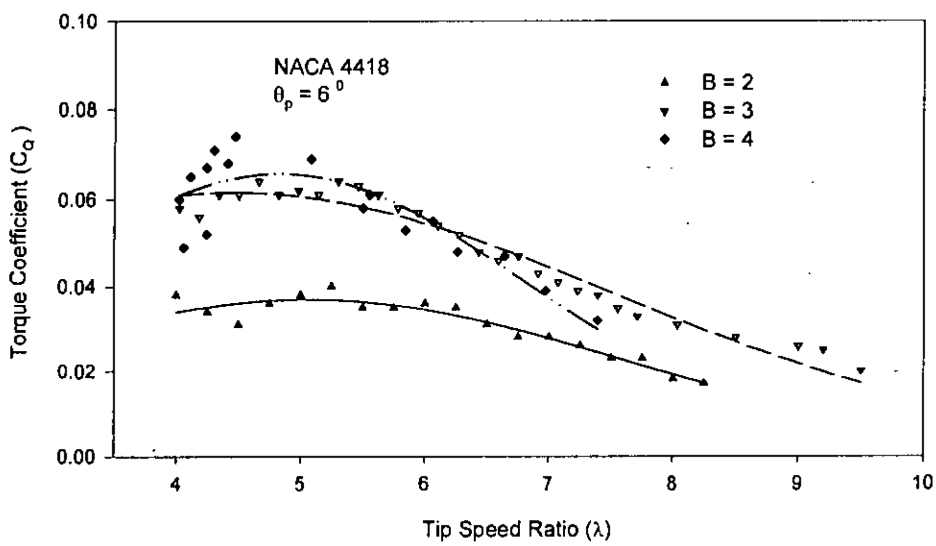

Figure 5.3.60 Torque Coefficient (C_Q) VS Tip Speed Ratio(λ)

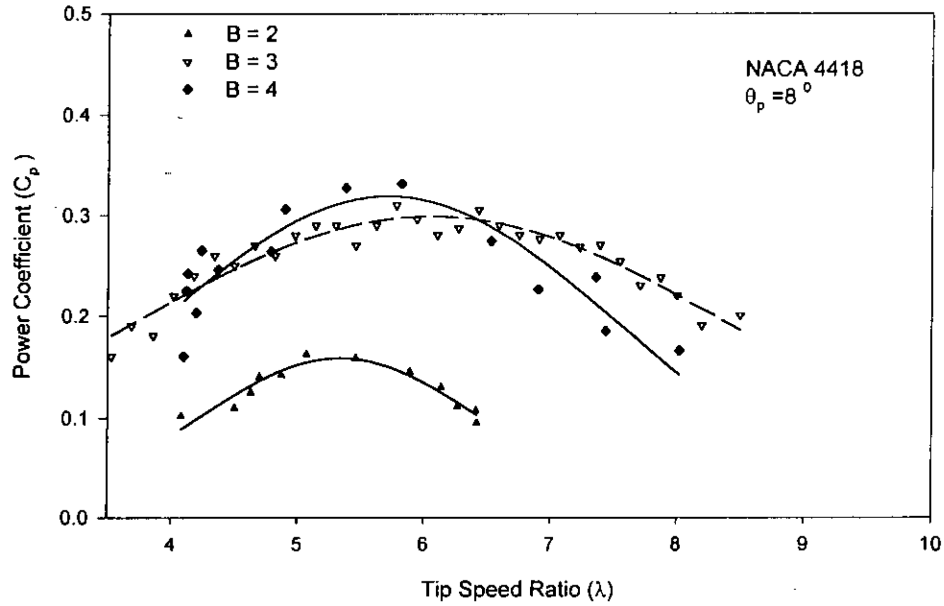

Figure 5.3.61 Power Coefficient (C_p) VS Tip Speed Ratio(λ)

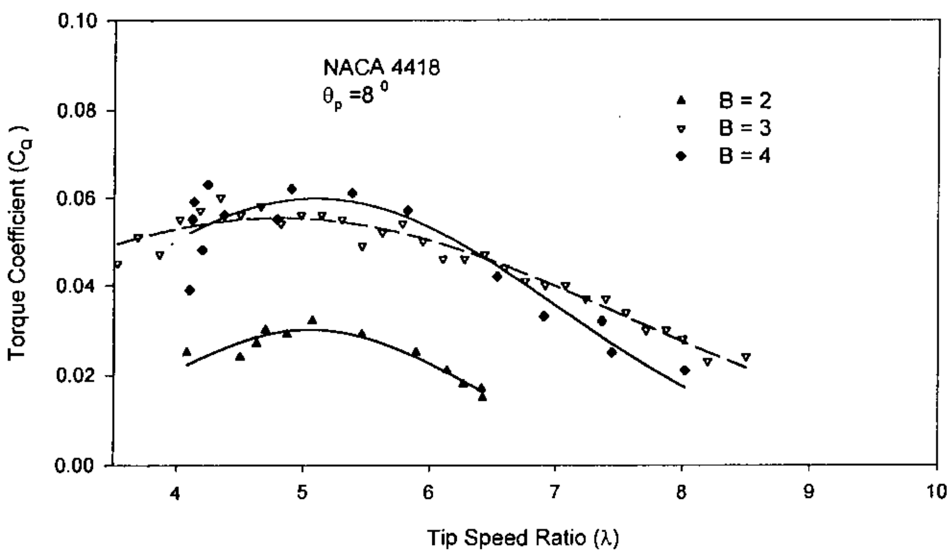

Figure 5.3.62 Torque Coefficient (C_Q) VS Tip Speed Ratio(λ)

CHAPTER 6

WIND PUMPING FOR IRRIGATION IN BANGLADESH

6.1 Introduction

For people, animals and crop irrigation, water is an essential need in every country. Frequently this water has to be pumped from under ground; the pumping requires energy. In the rural areas, this energy has traditionally been provided by people operating hand pumps or animal pumps. Where mechanized power is available, it is most commonly an internal combustion engine burning petrol or diesel oil. In the wake of the increasing world energy crisis, which hits the least developed countries most, the interest in alternative energy resources has increased considerably. Recently, there has been a growing interest in the new technology of solar-powered water pumps and a revival of interest in windpumps. Windmills have good potentials in many areas in the world, since they are relatively efficient energy converters. Their construction is relatively simple, cheap and can be carried out locally.

The ancient Egyptians used wind power 5000 years ago to propel boats. It is estimated that wind power was first used in land to power rotating machinery about 2000 years ago. The Chinese used windmills for low lift paddy irrigation for many centuries.

By the 18th century, windmills were a major form of technology particularly in some European country. They could produce 30-40 kW of power. In the mid 19th century settlers were moving into the great plain where there was a shortage of fuel and transport was difficult. With the need for water and the steady, regular wind across the great plains, windmills were ideal technology. By the 1880's the familiar all-steel windmills were American multi-bladed farm windpump had evolved. It looked not much different from many that are still in production [28].

Bangladesh farming needs adequate supply of irrigation water at right time and in right quantities for maximum agricultural production. About 50% of irrigation pump operate at a head of 6 m or less, depending on the terrain of the country. For driving these pumps, either diesel engine or electric motors are used. These pumps can be driven with the help of wind turbine [22].

6.1.1 Wind pumping technology

For a considerable length of time, the classical "American" wind pump depicted the basic wind pump technology. Around the 1970s, with the revival of wind energy development, various designs of a new generation of wind pumps came into being. Many such designs were based on grossly oversimplified engineering principles and they rarely went beyond the experimental stage. Some of the more successful designs, such as those developed by the Consultancy Services for Wind Energy in Developing Countries (CWD) in Netherlands, Intermediate Technology (IT) Power Ltd. in the United Kingdom and in country projects in China, India and Sri Lanka have reached the maturity for commercial production [57].

6.1.2 Principal benefits of windpumps

- Wind pumps are often more economical method of pumping water in the rural areas where the average wind speed in the least windy month is greater than about 3 m/s and no grid power is available.
- There are is no fuel requirements for wind pumps, contrary to engine-driven pumps which require expensive fuel that is difficult to obtain in the rural areas.
- Wind pumping systems represent an environmentally sound technology, though there is some noise, and visual impact.
- They are highly reliable with regular maintenance, and are also less vulnerable to theft or damage than other systems.
- Wind pumps last a long time, typically 20 years for a well-made, regular maintenance machine.
- They can be locally manufactured in most developing countries, creating indigenous skills and reducing foreign exchange requirements for costly diesel fuel and equipment [49].

6.1.3 Classification of wind pumping systems

Wind machines could be broadly categorized into two types: the vertical axis and the horizontal axis type. Primary advantage of the vertical axis type wind machine is its ability to capture wind from any direction without having to orient the wind rotor mechanically (Figure-6.1.1). Whereas the horizontal axis type wind machines comparatively have higher power coefficients. Within the class of horizontal axis wind pumps, the main difference between designs lies in the mode of power transmission.

Wind pumps with mechanical drives - In this category, the rotor is mechanically coupled either to a piston pump, centrifugal pump or screw pump. Coupling of piston pumps could be done either directly or through a gear transmission. Centrifugal pumps, which have to be operated at high rotational speeds, are always connected through a gear transmission. Screw pumps also need gearing primarily to change the geometry of transmission axis as well as for speed reduction at the pump. An indigenous wind pump of this category which has had a widespread use in Thailand and China, is the wind-driven "Ladder Pump" used for low-lift pumping (Figure-6.1.2).

Wind pumps with pneumatic transmission – A few manufacturers fabricate wind pumps in which the rotor drives a compressor and compressed air is used in an air lift pump or to drive a piston pump. Main advantage of this type of wind pumps is the absence of a pump rod, which is a significant parasitic load in deep well applications. The system also allows more freedom in sitting the wind pump as shown in Figure-6.1.3.

Wind pumps with electrical transmission – In this category, the rotor is coupled to an electrical generator, the output of which is used to power an electric motor-driven pump (Figure-6.1.4). Advantages are generally the same as those with pneumatic transmission. In the case of deep well pumping, electric submersible pumps may be used to pump water from narrow bore hole with flow rates far in excess of those attainable with piston pumps.

Of all these types of pumps, the wind pump with a mechanically coupled piston pump and centrifugal pump are the most common type and further discussion will be limited only to these types of wind pumps.

6.1.4 Components of a wind pump systems

A horizontal-axis wind machine with a mechanically coupled pump consists of the following main sub-systems.

Rotor

The rotor, which converts power of the wind into useful shaft power, consists of a number of blades mounted around the shaft. Those with a large number of blades, ranging from about 18 to 36, are supported by a structure of spokes and rims (Figure-6.1.5). Multi-bladed rotors possess high starting torque characteristics and run at slower speeds, typically at a tip speed ratio of around one.

Rotors of a more recent design have fewer blades, normally in the range of 4-8 blades mounted on individual spokes (Figure-6.1.6). Their design tip speed ratio is about 1.5-2 and the starting torque is comparatively lower.

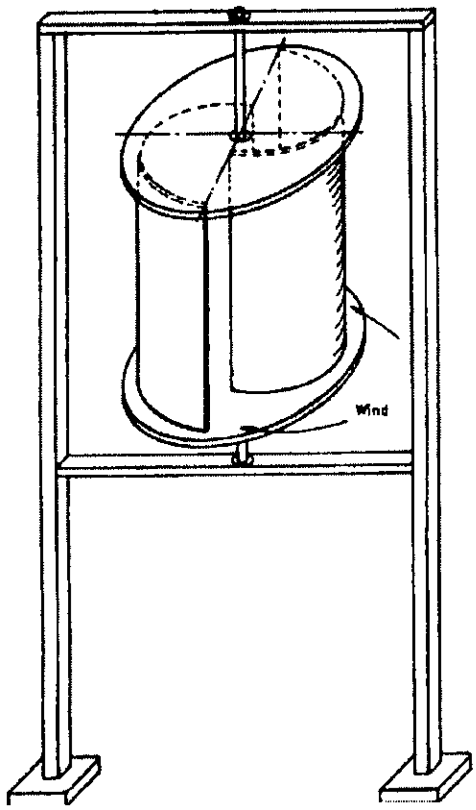

Figure 6. 1.1 Vertical Axis Wind Turbine, Savonius Rotor [28]

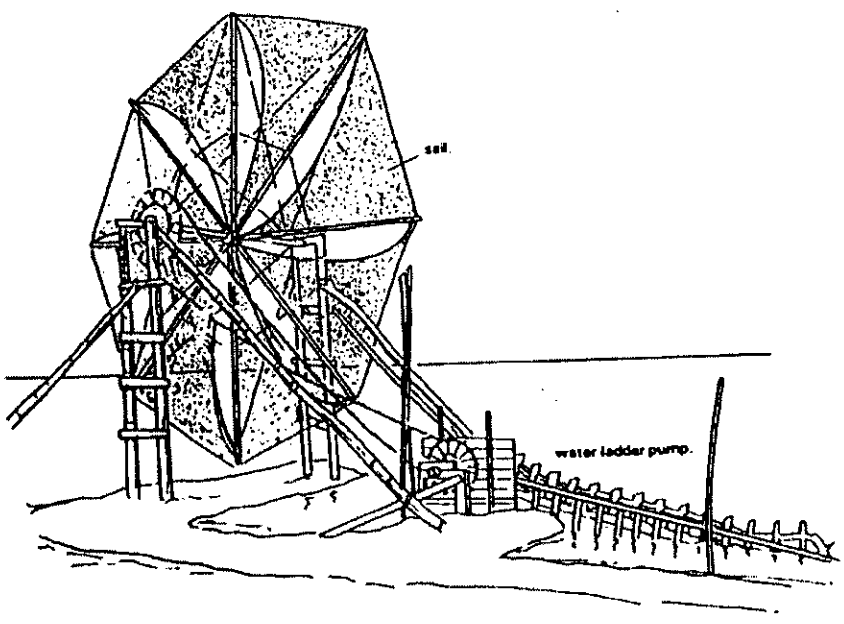

Figure 6.1.2 Horizontal Axis Wind Turbine Driven Ladder Pump [57]

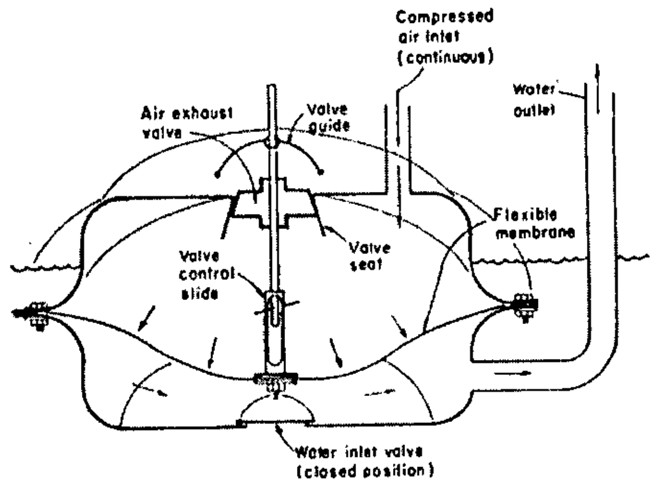

Figure 6.1.3 Water Pump Driven by Compressed Air [57]

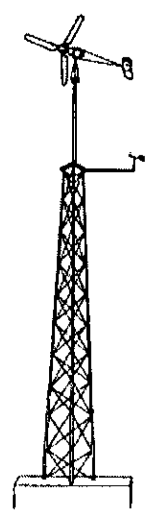

Figure 6.1.4 Wind Turbine Jacobs Design for Generating Electricity [28]

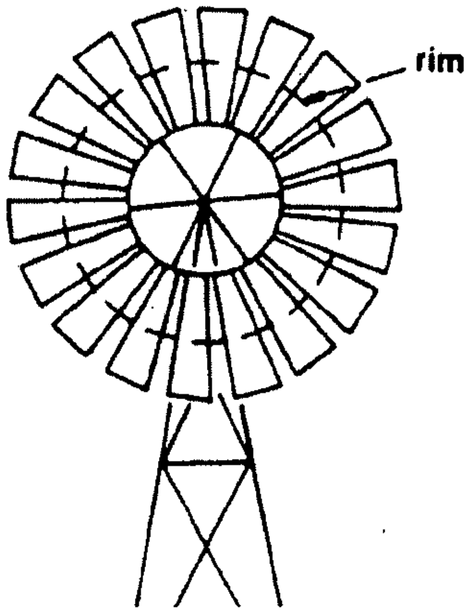

Figure 6.1.5 Classical Horizontal Axis Multi-Bladed Wind Turbine Rotor [57]

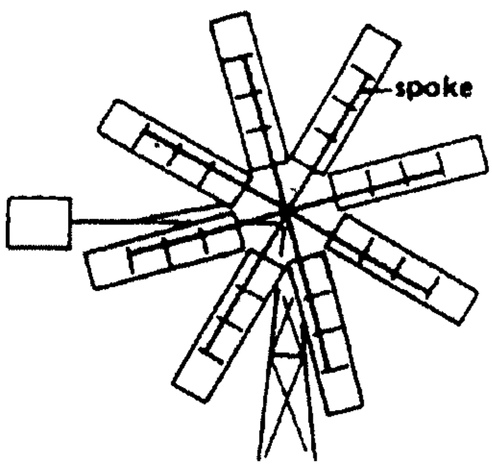

Figure 6.1.6 Modern Horizontal Axis Wind Turbine Rotor [57]

Transmission

The transmission system, which transmit power from the shaft to the pump, could either be a direct drive via a crank mechanism or a gear drive (Figure-6.1.7), the latter being used when speed reduction is necessary.

Due to reciprocating motion of the piston pump, the components of the transmission system undergo cyclic loading. Particularly in case of deep well pumping, the acceleration of oscillating masses, such as the pump rod and the water column in the rising main, would result in significant cyclic stresses on the system. Thus the components of the transmission system are some of the most heavily stressed ones in the entire machine. Incorporation of a speed reducing gear box in classical deep well wind pumps is basically a measure to contain the transmission loads within manageable limits [57].

Tails

The tails of a horizontal axis wind rotor serves two purposes. At low and medium wind speeds when the windpump is operating it keeps the rotor facing into the wind. At high speeds it causes the rotor to turn sideways on to the wind (i.e. to furl) so that it is not damaged during stormy weather. The power density is very high and they can therefore do a lot of damage. Windpump are usually designed furl at about 10-12 m/s, since the proportion of wind at speeds greater than this is usually very small.

Tower

Tower supports the energy conversion system at the desired height above the ground level. Very often the tower is designed as a self-supporting latticed structure. In more recent designs, slender masts supported by guy wires are also being used.

Pump

A pump in general may be defined as a machine, when driven from some external source, lifts water or other liquid from a lower level to a higher level. Or in other words, a pump may also be defined as a machine, which converts mechanical energy into pressure energy [27].

Piston Pump

The commonly used piston pump consists of a piston unit incorporating a sealing cup and a central valve. The cylinder unit has a foot valve at its bottom where the water inlet pipe is connected as shown in Figure-6.1.8. The principle of operation of the system is schematically shown in Figure-6.1.9. When a piston pump is operated at higher speeds, say over 120 rpm, the dynamic behavior of the valve system tends to generate shock loads over and above the force due to water lifting. In order to reduce such loads piston pumps running at high speeds are generally equipped with "air vessels", which reduce the mass of water being accelerated in each cycle.

Centrifugal Pump

The pump, which raises water or a liquid from a lower level to a higher level by the action of centrifugal forces, is known as centrifugal pump, shown in Figure 6.1.10. The action of a centrifugal pump is that of a reversed reaction turbine. In a reaction turbine, the water at higher pressure is allowed to enter the casing which gives out mechanical energy at its shaft. Whereas in case of pump the mechanical energy is fed into the shaft and water enters the impeller (attached to the rotating shaft) that increases the pressure energy of the out going fluid. The water enters the impeller axially and leaves the vanes radially.

The impeller is enclosed in a water-tight casing, having a delivery pipe in one of its sides. The casing of a centrifugal pump is so designed that the kinetic energy of the water in converted into pressure energy before the water leaves the casing. This is considerably increases the efficiency of the pump [27].

Main vane and speed control system

Under normal operating conditions, the main vane performs the function of orienting the rotor into the wind as the wind direction changes. At high wind speeds, the main vane becomes a part of the speed control system, which is present in practically every design of commercially produced wind pumps. Purpose of the speed control system is to limit the rotor speed and therefore, the power output to the rated level.

In most wind pumps speed control is often accomplished by turning the rotor away from the wind when the wind speed keeps increasing beyond a certain pre-determined value. Its principle of operation is based on the equilibrium of aerodynamic forces (acting on one or two vanes and the rotor) and gravity forces, or that of a spring, counteracting the aerodynamic forces.

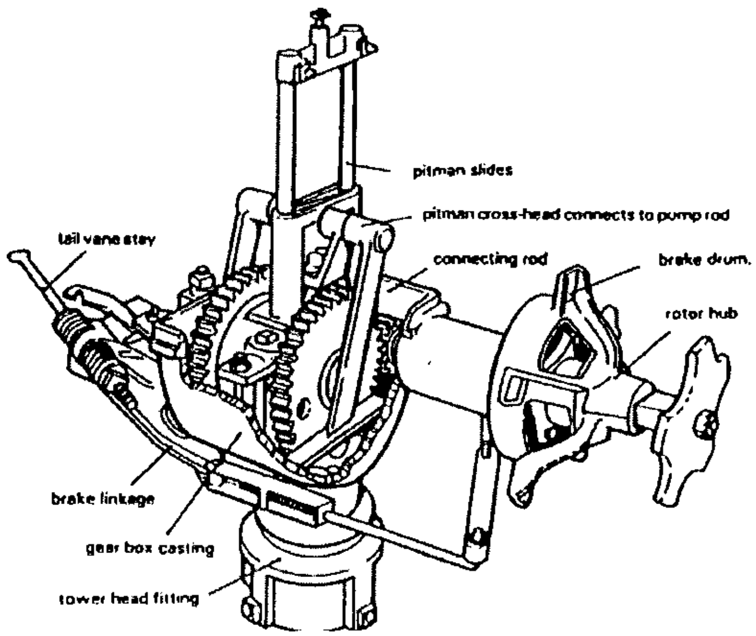

Figure 6.1.7 Gear Box of Classical Back Geared Wind Pump [57]

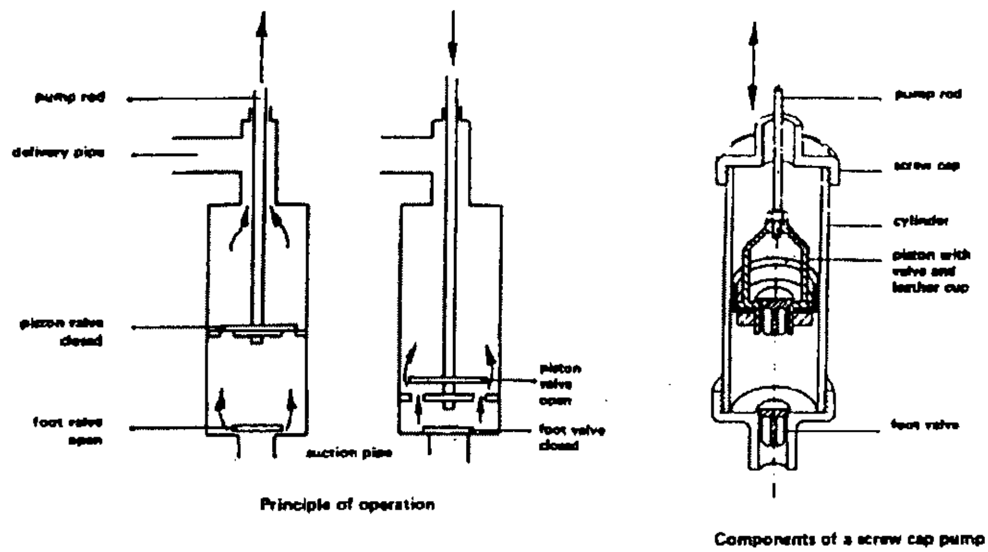

Figure 6.1.8 Principal Operation of the Piston Pump Used in Wind Pump [57]

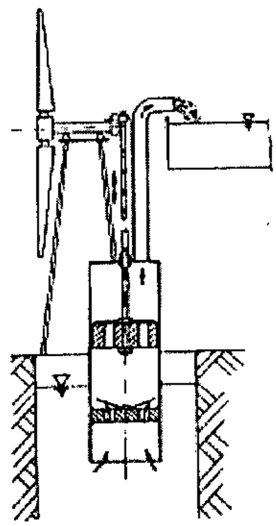

Figure 6.1.9 Horizontal Axis Wind Turbine Piston Pump [42]

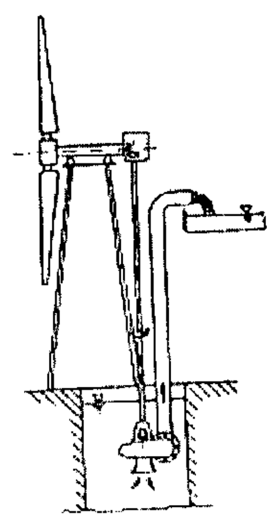

Figure 6.1.10 Horizontal Axis Wind Turbine CentrifugaL Pump [42]

Figure-6.1.11 shows the operating principle of a speed control system commonly used in wind pumps. The tail vane is hinged and fixed in place by means of a pre-loaded spring. The rotor axis has an offset from the pivot axis, which enables the development of a turning moment around the pivot axis under the action of wind force on the rotor. During low winds, the turning moment on the rotor is counteracted by the moment created by the wind force acting on the tail vane, and the rotor tail vane system behaves as a fixed system. Under this condition the tail vane performs the function of orienting the rotor into wind (Figure-6.1.11 a).

As the wind speed increases, the thrust on the rotor increases and the rotor starts turning out of wind. At the same time, the increased wind force on the tail vane tries to keep the vane parallel to wind thereby pulling on the spring (Figure-6.1.11 b). With further increase in the wind speed the rotor is pushed totally out of wind and comes almost parallel to wind thereby reducing the power output drastically (Figure-6.1.11 c). As wind speed drops, the thrust on the rotor reduces and the tension on the spring brings the rotor back into the wind.

The control system shown in Figure-6.1.12 operates on the same principle, but uses an extra vane to the side of the rotor (instead of the offset) to generate the rotor turning moment. In this arrangement, the tail vane is mounted on an inclined axis thereby allowing gravity force to replace the spring in the previous design.

6.1.5 Common types of wind pumps

Within the category of wind pumps equipped with piston pumps, two basic types of machines could be further identified on the basis of the rotor solidity. The two types are generally referred to as wind pumps with high solidity rotors and those with low solidity rotors, exhibiting distinct technical characteristics. As the rotor and the load should have matching characteristics, the two types of wind pumps do have specific applications.

Wind pumps with high solidity rotors are primarily used in deep well pumping where the wind pump should possess high starting torque to overcome the weight of water column in the rising main and the pump rod weight during start-up, and to provide the force of accelerating them during starting. Besides this, the wind pump should also operate at a low design speed to contain the dynamic loads associated with acceleration and deceleration of reciprocating masses within acceptable limits. Therefore, wind pumps used in deep well pumping also incorporate a speed reducing gear transmission. A typical example of this type of wind pump is the classical "American" wind pump shown in Figure-6.1.13.

Most modern wind pump designs evolved in recent times are based on the use of low solidity rotors running at moderate speeds, with direct transmission to the pump (Figure-6.1.14). The absence of a gear transmission and the use of lighter low solidity rotors have made these machines substantially cheaper than the classical designs. The designs also use fabricated steel components in place of forged and cast ones in order to facilitate the manufacture of such machines in developing countries. Just as much as they are cheaper, the application of most modern wind pumps is also limited to a very narrow range. Experience suggests that most modern wind pumps have so far been successful in low head pumping, typically less than about 20 m.

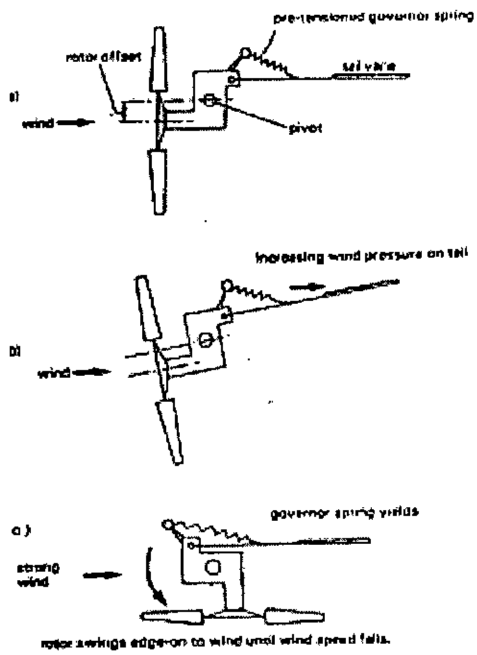

Figure 6.1.11 Safety System for Classical Wind Pump [57]

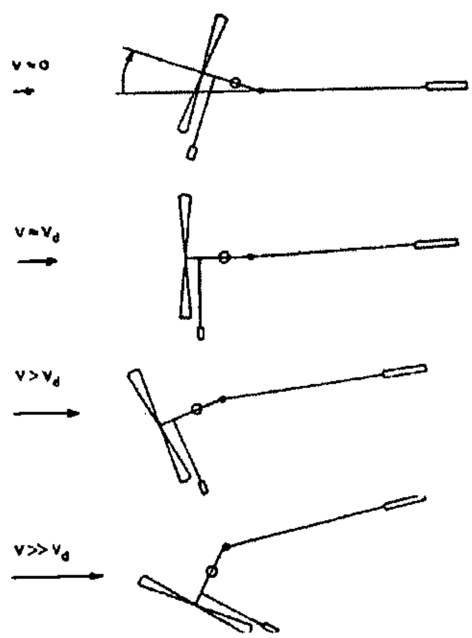

Figure 6.1.12 Principal Operation of the 'Inclined-hinge' Wind Turbine Safety System [57]

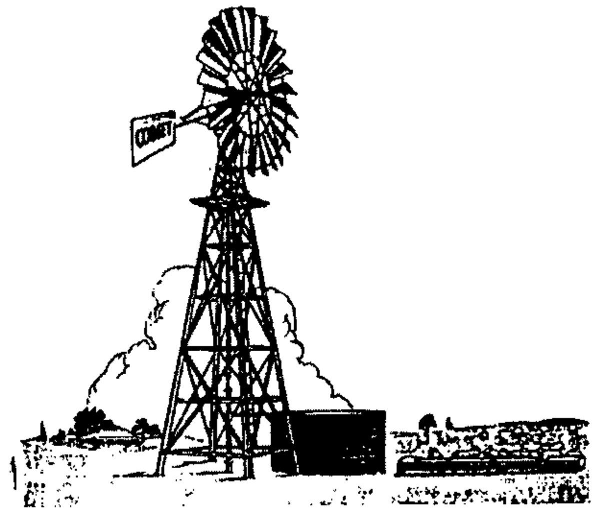

Figure 6.1.13 Classical American Farm Wind Pump [57]

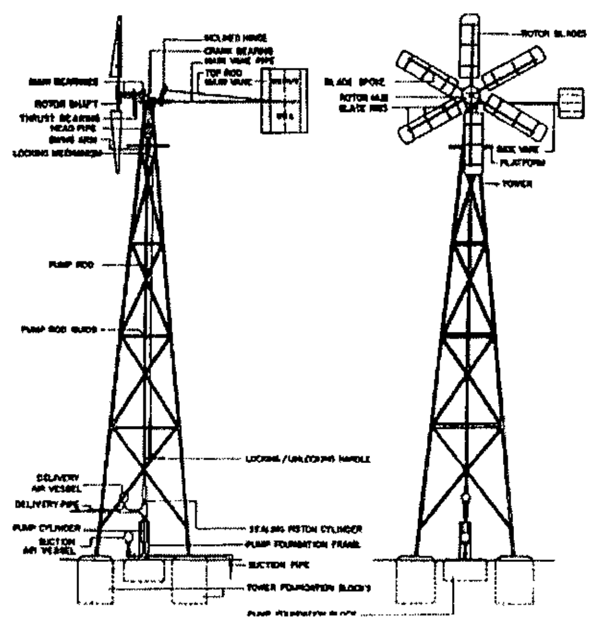

Figure 6.1.14 Design of Modern Wind Pump [57]

6.2 Performance of the Wind Pumps

6.2.1 Matching of windmill and wind pump

In order to achieve the desire performance of a wind pump, it is necessary to match the windmill to the wind regime as well as with the load. In order to understand this, it seems necessary to analyse the load characteristics, in this case, the characteristics of a piston pump and centrifugal pump.

In Figure-6.2.1, the torque of a single acting piston pump is cyclic, because it is only during the upward stroke that the pump gets loaded due to lifting water. During the downward stroke that the piston valve opens and the piston merely moves through the water. Once the pump is running, the rotor only feels the average torque demanded by the pump, because the cyclic torque variations get smoothened by the large inertia of the rotor. As the output of a piston pump is independent of the speed and the pumping head, the average torque remains almost constant.

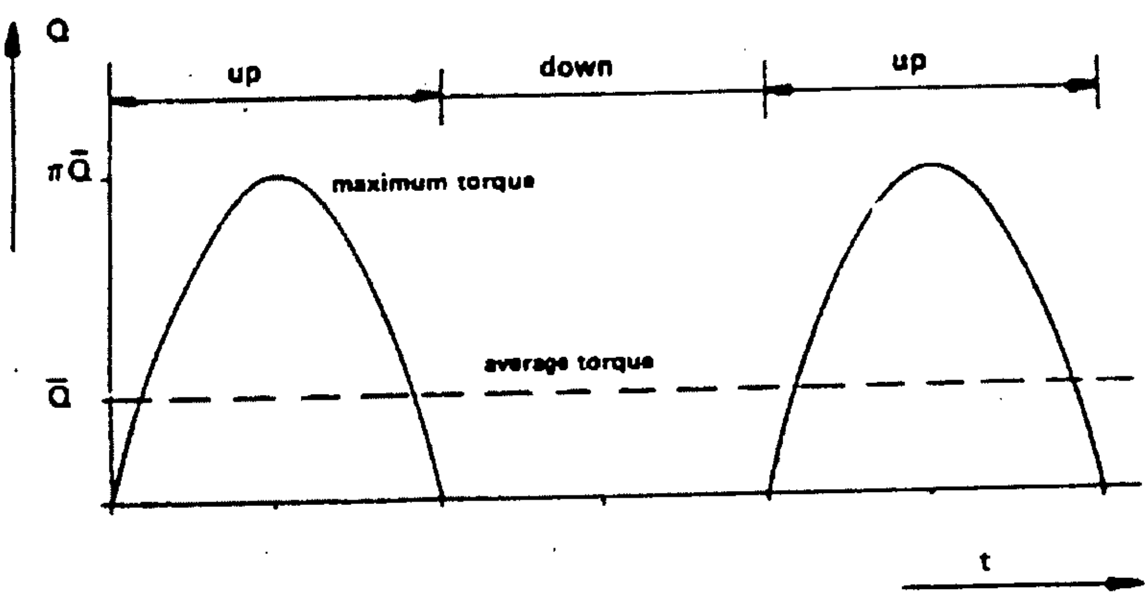

Figure 6.2.1 Torque of a Single Acting Piston Pump[57]

In Figure-6.2.2 a and Figure-6.2.2 b, the constant average torque of a piston pump is superimposed on the torque -speed and power-speed curves of a wind rotor for different wind speeds. In the starting region, the pump torque reaches a value that is π times the average torque, as this stage the rotor has to overcome the torque of the pump.

As any other machine, the wind pump system operates at the point where the torque demanded by the load is equal to the torque supplied by the rotor. Thus as the wind speed increases, the point of operation of the system would move to the right along the line of constant pump torque. Corresponding operating points are also shown in the power-speed curve. The dotted line indicates the locus of maximum power of the wind rotor. It is evident from the two sets of curves that it is only at the point D that the system operates. It is also clearly seen that, as the wind speed increase, the point of operation of the system moves away from the line of maximum power thereby shedding much of the available power from the wind. The wind speed corresponding to the point D is referred to as the "design wind speed" and is denoted by V_d. This is also illustrated in the curve depicting the overall performance ($Cp\eta$) against the wind speed in Figure-6.2.2c and in the output curve shown in Figure-6.2.2 d.

The matching of a windmill to the wind regime and the pump is essentially a matter of choosing the design wind speed. Up to a point, a higher design wind speed tends to increase the overall system output, but the wind availability may be lower (i.e. the wind pump will often stand still). Selection of lower V_d has an opposite effect. Thus, the selection of the design wind speed V_d is a compromise between the water output and the wind availability. For example, a farmer having a large water tank would prefer to have a large water output with lower availability, as the resulting intermittent nature of output does not influence his irrigation water supply coming from the tank. On the other hand, a wind pump for drinking water supply should be matched with a lower V_d so as to increase the availability thereby maintaining a regular water output from the wind pump throughout the year.

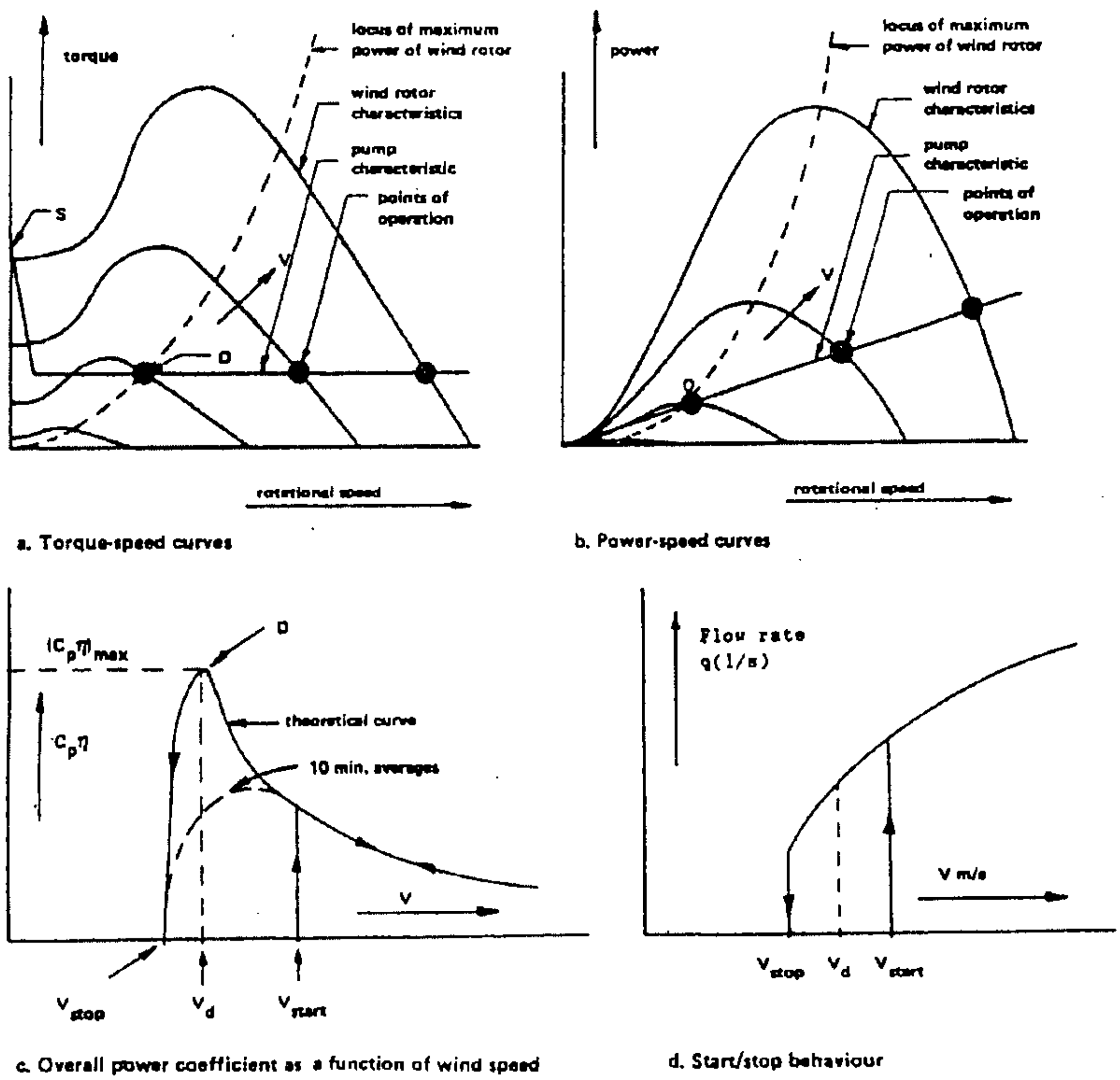

Figure 6.2.2 Matching of Wind Turbine and Piston Pump [57]

The shaft power of a centrifugal pump is superimposed on the same wind turbine characteristics. The centrifugal pump, once delivery has commenced, operates close to the optimum conditions even when wind speeds increases strongly. The power requirement of centrifugal pump fits the characteristics much better as shown Figure-6.2.3 than the case of the piston pump.

In Figure-6.2.4 and Figure-6.2.4 b the curves of delivery of the two pump types and their total efficiency are shown as a function of wind speed. It can be seen from the curve of delivery that after delivery begins (V_{beg} = 2.7 m/s) the piston pump initially deliver more. However, as soon as the wind speed is above 4 m/s the centrifugal pump delivers more. Above 4 m/s the total efficiency of the wind pump system with centrifugal pump is higher than the wind pump system with piston pump. At higher wind speeds (around 9 m/s) it is nearly twice as efficient [42].

Start and stop behavior of the piston pump

Due to the specific torque characteristic of the single acting piston pump, a wind pump exhibits a peculiar behavior in the lower end of the output curve. As shown in Figure 6.2.2 d, the wind speed needed to start a wind pump (V_{start}) is higher than the wind speed at which the machine would stop (V_{stop}). The higher V_{start} is necessary to overcome the starting torque of the pump and, once the wind pump starts operating, it experiences only the average pump torque. As the wind speed comes down, the pump speed and output keep on reducing, but due to rotor inertia the machine continues to operate until the wind speed reaches V_{stop}. At this point, if the wind speed start increasing, the wind pump would not start until V_{start} is reached. It could thus be expected that within the range of wind speeds between V_{stop} and V_{start} the wind pump may or may not be pumping depending on whether the wind speed was decreasing or increasing. This region in the output curve is referred to as the hysteresis region [30].

It is due to this peculiar starting behavior that the 10 min. average values of the $C_p\eta$ (Figure 6.2.2 c) is very much below the computed value around the design wind speed. Following are some of the methods, which could mitigate the adverse effects of this starting behavior on the wind pump performance.

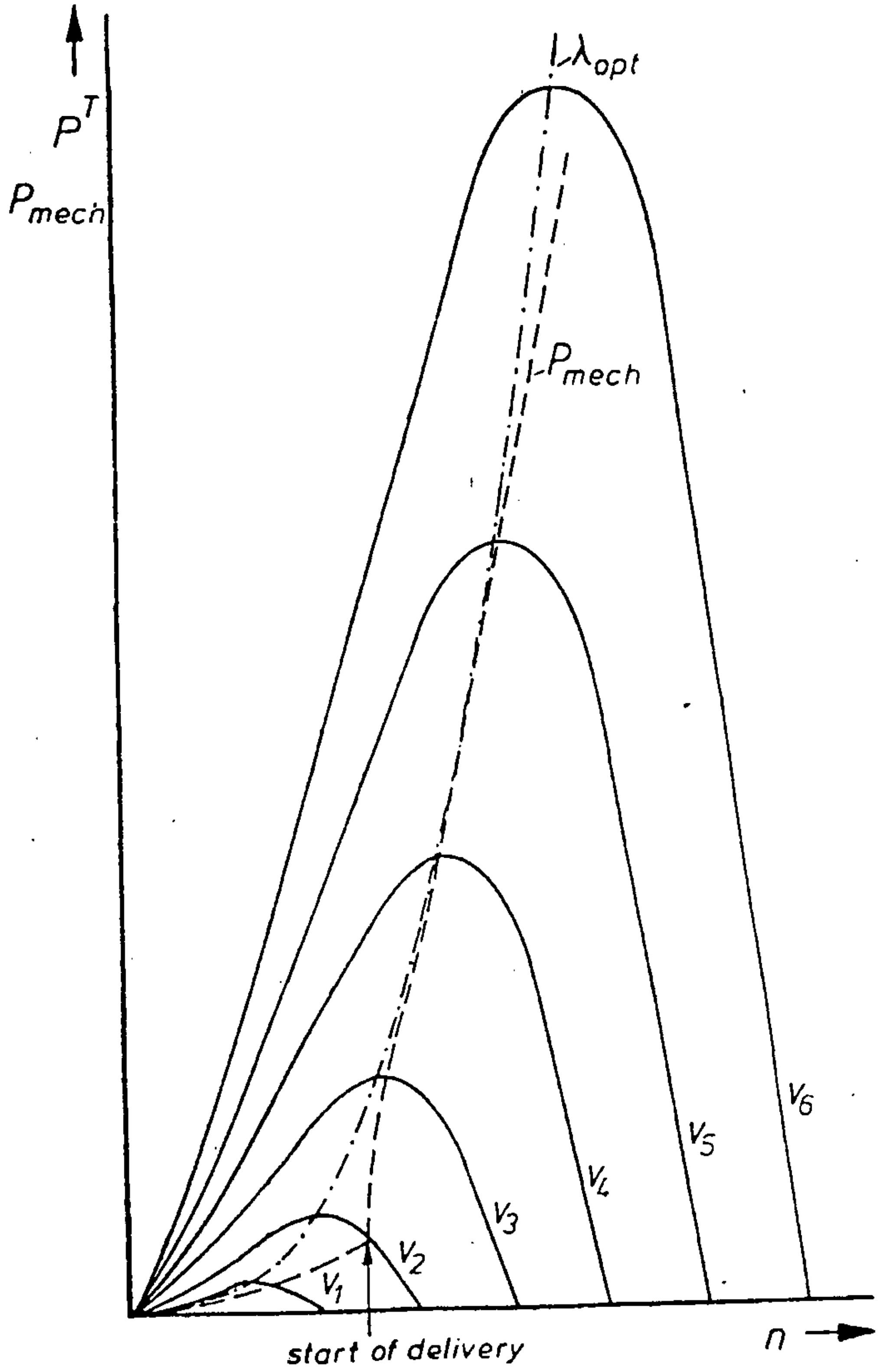

Figure 6.2.3 Operation of Centrifugal Pump [42]

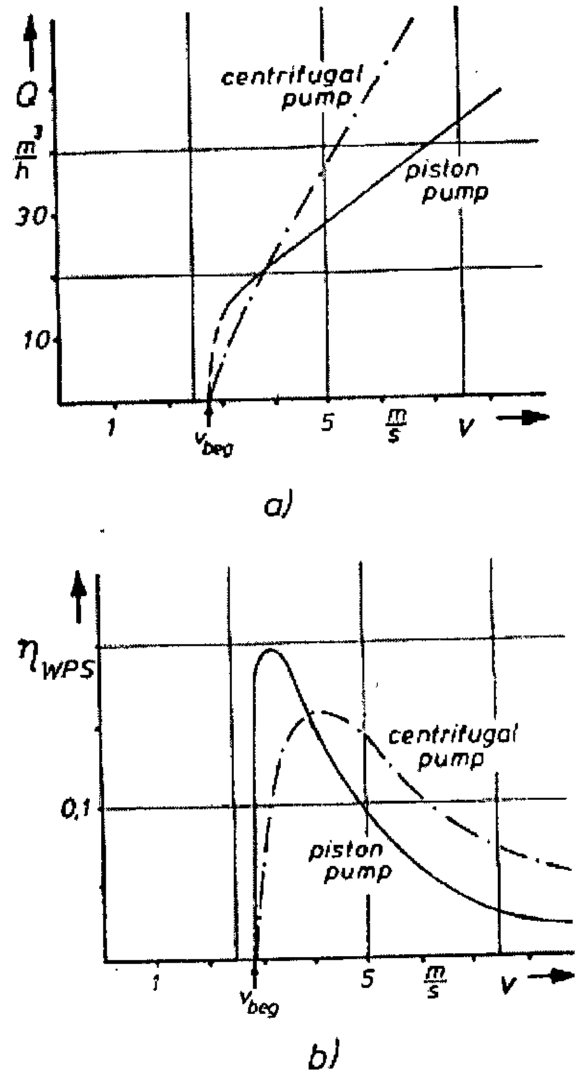

Figure 6.2.4 a) Curve of Delivery of Piston and Centrifugal Pump System
b) Comparison of Total Efficiency [42]

Variable stroke transmission: In this design, the pump torque is continuously varied to follow the varying rotor torque (due to change in wind speed) in such a manner that the system would follow the locus of maximum power. Such a design would allow a wind pump to operate close to the theoretical curve, but, as far is known, a practical design of a variable stroke transmission is yet to develop.

Starting nozzle: In this design, at low wind speeds water leaks through small orifice (of pre-determined diameter) in the piston body, thereby reducing the starting torque. As the wind speed increases, the system starts pumping more and more water, letting only a specified amount of water to leak through the starting nozzle, typically 10 percent of the stroke volume. However, clogging of the nozzle (which is less than 3-4 mm in diameter) by particles in water could easily set the mechanism out of action.

Controlled valve: The design incorporates a method of keeping the piston valve open during low wind speeds so that the rotor could start without experiencing the pump starting torque. As the wind speed increases beyond a pre-determined value, the valve closes and the wind pump starts pumping. This principle is now being tried with the aid of a "floating valve" with encouraging results.

6.2.2 Energy output and availability

The performance of a wind pump resulting from the matching of wind machine and pump can be summarized by two characteristic quantities, related to output and availability [30].

Energy production coefficient C_E, defined as the real hydraulic energy output (E) in time period T, divided by the reference energy which would be obtained during the same period, if the wind pump was operating at a constant wind speed equal to the average site wind speed, assuming that the machine is operating at the maximum power coefficient (Cp) and transmission efficiency (η) during the whole period T:

$$C_E = \frac{E}{0.5\,\rho V_{av}^{\ 3} A(Cp\eta)_{\max} T} \qquad (6.2.1)$$

Output availability, defined as the percentage of the time during which sufficient wind is available to operate the wind pump at more than 10 percent of its average pumping rate.

Both these quantities depend on the type of pump and the design wind speed. Some typical values of these two quantities for different versions of wind pumps are given in Table 6.2.1. These values are based on what have been found in practice and are supported by the theory. As can be seen in the expression for the energy production coefficient, one also needs to know the maximum overall power coefficient $(Cp\eta)_{max}$. Typical values of $(Cp\eta)_{max}$ for different pumping heights are also presented in Table-6.2.1a and Table-6.2.1b. The effect of these three factors may be represented through a "quality factor" defined as:

$$\beta = \frac{P_{av}}{A\,V_{av}^{3}} = 0.5\rho(Cp\eta)_{max}\,C_E \tag{6.2.2}$$

The average power referred to above is in fact the hydraulic power output of the system. Values of the quality factor are presented in Table 6.2.1, taking ρ = 1.2 kg/m^3.

Table-6.2.1a: Design and Performance Characteristics for Wind Pumps [57]

Choice of design wind speed V_d, energy production coefficient C_E and output availability			
	V_d/V_{av}	C_E	Availability
Wind machines driving piston pumps			
• Classical deep well	0.6	0.40	60%
• Classical shallow well or deep well with balanced pump rod	0.7	0.55	60%
• Starting nozzle and balanced	1.0	0.90	50%
• Ideal (Future)	1.3	1.20	50%
Wind machines driving rotating pumps	1.2	0.80	50%

Table-6.2.1b: Peak overall Power Coefficient $(C_p\eta)_{max}$ [57]

Pumping Head	<3 m	3 m	10 m	>20 m
Wind machines driving piston pumps				
• Classical	0-0.15	0.15	0.20	0.30
• Starting nozzle	0-0.13	0.13	0.18	0.27
Wind machines driving rotating pumps				
• Mechanical transmission			0.15-0.25	
• Electric transmission			0.05-0.10	
Quality factor: 0.05 – low, 0.10 – medium, 0.15 – high.				

6.3.Design of Wind Pump Systems

Wind turbines are becoming an attractive proposition for agricultural pumping in the developing countries. For designing a wind pumping system for a particular area, water requirement per day of that area should be known.

6.3.1 Assessment of water requirements

Main applications of wind pumps in rural areas of developing countries are water supply for drinking and irrigation, with other limited end uses such as water pumping in fish breeding centers, salterns, drainage, etc.

Irrigation

Water requirements for irrigation depend on a number of factors, which need to be carefully analyzed in order to optimize the wind pumping system to the given situation. Factors which have the most direct influence on the assessment of water requirements are;

i. cropping system followed by the farmer;
ii. crop water requirements under given climatic conditions;
iii. type and condition of soil;
iv. topography of the area.

The annual cropping system followed by farmers basically reflects the seasonality of the agricultural practices as well as the crop mix during each season. The choice of cropping system would be mainly governed by the market considerations of the produce. Some typical cropping systems followed in Bangladesh are presented in Table-6.3.1. Wind pumping could be used for irrigation only during the cropping season, which coincides with the windy period in the region and also if it happens to be the season of irrigated agriculture.

Once the cropping system is identified, the net water supply for irrigation could be estimated from the data on crop water requirements. These are obtained from the Directorate of Agricultural Extension (DAE) in Bangladesh, as shown in Table-6.3.2. The gross water supply, which is also the desired wind pump output, depends on the efficiency of water conveyance through the field, which in turn depends primarily on the field canal network and soil conditions.

Table-6.3.1: Some Typical Medium Highland Cropping Systems followed in Bangladesh

Sl. No.	Crop	Season	
1.	Pulses Chilly Soyabean	October February July	January July September
2.	Chilly Vegetables	November May	May October
3.	Mustard Potato Vegetables	October December June	February February October
4.	Wheat Chilly	November March	February September
5.	Onion Vegetables Soyabean	October March July	January July September
6.	Garlic Chilly Vegetables	September February June	January May August
7.	Potato Rice (Boro) Chilly	November February May	January May September

Source: Irrigated Crop Production Manual, DAE, Bangladesh

Table-6.3.2:Irrigation Water Requirements of Medium Highland Crops Grown in Bangladesh

Crops	Crop duration (days)	Number of irrigation	Irrigation frequency (days)	Water requirement per irrigation (m^3/ha)	Daily water requirement per irrigation on rotation basis
Chilly	150	19	8	184	23
Onion	95	11	7	273	39
Garlic	90	15	6	200	33
Soybean	110	4	28	750	27
Wheat	120	5	24	700	29
Rice (Boro)	120	5	24	2150	90
Potato	100	10	10	350	35
Mustard	96	4	24	750	31
Vegetables	100	17	6	176	29

Source: Irrigated Crop Production Manual, DAE, Bangladesh

Drinking water supply

In general, drinking water requirements could be estimated as the product of the per capita consumption and the human or animal population as the case may be. Domestic water requirements per capita vary markedly in response to the actual availability of water. If there is home supply, the consumption may be five or more times greater than if water has to be collected at the public water point. Where groundwater is scarce, the per capita allocation of water will be determined more by supply constraints than by the demand. Subject to availability of water, it seems reasonable to assume a consumption rate of 40 litres per capita per day for the purpose of designing village drinking water supply schemes [28]. Typical daily water requirements for a range of livestock are presented in Table-6.3.3.

Table-6.3.3: Typical Daily Water-Requirement of Livestock [28]

Species	Litres of water per day
Camels	40 – 90
Horses	30 – 40
Cattle	20 – 40
Milch Cow	70 – 100
Sheep and Goats	1 – 5
Swine	3 – 6
Lactating	25
Poultry	0.2 – 0.3

For example, population at Patenga (5 villages) where water to be supplied by the windpump is 5000 peoples, 2000 cattle, 9000 goats and 100000 chickens.

Then present daily water demand is:

5000 People = 5000 x 40 L = 200000 Litres

2000 Cattle = 2000 x 40 L = 80000 Litres

10000 Goats = 10000 x 5 L = 50000 Litres

100000 Chickens =100000 x 0.1 L = 10000 Litres

Total Demand = 340,000 Litres

= 340 m^3

6.3.2 Hydraulic power requirements

Once the water requirements are established, the hydraulic power requirements could be estimated using the following equation [57]:

$$P_{hyd} = 0.1134\, q\, H \text{ (W)} \tag{6.3.1}$$

Where

P_{hyd} - average hydraulic power (W)

q - pumping rate (m^3/day)

H - total pumping head (m)

The total pumping head includes the static head, draw down in the well (the lowering of the water level due to pumping), and the head losses in pipes and fittings.

Data for a hypothetical water supply scheme in Bangladesh are presented as a design example in Table-6.3.4.

Table-6.3.4: Hydraulic Power Requirements in the Design Example

Total static pumping head: 20 m				System head loss: 10%	
Month	Required water output (m^3/day)	Static head (m)	Head loss (m)	Total head (m)	Average hydraulic power required (W)
January	340.00	20.0	2.0	22.0	845.24
February	340.00	20.0	2.0	22.0	845.24
March	340.00	20.0	2.0	22.0	845.24
April	340.00	20.0	2.0	22.0	845.24
May	340.00	20.0	2.0	22.0	845.24
June	340.00	20.0	2.0	22.0	845.24
July	340.00	20.0	2.0	22.0	845.24
August	340.00	20.0	2.0	22.0	845.24
September	340.00	20.0	2.0	22.0	845.24
October	340.00	20.0	2.0	22.0	845.24
November	340.00	20.0	2.0	22.0	845.24
December	340.00	20.0	2.0	22.0	845.24
Total annual water requirement : 124100 m^3/year					

6.3.3 **Available wind power resources**

Once the demand considerations are specified, the next step of the design process is to ascertain the availability of wind power resources to meet the hydraulic power demanded by the system. As wind is very often a seasonal phenomenon, it is necessary to evaluate the availability of wind power resources on a monthly basis. Wind data required for such an analysis would have to be obtained from the nearest wind measuring station such as the local meteorological station. The process of designing a wind pump system for a given location required a further steps in estimating the site wind speeds using the station potential wind speeds.

For the example considered here, wind data are taken from the wind measuring station at Patenga, Chittagong. Both potential wind speeds and the estimated site wind speeds are presented in Table-6.3.5. Specific wind power at the site could be calculated as the available wind power divided by the rotor area ($P_{wind}/0.5\ \rho V^3$).

Table-6.3.5: Wind Power Resources in the Design Example

Location: Patenga, Chittagong		Assumed wind pump hub height: 20 m		
Month	Average potential wind speed at 10 m height (m/s)	Average wind speed at hub height (m/s)	Density of air (kg/m^3)	Specific wind power (w/m^2)
January	5.10	6.22	1.2	144.39
February	5.20	6.34	1.2	152.90
March	6.04	7.37	1.2	240.19
April	6.49	7.92	1.2	298.08
May	6.94	8.47	1.2	364.59
June	7.12	8.69	1.2	393.74
July	7.54	9.20	1.2	467.21
August	7.00	8.54	1.2	373.70
September	6.13	7.48	1.2	251.11
October	5.68	6.93	1.2	199.69
November	5.50	6.71	1.2	181.27
December	4.84	5.91	1.2	123.86

6.3.4. Determining the design month

There are two options for operating wind pump: either as a stand alone system providing water throughout the year or a fuel saver operated during the windy months to reduce the fuel consumption of the water supply system equipped with an engine-driven water pump set.

The sizing methodology for a wind pump in the fuel saver mode is an iterative process , going from sizing to economic analysis, and back to sizing, until the most cost effective combination of the engine-pump set and wind pump is established.

For the example considered in this chapter, a storage tank of three days capacity or 120 m^3 is chosen. In the case of a stand alone wind pumping system, the requirement is that the system should provide output during the entire year without any back-up system. Therefore, the wind pump size is chosen on the basis of the "design month", which is the month during which the ratio of the hydraulic power to the specific wind power is highest. If the hydraulic power demand is constant throughout the year (e.g. in drinking water supply schemes), then the design month is essentially the month having the lowest wind power potential.

This ratio has the dimension of an area and will be referred as the "reference area". It is related to the rotor area needed to capture sufficient power from the wind to meet the demand. Results of this computation as applied to the design example are presented in Table-6.3.6, and the design month is December.

Table-6.3.6: Calculation of the Design Month for Wind Pump Sizing in the Design Example

Month	Average hydraulic power, P_{hyd} (W)	Average wind speed at hub height (m/s)	Specific wind power, P_{wind} (W/m^2)	Reference Area P_{hyd}/P_{wind} (m^2)	Design months
January	845.24	6.22	144.39	5.85	
February	845.24	6.34	152.90	5.52	
March	845.24	7.37	240.19	3.52	
April	845.24	7.92	298.08	2.83	
May	845.24	8.47	364.59	2.31	
June	845.24	8.69	393.74	2.14	
July	845.24	9.20	467.21	1.80	
August	845.24	8.54	373.70	2.26	
September	845.24	7.48	251.11	3.36	
October	845.24	6.93	199.69	4.23	
November	845.24	6.71	181.27	4.66	
December	845.24	5.91	123.86	6.82	****

6.3.5 Sizing the wind pump

Prior to determining the size of the wind pump, it is necessary to outline the system demand characteristics in relation to output: high output or high availability. Equally important is the choice of the technology: modern light weight designs with high maintenance duty or classical wind pumps offering greater reliability and prolonged unattended operation.

Experience so far indicates that most modern designs have yet to prove their ability to withstand the conditions of deep well pumping. According to available experience, most modern wind pumps are suitable for low head pumping, where structural loads are manageable and frequent maintenance is more easily carried out, than in deep well pumping. Therefore, it is advisable to consider classical wind pumps when a choice is made on the technology for deep well wind pumping. Accordingly, classical type of a wind pump is chosen for the case in the example.

Sizing of the wind pump is basically the determination of the required diameter of the rotor. This could be done using equation 6.2.2, or more easily from the nomogram given in Figure-6.3.1:

Step-1: Locate the reference area along the X-axis on the graph on the right side. In the case of the example, the reference area is taken as 6.82 m^2.

Step-2: Move upwards to intercept the line conforming to the chosen energy production coefficient C_E (values could be chosen by referring to Table-6.2.1). Chose 0.4 for classical wind pump for deep well application: H=20 m.

Step-3: Move horizontally to intercept the lines of peak overall power coefficient on the graph on the left-hand side. Chose $(Cp\eta)_{max} = 0.3$.

Step-4: Move downwards to intercept the X-axis referring to the rotor diameter. This results in $D_{rotor} = 7.75$ m.

When selecting a 7.75 m wind pump from available commercial, designs, it might become necessary to alter the hub height to conform to standard designs.

When selecting the appropriate pump for the chosen machine, it is necessary to evaluate the design wind speed V_d. Choosing $V_d/V_{av} = 0.6$ from Table 6.2.1 and the average wind speed during the design month equal to 5.91 m/s, the design wind speed works out to 3.55 m/s. Referring to the nomogram in Figure-6.3.2, the following steps should be taken for selection of the pump size:

Step-1:Locate the rotor diameter on the X-axis on the graph on the right side.

Step-2:Move upwards to intercept the lines of design wind speeds. The lowest design wind speed marked is 4 m/s, which is close enough to the value of 3.55 m/s in the example.

Step-3:Move to the left to intercept the speed of operation represented by the product of TSR x gear ratio(i). Choose TSR of classical wind pumps as unity and gear ratio of back-geared transmission as 0.3. Substituting for the chosen $(Cp\eta)_{max}$ of 0.3, the result is 0.25.

Step-4:Move downwards to lines of total pumping head, which is 22 in this case, and moving horizontally to the right gives the design stroke volume of approximately 22.50 litres. This might have to be increased by dividing by the volumetric efficiency, which is typically 0.9. The resulting geometrical stroke volume would then be 25 litres.

The diameter of the pump could be established from the supplier's catalogues, depending on the stroke adjustment scale and standard pump diameters.

6.3.6 Sizing the wind pump for Patenga, Bangladesh

Empirical equation developed for wind pump rotor sizing for Bangladesh is given below :

$$HQ = C \times D^2 \times V^3 \tag{6.3.1}$$

Where,

C = Constant (here, 8.47)

HQ = Volume-Head product (m^4/day)

Q = Water requirement per day (m^3/ day)

H = Water tank height (m)

D = Diameter of the rotor (m)

V = Average wind velocity (m/s)

When the water requirement per day for a particular region is known, then the following steps could easily do rotor sizing.

Sizing of the wind pump for Patenga, Bangladesh could be carried out using equation 6.3.1, or more easily from the nomogram given in Figure-6.3.3.

Step-1: Locate the volume-head product along the Y-axis on the graph on the left side. In the case of the example, the volume-head product is 7480 m^4/day.

Step-2: Move horizontally right to intercept the line for the average wind velocity 5.91 m/s.

Step-3: Move downward to intercept the X-axis referring to the rotor diameter. This results in D = 2.07 m.

When selecting a 2.07m wind pump from available commercial, designs, it might become necessary to alter the hub height to conform to standard designs.

Another way, sizing of the wind pump for Patenga, Bangladesh could be carried out using equation 6.3.1, or more easily from the nomogram given in Figure-6.3.4, if the average wind velocity (m/s) is known:

Step-1: Locate the average wind velocity along the X-axis on the graph on the right side. In the case of the example, average wind velocity is taken as 5.91 m/s.

Step-2: Move upwards to intercept the line for A =1 m^2.

Step-3: Move horizontally left to intercept the Y-axis referring to the volume-head product. This results in HQ = 1750 m^4/day.

When selecting a wind pump from available commercial, designs, it might become necessary to alter the hub height to conform to standard designs.

The diameter of the pump could be established from the supplier's catalogues, depending on the stroke adjustment scale and standard pump diameters.

6.3.7 Sizing of storage tank

In wind-powered water supply systems, there is a need for storage of water for two basic reasons: to maintain supply during windless periods (Lull periods) and to store water that is pumped during the period of low consumption. For example, in an irrigation system water is used for irrigation only during the day time, whereas pumping may go on throughout the night. Thus, storage of water during the night would enhance the command area of the cultivation. For this purpose, a storage tank of about half the typical daily output would be sufficient. But, if it is necessary to guarantee the supply of water during intermittent windless days as well, then the storage tank capacity would have to be considerably higher and would depend on the probability of occurrence of such events. In most locations, it is very rare for the wind to be too low to operate the pump more than three days, so a tank sized for three days would normally be adequate.

In practice, however, for example, the use of large water storage tanks to account for windless day is rare among the farmers. Although water scarcity could seriously hamper the farming operations, most farmers are unable to afford the high cost of tank construction. Instead, farmers often use an engine pump, either his own or taken on rent, to meet the water deficit during windless days. Thus, the final choice of the storage tank or an alternative power source depends very much on the cost involved and other factors such as the availability of alternative pumping systems within close proximity of the users.

In the case of wind pumping for drinking water supply, a storage tank is an indispensable item, at least from the viewpoint of design of the distribution piping system. Such systems are always designed for a given range of supply head variations and any fast fluctuating outputs (such as the direct output from a wind pump) could cause considerable technical problems.

On the user side, there is also the possibility of having periods of peak demand, when the demand may exceed the supply and a storage tank of a pre-determined size would be essential to meet such situations. The tank could then store water pumped during the periods of low consumption as well as during the times of strong winds to meet such situations. The sizing of the tank may also take into account the supply of water during windless days. Although it might involve a high cost, such expenditures are well within the capacity of community drinking water supply projects. The storage capacity is calculated as follows:

Storage capacity = Daily water requirement x Longest lull Period x Safety factor

A safety factor of two is recommended. The example considered in this text, a storage tank of

three days capacity or 960 m^3 is chosen.

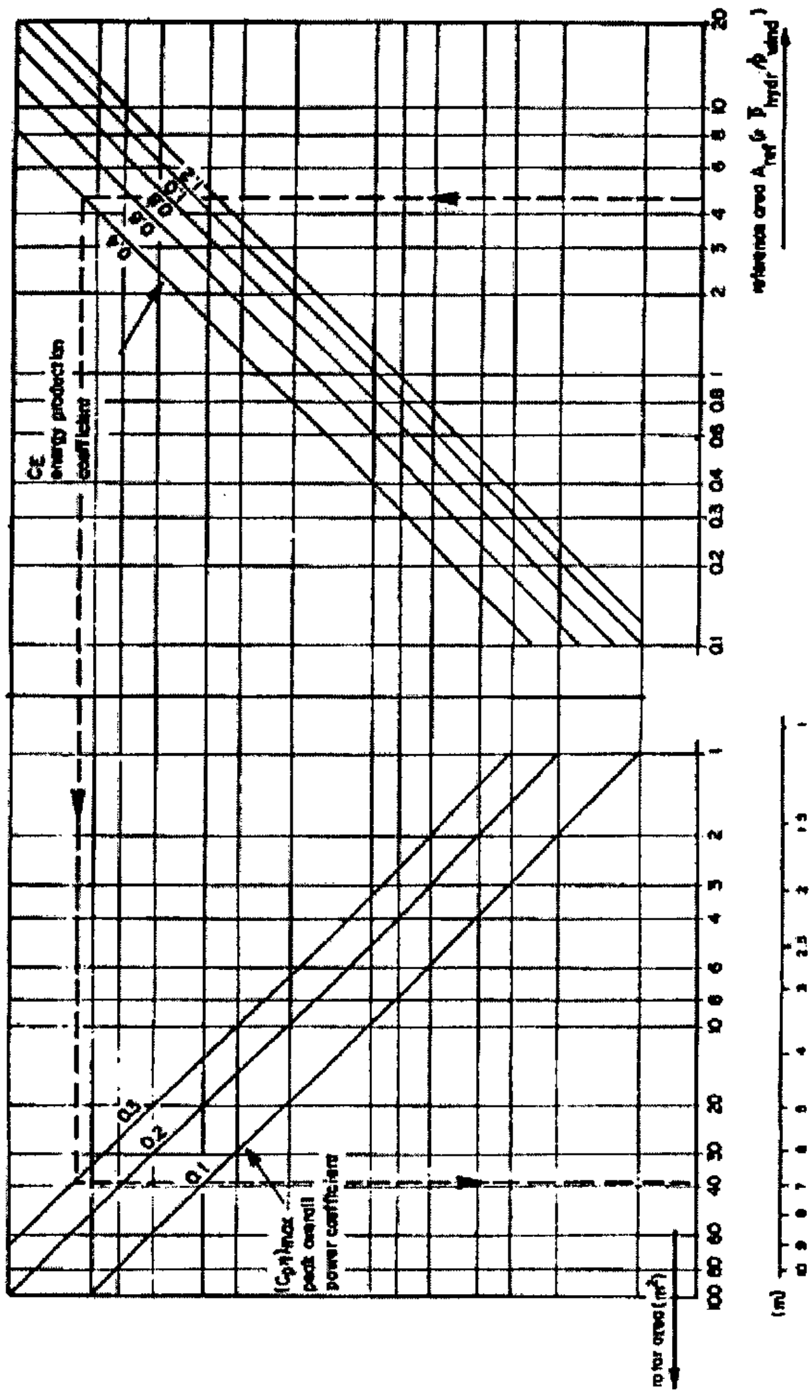

Figure 6.3.1 Nomogram to Determine the Rotor Size of a Wind Turbine [57]

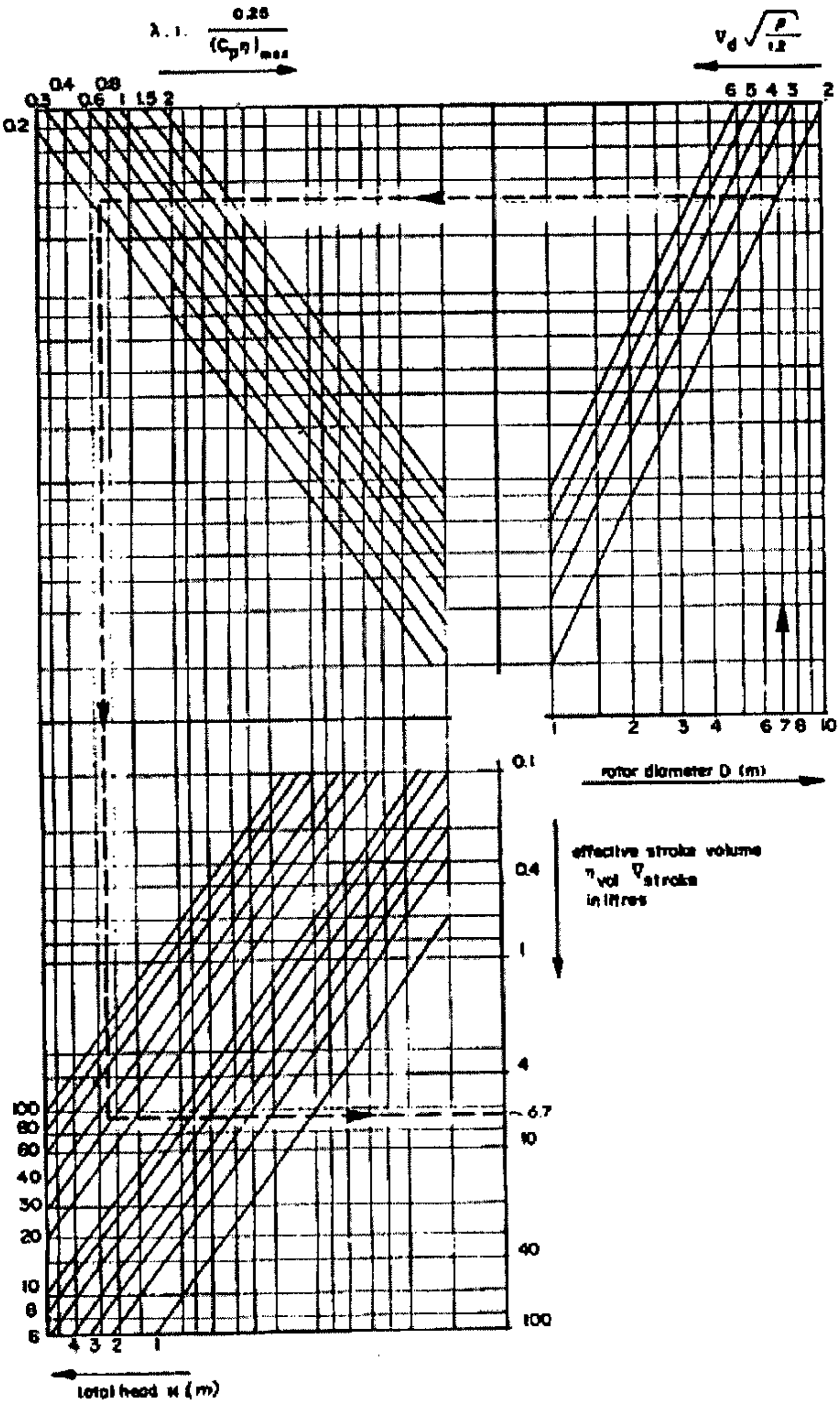

Figure 6.3.2 Nomogram to Determine the Size of a Wind Pump [57]

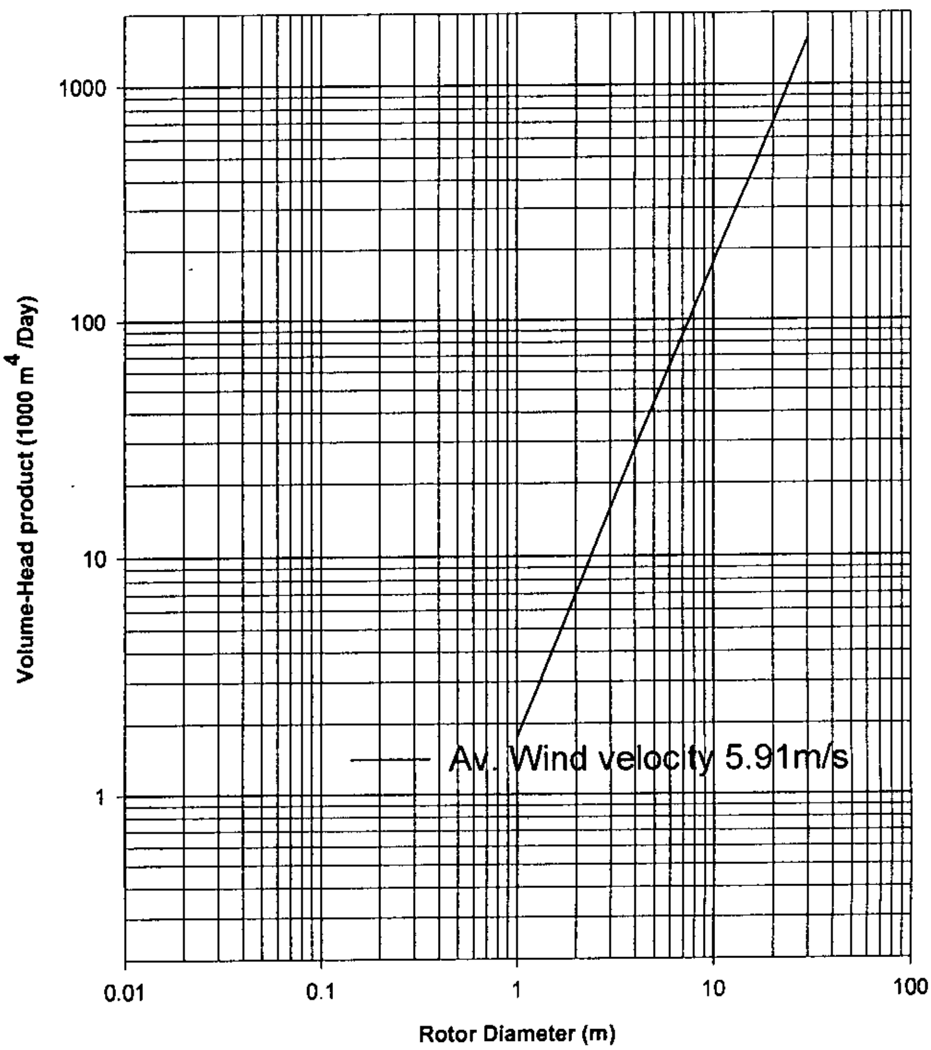

Figure 6.3.3 Wind Pump Rotor Sizing Nomogram for Patenga, Bangladesh

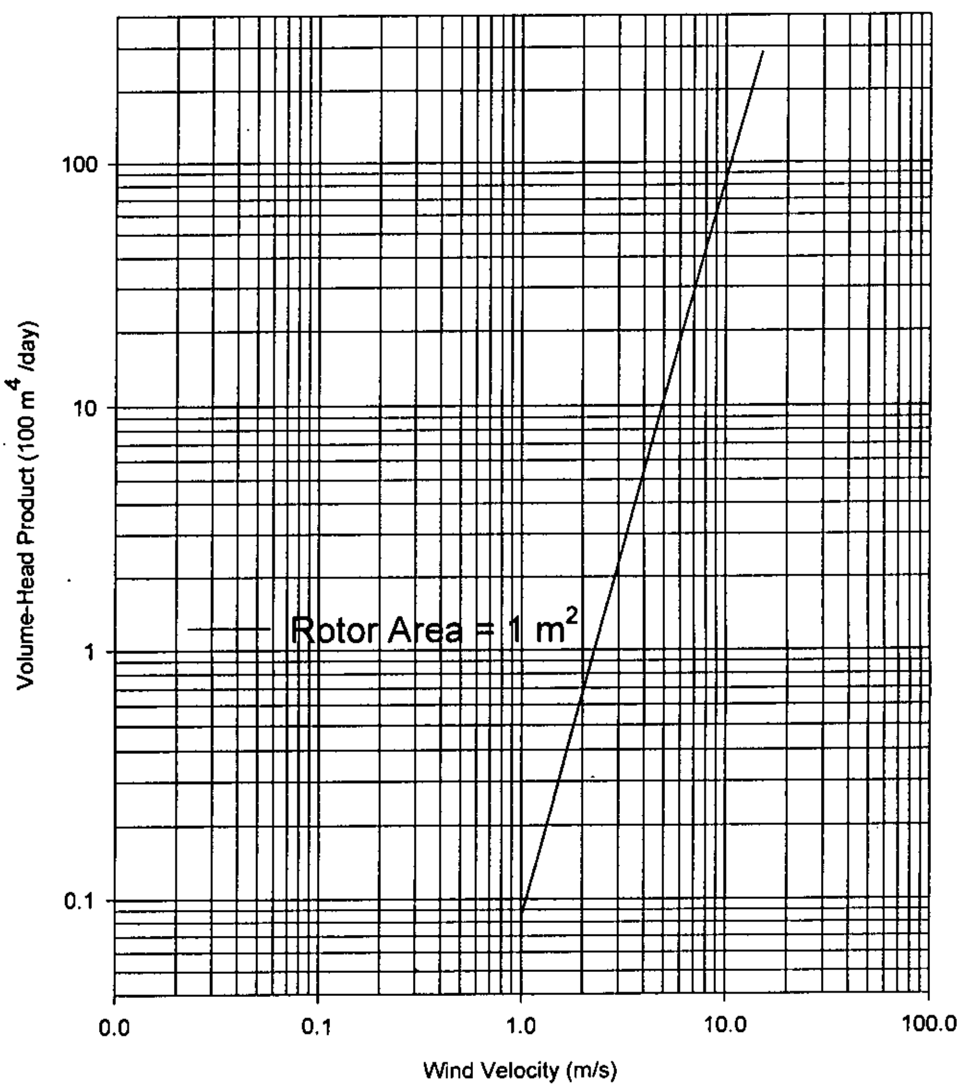

Figure 6.3.4 Nomogram for Wind Pump Rotor Sizing

CHAPTER 7

CONCLUSIONS AND RECOMMENDATIONS

7.1 Conclusions

In regard to the present experimental investigation and design analysis of the horizontal axis wind turbines the following conclusions are drawn:

1. Winds are available in Bangladesh during the monsoon and one to two months before and after the monsoon in general. However, in some regions at 20 meters height, the wind speed is satisfactory for pumping water and generating electricity.

2. At Patenga of Bangladesh wind speed available in the range of about 6.0 m/s to 9.0 m/s almost throughout the year, which is prospective for extraction of power.

3. For horizontal axis wind turbines, classical strip theory has been found to give adequate results under normal operating conditions near the design tip speed ratio. At both high and low tip speed ratios, however, the wind turbine may operate in flow conditions, which are not easily analyzed by classical theory.

4. It is observed that there is a good correlation between the calculated results performed by the present method and those done by references [38, 24].

5. The wind tunnel experimental results obtained from the various wind turbine model consisting of 2-blades, 3-blades and 4-blades show reasonable agreement with the calculated results done by classical theory.

6. A nomogram and an empirical relation to design the rotor size of a horizontal axis wind turbine and pump size have been developed for a particular region Patenga, Bangladesh. The same design procedure can be applied for any prospective wind regime.

7.2 Recommendations

From the knowledge developed while conducting the experimental investigation and doing analysis of the horizontal axis wind turbine, the following recommendations are made:

1 For the design of a horizontal axis wind turbine the combined influence of coning, tilting, yawing and different wind conditions such as, wind shift, wind shear and tower shadow effect may be studied.

2 Estimation of the rotor blades loading and stresses developed in the deformed blade due to blade flexibility may also be studied.

3 Mass distribution of the blade calculation by the present method is not possible and manufacturing of these blades may be difficult. Linearization or other method may be applied for this purpose.

4 For actual design the flapping and lagging mode shapes with frequencies may be taken into consideration for study.

5 Cost–benefit ratio of wind pumping system with the other existing system can be studied.

REFERENCES

[1] Ahmad, D. (1983)."***Design of a Simple, Low- Lift, Wind Powered Pump for Rural Use in Thailand***", Journal of Agricultural Mechanization in Asia, Africa and Latin America. Vol.14, No.1: pp 20-26.

[2] Alam , M. M. and Burton, J. D. (1998). "***The Coupling of Wind Turbines to Centrifugal Pumps*** ", Journal of Wind Engineering. Vol.22, No.5: pp 223- 234.

[3] Aldoss, T.K. and Obeidat, K.M. (1987). "***Performance Analysis of Two Savonius Rotors Running Side by Side using The Discrete Vortex method***". Journal of Wind Engineering, Vol.11, No.5.

[4] Beurskens, H. J. M. (1978). "***Feasibility Study of Windmills for Water Supply in Mara Region, Tanzania***", Steering Committee on Wind-Energy for Developing Countries, P.O. Box 85/ Amersfoort, The Netherlands.

[5] Beurskens, H.J.M. (1980). "***Low Speed Water Pumping Wind Mills: Rotor Tests and Overall Performance***", Proc. of 3rd Int. Symp. on Wind Energy Systems, Copenhagen, Denmark, August 26-29,pp K2 501-520.

[6] Bowden, G.J. and McAleese, S.A. (1984). "***The Properties of Isolated and Coupled Savonius Rotors***", Journal of Wind Engineering. Vol.8, No.4, pp. 271-288.

✓[7] Burton, J. D.; Hijazin, M. and Rizvi, S. (1995)." ***Wind and Solar Driven Reciprocating Lift Pumps***", Journal of Wind Engineering. Vol.15, No.2: pp 95-108.

[8] Burton, J.D. and Ghorap, A. (1995)."***Seals and Sealing for Wind Driven Lift Pumps***", Journal of Wind Engineering. Vol.19, No.2: pp 67-81.

[9] Chowdhry, S.C.; Ramana Rao, B. V. and Sharma P. (1981)."***Performance of Low-cost Sail-Wing Windmill***", Journal of Agricultural Mechanization in Asia, Africa and Latin America. Vol.12, No.1: pp 66-68.

[10] Clerk, R. N.; Nelson, V.; Barieau, R. E. and Gilmore, E. (1981)." ***Wind Turbine for Irrigation pumping***", Journal of Energy. Vol.5, No.2: pp 104-108.

[11] Currie, I.G. (1974). "***Fundamental Mechanics of Fluids***", McGraw Hill.

[12] Fanucci, J.B. and Watters, R.E. (1976). "***Innovative Wind Machines: The Theoretical Performance of a Vertical-Axis Wind Turbine***", proceedings of the Vertical-Axis Wind Turbine Technology Workshop, Sandia Laboratories, SAND 76-5586, pp. III-61-95.

✓[13] Garman P., (1986). ***Water Current Turbines: A Fieldworker's Guide***, Intermediate Technology Publications, London.

[14] Gavalda, J.; Massons, J. and Diaz, F. (1991). ***"Drag and Lift Coefficients of the Savonius Wind Machine"***, Journal of Wind Engineering. Vol.15, No.5, pp. 240-246.

[15] Hirsch, Ch.; Derdelinckx, R. and Islam, M.Q.(1984).*"**A Theoretical Investigation of the Design of a Horizontal Axis Wind Turbine**"*, Proceedings of the European Wind Energy Conference, Hamburg, October 22-26.

[16] Holme, O. (1976). "***A Contribution to the Aerodynamic Theory of the Vertical Axis Wind Turbine",*** proceedings of the International Symposium on Wind Energy Systems, Cambridge, pp. C4-55-72.

[17] Hossain, M. A. and Islam, M.Q. (1982)."***Sailwing Rotor for Pumping Water in Bangladesh***", Renewable Energy Review Journal. Vol.4, No.1: pp 29-35.

[18] Huda, M.D.; Selim, M.A.; Islam, A.K.M.S. and Islam, M.Q.(1992). "***The Performance of an S-shaped Savonius Rotor with a Deflecting Plate***", RERIC Int. Energy Journal. Vol.14, No.1, pp. 25-32.

[19] Hussain, M.; Alam, S.; Reza,K.A. and Sarkar, M. (1986). "***A study of wind speed and wind energy available in Bangladesh",*** Journal of Energy Conversion Management. Vol.26 No.3/4, pp 321-327.

[20] Islam, A.K.M.S.; Islam, M.Q.; Mandal, A.C. and Razzaque, M.M. (1993). "***Aerodynamic Characteristics of a Stationary Savonius Rotor***", RERIC Int. Energy Journal. Vol.15, No.2, pp.125-135.

[21] Islam, A.K.M.S.; Islam, M.Q.; Razzaque, M.M. and Ashraf, R.(1995). "***Static Torque and Drag Characteristics of an S-shaped Savonius Rotor and Prediction of Dynamic Characteristics"***, Journal of Wind Engineering. Vol.19, No.6. pp 363-370

[22] Islam, M.Q.; Islam, S.M.N.; Islam, A.K.M.S. and Razzaque, M.M.(1995). "***Application of Wind Energy for Irrigation Bangladesh***", Journal of Agricultural Mechanization in Asia, Africa and Latin America. Vol.26, No.2: pp 24-28.

[23] Islam, M.Q.; Mandal, A.C. and Islam, A.K.M.S. (1993)."***The prospect of Wind Energy Application in Bangladesh",*** Journal of Mechanical Engineering research and developments. Vol.16, pp 27-40.

[24] Islam, M.Q (1986), "***A theoretical Investigation of the Design of Horizontal-Axis Wind Turbines",*** Ph. D. Thesis.

[25] Jansen W.A.M. and Smulders P.T.,(1977). "***Rotor Design for Horizontal Axis Windmills"***, Steering Committee for Windenergy in Developing Countries (SWD), P.O. Box 85 / Amersfoort / The Netherlands.

[26] Jones, C.N.; Littler, R.D. and Manser, B.L. (1979). ***"The Savonius Rotor Performance and flow"***, Proceedings of 1st British Wind Energy Association (BWEA) Workshop.

[27] Khurmi, R. S. (1987). ***A Textbook of Hydraulics, Fluid Mechanics and Hydraulic Machines***. Published by S. Chand and Company(Pvt.) Ram Nagar, New Delhi - 110055.

√[28] Lancashire, S., Kenna, J. and Fraenkel, P., (1987). ***Wind pumping Handbook***. IT publications.

[29] Lysen, E. H.; Bos, H.G. and Cordes, E.H. (1978). ***"Savonius Rotors for Water Pumping"***, SWD publication, P.O. Box 85, Amersfoort, The Netherlands.

[30] Lysen, E.H. (1983). ***"Introduction to Wind Energy"***, 2nd. Edition. SWD Publication, P.O. Box 85, Amersfoort, The Netherlands.

[31] Mahar, S.A. (1983)." ***Use of Wind Power in New Zealand: Its Scope in Pakistan***", Journal of Agricultural Mechanization in Asia, Africa and Latin America. Vol.14, No.2: pp 77-81.

√[32] Mishra, S.P. and Sharma, K.N. (1992)." ***Utilization of Windmill in Coastal Belt of Orissa",*** Journal of Agricultural Mechanization in Asia, Africa and Latin America. Vol.23, No.4: pp 47-49.

[33] Noll, R.B. and Ham, N.D. (1980). "***Analytical Evaluation of the Aerodynamic Performance of a High-Reliability Vertical-Axis Wind Turbine",*** Proceedings of American Wind Energy Association (AWEA) National Conference.

[34] Panda, R.K, and Clerk, R.N.(1999). "***Stochastic Study of Windpumps with Reservoir in Southern High Planes",*** Journal of Energy Engineering. Vol.125, No.3: pp 79-93.

[35] Paraschiviu, I.; Fraunie, P. and Beguier, C. (1985). "***Stream tube Expansion Effects on the Darrieus Wind Turbine",*** Journal of Propulsion. Vol.1, No.2, pp. 150-155.

[36] Paraschivoiu, I. and Delclaux, F. (1983). "***Double Multiple Streamtube Model with Recent Improvements***", Journal of Energy. Vol.7, No.3, pp. 250-255.

[37] Park, J. (1975). "***Simplified Wind Power System for Experimenters***", Helion Inc., California, USA.

[38] Puthoff R. L. , Collins J. L. and Wolf R.A. (1974), ***"Installation and Checkout of the DOE/NASA MOD-1 2000 -kW Wind Turbine***", National Aeronautics and Space Administration, Lwis Research Center, Cleveland, Ohio.

[39] Rahman, M.F. (1995), "***Wind Energy Prospects in Bangladesh***", Paper presented in Seminar on Fluid Mechanics Research, Dec.27-28, Dhaka, Bangladesh.

[40] Rahman, M.F.(1996). "***Prospects of wind energy in Bangladesh***", Proceedings of World Renewable Energy Congress (WREC), 15-21 June, Denver,Colorado, USA, PP 806- 809.

[41] Ramana Rao, B. V.; Sharma P. and Chowdhry, S.C.(1985)."***Design characteristics and Performance of Wind Mills for Pumping Irrigation Water***", Journal of Agricultural Mechanization in Asia, Africa and Latin America. Vol.16, No.2, pp 27-29.

[42] Robert, G.; Kortenkamp, R. and Twele, J. (1987)."***A Simple Method for Near Optimum Design of Wind Turbines with Centrifugal Pumps"***, Journal of Wind Engineering. Vol.11, No.5, pp 293- 312.

√[43] Sarkar, M. and Hussain, M. (1991). ***"The potential of wind electricity generation in Bangladesh"***, Renewable energy journal. Vol.1 No.5/6, pp 855-857.

[44] Sawada, T.; Nakamura, M. and Kamada, S. (1986). "***Blade Force measurement and Flow Visualisation of Savonius Rotors***", Bull. JSME. Vol.29, pp. 2095-2100.

[45] Siddig, M. H. (1996)."***Design Optimization of Wind- Powered Piston Pumps",*** Journal of Wind Engineering. Vol.20, No.2: pp 63- 71.

√[46] Siddig, M. H. (1997). "***The Feasibility of Using Wind-Pumps in Zimbabwe***". Journal of Wind Engineering". Vol.21, No.4: pp 227- 236.

[47] Sivasegaram, S. and Sivapalan, S. (1983). "***Augmentation of Power in Slow Running Vertical-Axis Wind Rotors Using Multiple Vanes***", Journal of Wind Engineering. Vol.7, No.1.

[48] Smulders , P. T.; Alam, M.M. and Burton, J. D. (1991)." ***Wind rotors and rotodynamic pumps"***, Proceedings of Wind energy technology and Implementation, Amsterdam, European Wind Energy Conference (EWEC), pp 692-696.

[49] Special Issue on Windpumps, (1993). ***Renewable Energy for Development***. Vol. 6 (1). Stockholm Environmental Institute Newsletter.

[50] Strickland, J.H. (1975). "***The Darrieus Turbine: A Performance Prediction Model Using Multiple Stream tubes***", Sandia Laboratories Report, SAND75-0431.

[51] Suresh, R. and Block, D.S. (1998). "***Field Testing of Geared Type Deep Well Wind pumps in India***", Journal of Wind Engineering. Vol.22, No.2: pp 117- 129.

[52] Swift, R. H., (1987). "***On Maximizing the Long-Term Efficiency of Water Pumping Windmills***", Journal of Wind Engineering. Vol.11, No.5: pp 277- 292.

[53] Templin, R.J. (1974). "***Aerodynamic Performance Theory for the NRC Vertical-Axis Wind Turbine***", National Research Council of Canada, Report LTR-LA-160.

[54] Vries, O. (1979). "***Fluid Dynamics Aspects of Wind Energy Conversion***", NATO Advisory Group for Aerospace Research and Development, The Netherlands, July.

[55] Wilson, R.E. (1978). "***Vortex Sheet Analysis of the Giromill***", ASME Journal of Fluids Engineering. Vol.100, No.3, pp.340-342.

[56] Wilson, R.E. and Lissaman, P.B.S. (1974). "***Applied Aerodynamics of Wind Power Machines***", Oregon State University, USA.

[57] ***Wind-powered Water Pumping in Asia and The Pacific***.(1991). Economic and Social Commission For Asia and Pacific, United Nations, New York.

[58] Yongfen, W. (1995)."***The Development of Small Wind-Solar Generating Systems in China***", Journal of Wind Engineering. Vol.19, No.1: pp 17- 19.

APPENDICES

Appendix -A : Selection of Design Parameters

Appendix –A$_1$ Determination of Minimum C_d / C_l Ratio

airfoil name	geometrical description	$(C_d/C_l)_{min}$	α^o	C_l
sail and pole	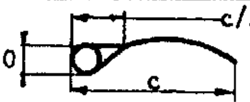 c/10, c/3, c	0.1	5	0.8
flat steel plate		0.1	4	0.4
arched steel plate	 f f/c=0.07	0.02	4	0.9
	f/c=0.1	0.02	3	1.25
arched steel plate with tube on concave side	 d, d<0.1c f/c=0.07	0.05	5	0.9
	f/c=0.1	0.05	4	1.1
arched steel plate with tube on convex side	 f/c=0.1	0.2	14	1.25
sail wing	 cloth or sail, c/10, tube, steel cable	0.05	2	1.0
sail trouser $f/c \approx 0.1$ $d_{tube} \approx 0.6f$	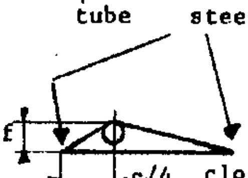 f, c/4, cloth or sail	0.1	4	1.0
NACA 4412	see appendix II	0.01	4	0.8
NACA 23015	see Lit(I) in appendix I	0.01	4	0.8

Appendix –A_2 Determination of Design Lift Coefficient and Design Angle of Attack

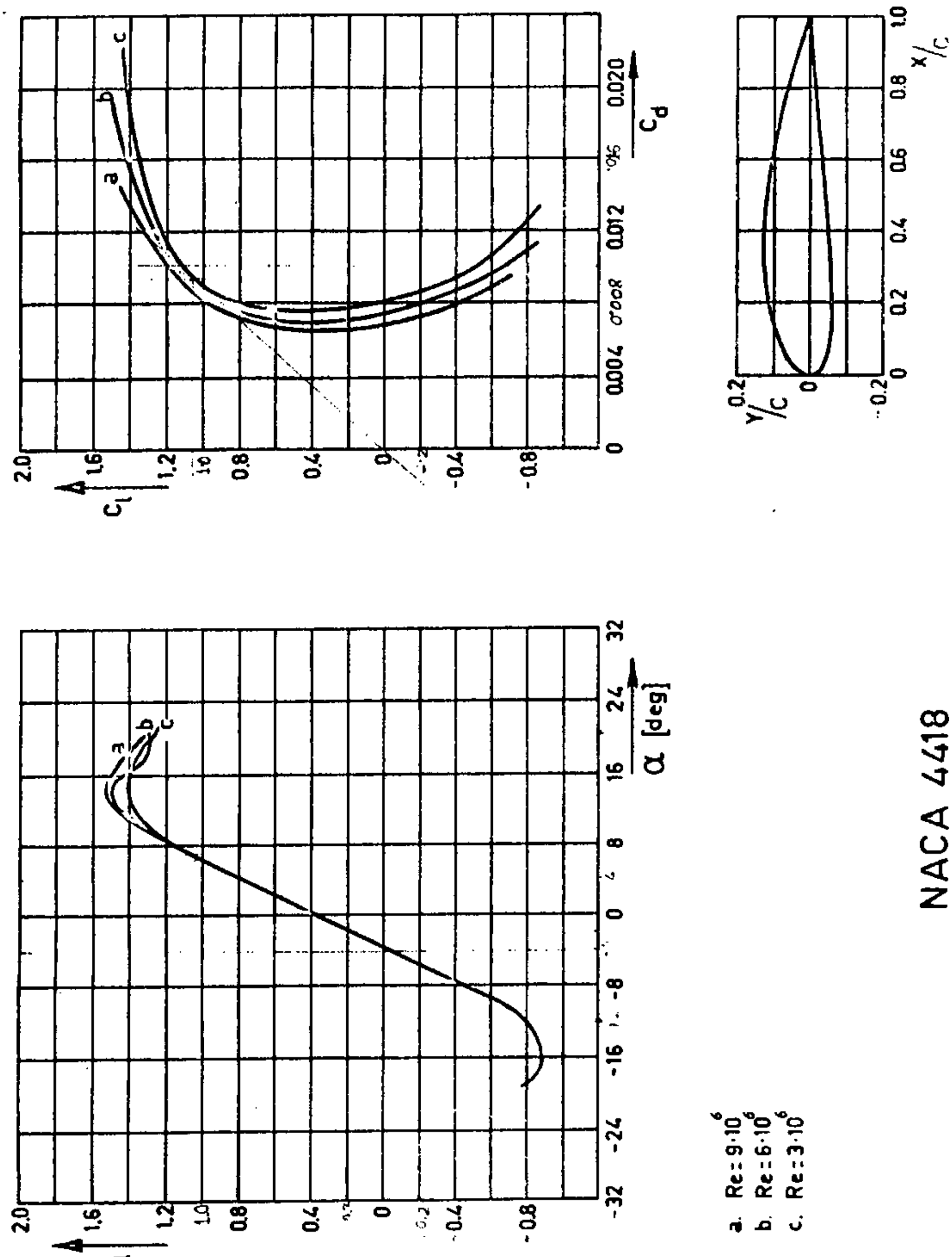

Appendix –A_3 Determination of Design Power Coefficient (C_p)

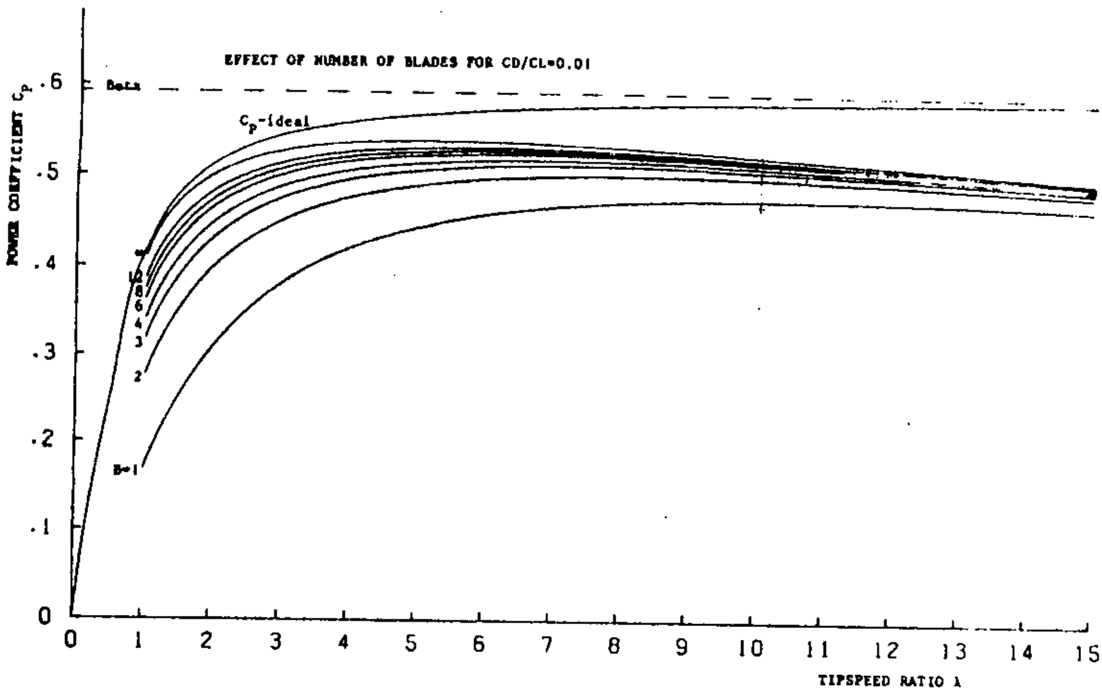

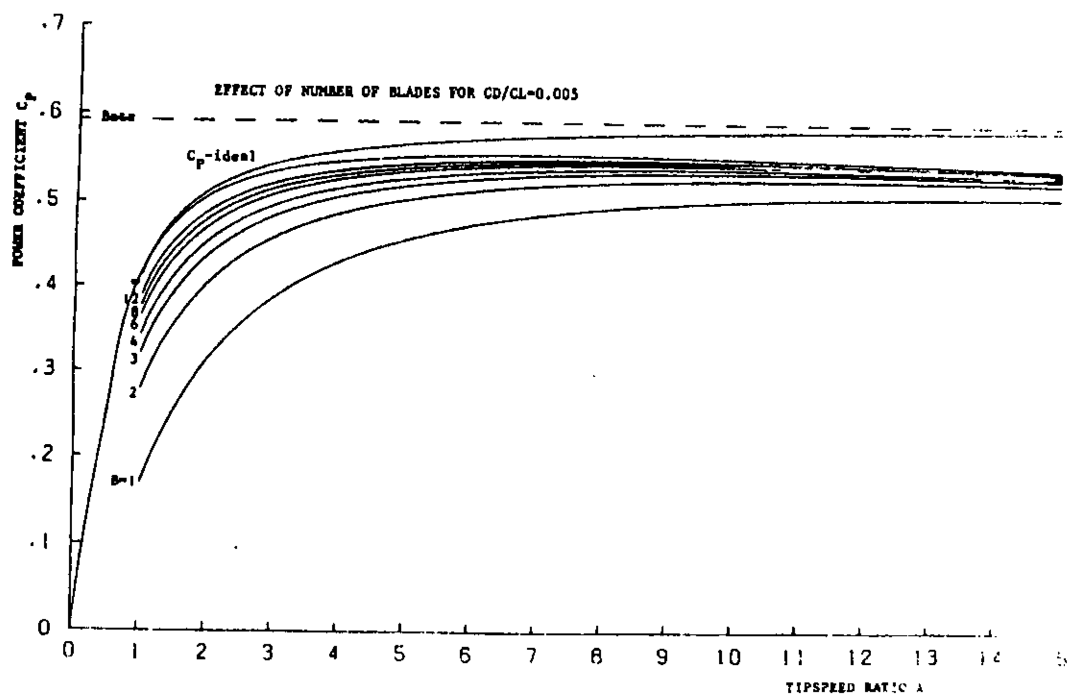

Appendix –A$_4$: Determination of Maximum Power Coefficient (C_p)

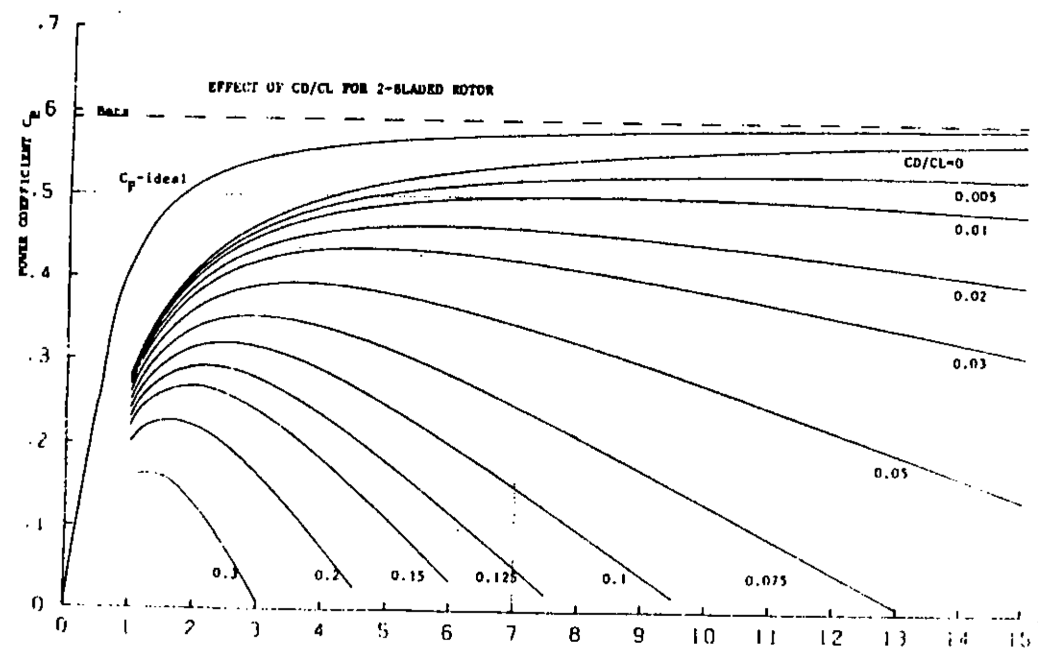

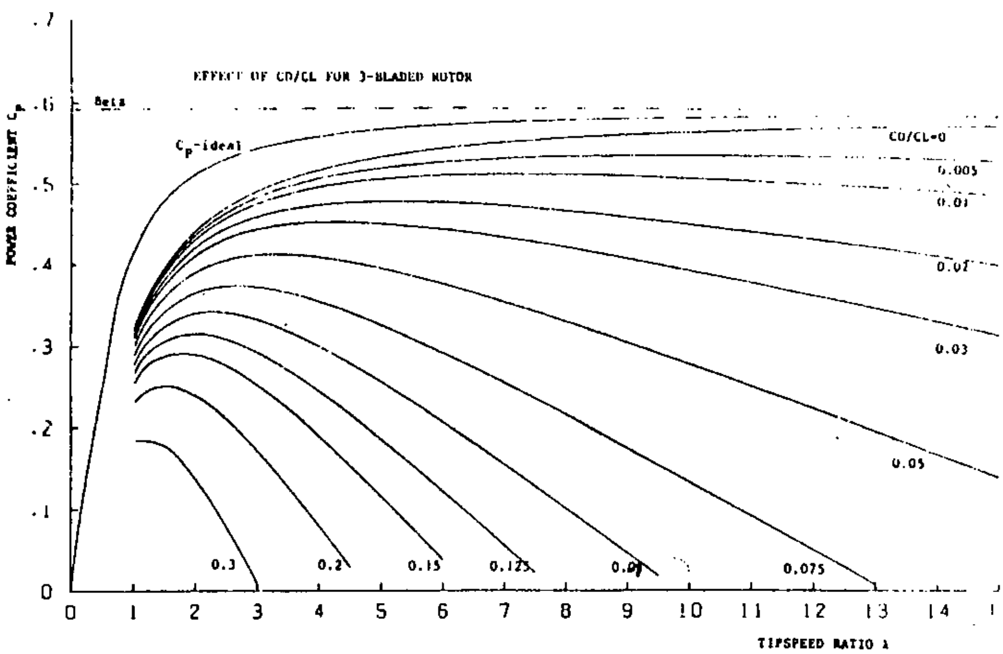

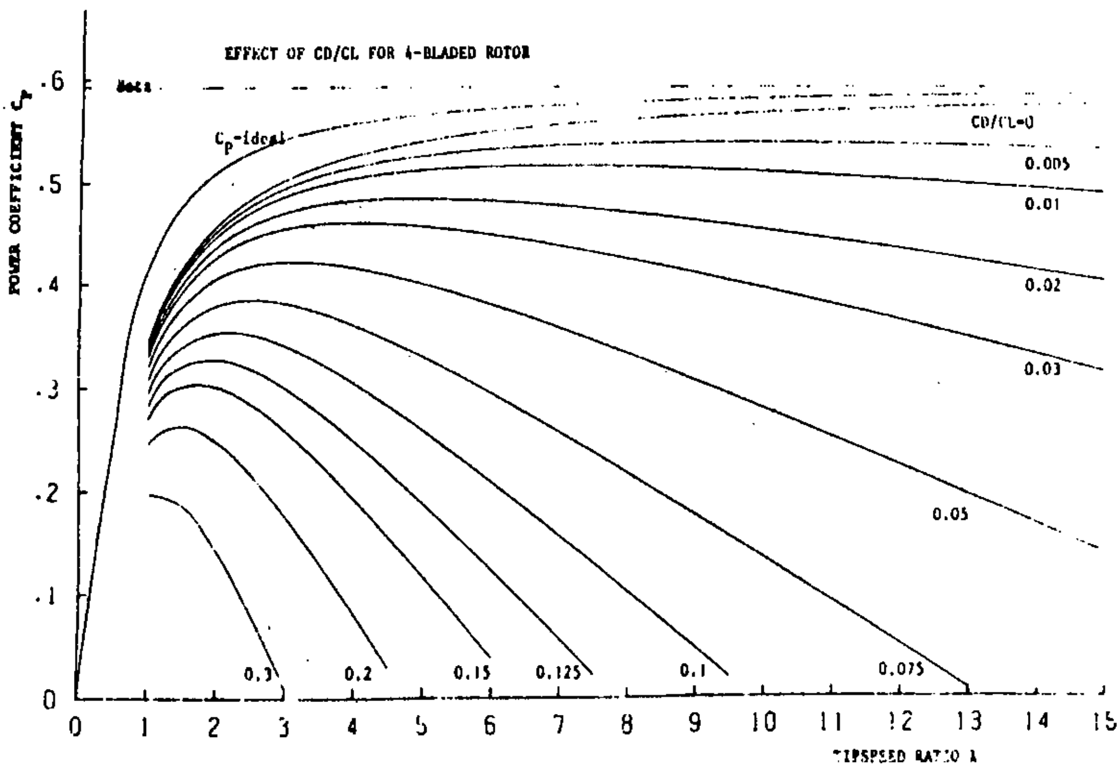
EFFECT OF CD/CL FOR 4-BLADED ROTOR
POWER COEFFICIENT C_p
TIPSPEED RATIO λ
Betz
C_p-ideal
CD/CL=0
0.005
0.01
0.02
0.03
0.05
0.075
0.1
0.125
0.15
0.2
0.3
0
.1
.2
.3
.4
.5
.6
0 1 2 3 4 5 6 7 8 9 10 11 12 13 14 15

APPENDIX-B: EXPERIMENTAL DATA

Appendix-B_1: Experimental Data for 2-Blade HAWT Model

Airfoil = NACA 4418, Number of Blade = 2, Blade Setting Angle, $\theta_p = 0^0$

Theoretical			Experimental		
Tip Speed Ratio (λ)	Torque Coefficient (C_Q)	Power Coefficient (Cp)	Tip Speed Ratio (λ)	Torque Coefficient (C_Q)	Power Coefficient (Cp)
1.11	0.00	0.00	8.50	0.02	0.17
1.59	0.02	0.02	8.30	0.02	0.19
2.06	0.02	0.03	8.00	0.03	0.25
2.54	0.02	0.06	7.50	0.04	0.26
3.01	0.03	0.09	7.00	0.04	0.30
3.49	0.03	0.11	6.45	0.04	0.27
3.97	0.04	0.16	6.29	0.05	0.29
4.44	0.05	0.20	6.00	0.04	0.26
4.92	0.05	0.24	5.84	0.05	0.27
5.39	0.05	0.27	5.68	0.04	0.24
5.87	0.05	0.30	5.51	0.04	0.20
6.35	0.05	0.32	5.00	0.04	0.19
6.82	0.05	0.33	4.60	0.04	0.17
7.30	0.04	0.32	4.30	0.03	0.13
7.77	0.04	0.30	4.00	0.03	0.12
8.25	0.03	0.28			
8.73	0.03	0.25			
9.20	0.02	0.22			
9.68	0.02	0.18			
10.15	0.01	0.14			
10.63	0.01	0.12			
11.11	0.01	0.08			
11.58	0.01	0.06			
12.06	3.00e-3	0.04			
12.54	2.00e-3	0.03			
13.01	2.00e-3	0.02			
13.49	1.00e-3	0.01			
13.65	1.00e-3	0.01			

Airfoil = NACA 4418, Number of Blade = 2, Blade Setting Angle, $\theta_p = 2^0$

Theoretical			Experimental		
Tip Speed Ratio (λ)	Torque Coefficient (C_Q)	Power Coefficient (Cp)	Tip Speed Ratio (λ)	Torque Coefficient (C_Q)	Power Coefficient (Cp)
1.11	0.00	0.00	8.50	0.02	0.17
1.59	0.02	0.02	8.30	0.02	0.18
2.06	0.02	0.05	8.00	0.03	0.25
2.54	0.04	0.09	7.50	0.04	0.26
3.01	0.04	0.13	7.00	0.04	0.31
3.49	0.05	0.16	6.45	0.05	0.32
3.97	0.05	0.21	6.29	0.05	0.31
4.44	0.06	0.26	6.00	0.05	0.32
4.92	0.06	0.30	5.84	0.05	0.31
5.39	0.06	0.34	5.68	0.05	0.30
5.87	0.06	0.37	5.51	0.05	0.28
6.35	0.06	0.38	5.00	0.05	0.25
6.82	0.05	0.37	4.60	0.05	0.22
7.30	0.05	0.36	4.30	0.04	0.18
7.77	0.04	0.34	4.00	0.04	0.16
8.25	0.04	0.31			
8.73	0.03	0.27			
9.20	0.02	0.22			
9.68	0.02	0.16			
10.15	0.01	0.10			
10.63	0.01	0.08			
11.11	0.01	0.12			
11.58	0.01	0.10			
12.06	0.03	0.40			
12.54	0.03	0.40			
13.01	0.03	0.40			
13.49	0.03	0.39			
13.65	0.03	0.38			

Airfoil = NACA 4418, Number of Blade = 2, Blade Setting Angle, $\theta_p = 4^0$

Theoretical			Experimental		
Tip Speed Ratio (λ)	Torque Coefficient (C_Q)	Power Coefficient (Cp)	Tip Speed Ratio (λ)	Torque Coefficient (C_Q)	Power Coefficient (Cp)
1.27	0.01	0.01	8.90	0.02	0.16
1.59	0.02	0.03	8.52	0.02	0.18
1.90	0.03	0.05	7.79	0.03	0.27
2.22	0.04	0.08	7.12	0.04	0.27
2.54	0.04	0.11	6.25	0.04	0.26
2.86	0.05	0.13	5.78	0.04	0.24
3.17	0.03	0.10	5.72	0.04	0.24
3.49	0.04	0.14	5.53	0.04	0.24
3.81	0.04	0.18	5.40	0.04	0.23
4.13	0.05	0.21	5.08	0.04	0.21
4.44	0.05	0.24	4.47	0.05	0.20
4.76	0.06	0.27	3.75	0.03	0.13
5.08	0.06	0.29			
5.39	0.06	0.31			
5.71	0.06	0.32			
6.03	0.05	0.33			
6.35	0.05	0.34			
6.66	0.05	0.34			
6.98	0.05	0.34			
7.30	0.04	0.33			
7.62	0.04	0.32			
7.93	0.04	0.31			
8.25	0.04	0.29			
8.57	0.03	0.27			
8.89	0.03	0.25			
9.20	0.02	0.22			
9.65	0.02	0.18			
10.03	0.01	0.14			
10.42	0.01	0.14			
11.10	0.01	0.16			
11.30	0.01	0.12			
11.90	0.01	0.08			
12.40	0.01	0.07			
13.13	2.00e-3	0.02			
12.06	0.03	0.36			
12.38	0.03	0.35			
12.69	0.03	0.34			
13.01	0.03	0.33			
13.33	0.02	0.31			
13.65	0.02	0.30			

Airfoil = NACA 4418, Number of Blade = 2, Blade Setting Angle, $\theta_p = 6^0$

Theoretical			Experimental		
Tip Speed Ratio (λ)	Torque Coefficient (C_Q)	Power Coefficient (Cp)	Tip Speed Ratio (λ)	Torque Coefficient (C_Q)	Power Coefficient (Cp)
1.27	0.01	0.02	8.25	0.02	0.14
1.59	0.01	0.02	8.00	0.02	0.14
1.90	0.02	0.03	7.75	0.02	0.18
2.22	0.03	0.08	7.50	0.02	0.17
2.54	0.04	0.10	7.25	0.03	0.19
2.86	0.03	0.13	7.00	0.03	0.20
3.17	0.03	0.15	6.75	0.03	0.19
3.49	0.04	0.16	6.50	0.03	0.20
3.81	0.05	0.19	6.25	0.04	0.22
4.13	0.05	0.22	6.00	0.04	0.22
4.44	0.05	0.24	5.75	0.04	0.20
4.76	0.05	0.26	5.50	0.04	0.20
5.08	0.05	0.27	5.25	0.04	0.21
5.39	0.05	0.28	5.00	0.04	0.19
5.71	0.05	0.29	4.75	0.04	0.17
6.03	0.05	0.30	4.50	0.03	0.14
6.35	0.04	0.30	4.25	0.03	0.15
6.66	0.04	0.30	4.00	0.04	0.15
6.98	0.04	0.29			
7.30	0.04	0.27			
7.62	0.03	0.25			
7.93	0.03	0.23			
8.25	0.03	0.21			
8.57	0.02	0.19			
8.89	0.02	0.17			
9.20	0.02	0.15			
9.52	0.01	0.13			
9.84	0.01	0.10			
10.15	0.01	0.07			
10.47	0.01	0.07			
10.79	0.03	0.32			
11.11	0.03	0.31			
11.42	0.03	0.30			
11.74	0.03	0.29			
12.06	0.02	0.27			
12.38	0.02	0.26			
12.69	0.02	0.24			

Airfoil = NACA 4418, Number of Blade = 2, Blade Setting Angle, $\theta_p = 8^0$

Theoretical			Experimental		
Tip Speed Ratio (λ)	Torque Coefficient (C_Q)	Power Coefficient (Cp)	Tip Speed Ratio (λ)	Torque Coefficient (C_Q)	Power Coefficient (Cp)
1.27	0.02	0.02	6.42	0.02	0.10
1.59	0.02	0.04	6.41	0.02	0.11
1.90	0.03	0.06	6.27	0.02	0.11
2.22	0.04	0.09	6.14	0.02	0.13
2.54	0.02	0.08	5.89	0.03	0.15
2.86	0.02	0.09	5.46	0.03	0.16
3.17	0.03	0.07	5.07	0.03	0.16
3.49	0.03	0.14	4.87	0.03	0.14
3.81	0.04	0.18	4.70	0.03	0.14
4.13	0.04	0.21	4.63	0.03	0.13
4.44	0.05	0.23	4.50	0.02	0.11
4.76	0.05	0.25	4.08	0.03	0.10
5.08	0.05	0.26			
5.39	0.04	0.26			
5.71	0.04	0.25			
6.03	0.04	0.23			
6.35	0.03	0.21			
6.66	0.03	0.19			
6.98	0.02	0.17			
7.30	0.02	0.15			
7.62	0.02	0.13			
7.93	0.01	0.10			
8.25	0.01	0.07			
8.57	0.01	0.08			
8.89	0.01	0.07			
9.20	0.01	0.06			
9.52	0.01	0.05			
9.84	4.00e-3	0.04			
10.15	3.00e-3	0.06			
10.47	1.00e-3	0.25			
11.00	0.02	0.24			
11.25	0.02	0.23			
11.50	0.02	0.22			
11.75	0.02	0.21			
12.00	0.02	0.20			

Appendix-B_2: Experimental Data for 3-Blade HAWT Model

Airfoil = NACA 4418, Number of Blade = 3, Blade Setting Angle, $\theta_p = 0^0$

Theoretical			Experimental		
Tip Speed Ratio (λ)	Torque Coefficient (C_Q)	Power Coefficient (Cp)	Tip Speed Ratio (λ)	Torque Coefficient (C_Q)	Power Coefficient (Cp)
0.80	0.00	0.00	10.70	0.01	0.11
0.96	0.01	0.01	10.00	0.02	0.20
1.12	0.02	0.02	9.39	0.02	0.22
1.29	0.02	0.03	8.88	0.03	0.24
1.45	0.03	0.04	8.90	0.03	0.30
1.61	0.03	0.05	8.36	0.04	0.34
1.77	0.04	0.07	7.53	0.05	0.34
1.93	0.04	0.08	7.30	0.04	0.30
2.09	0.05	0.10	6.75	0.05	0.32
2.57	0.05	0.10	6.43	0.05	0.31
3.05	0.02	0.11	6.41	0.04	0.25
3.21	0.03	0.13	5.78	0.05	0.30
3.37	0.03	0.14	5.62	0.05	0.27
3.50	0.04	0.15	5.30	0.05	0.24
3.86	0.04	0.19	5.83	0.04	0.22
4.02	0.05	0.21	4.82	0.04	0.20
4.34	0.05	0.25	4.50	0.04	0.19
4.50	0.06	0.26	4.18	0.03	0.14
4.66	0.06	0.28	4.15	0.03	0.14
4.98	0.06	0.31			
5.14	0.06	0.33			
5.30	0.06	0.34			
5.62	0.06	0.36			
6.10	0.06	0.38			
6.33	0.06	0.40			
6.65	0.06	0.40			
6.75	0.06	0.41			
6.89	0.06	0.41			
6.93	0.06	0.41			
7.12	0.06	0.42			
7.30	0.05	0.41			
7.64	0.05	0.40			
8.00	0.05	0.39			
8.58	0.04	0.36			
9.24	0.04	0.32			
9.75	0.03	0.28			
10.28	0.02	0.24			
10.89	0.02	0.22			
11.52	0.01	0.16			

Airfoil = NACA 4418, Number of Blade = 3, Blade Setting Angle, $\theta_p = 2^0$

Theoretical			Experimental		
Tip Speed Ratio (λ)	Torque Coefficient (C_Q)	Power Coefficient (Cp)	Tip Speed Ratio (λ)	Torque Coefficient (C_Q)	Power Coefficient (Cp)
0.80	0.00	0.00	8.03	0.03	0.24
0.96	3.00e-3	3.00e-3	7.87	0.04	0.32
1.12	0.01	0.01	7.71	0.04	0.30
1.29	0.01	0.02	7.55	0.04	0.33
1.45	0.02	0.03	7.39	0.05	0.35
1.61	0.02	0.04	7.23	0.05	0.37
1.77	0.03	0.05	7.07	0.05	0.36
1.93	0.04	0.07	6.91	0.05	0.38
2.09	0.04	0.09	6.75	0.06	0.37
2.25	0.05	0.11	6.59	0.06	0.39
2.41	0.05	0.13	6.43	0.06	0.40
2.57	0.05	0.16	6.27	0.06	0.40
2.73	0.06	0.18	6.10	0.06	0.37
2.89	0.06	0.22	5.94	0.06	0.38
3.05	0.04	0.22	5.71	0.07	0.38
3.21	0.05	0.23	5.62	0.06	0.35
3.37	0.05	0.24	5.46	0.06	0.34
3.53	0.06	0.25	5.30	0.07	0.35
3.69	0.06	0.27	5.14	0.06	0.32
3.86	0.07	0.29	4.98	0.06	0.30
4.02	0.07	0.31	4.82	0.07	0.32
4.18	0.07	0.33	4.66	0.06	0.28
4.34	0.07	0.35	4.50	0.06	0.26
4.50	0.07	0.36	4.20	0.06	0.25
4.66	0.08	0.37	4.00	0.06	0.22
4.82	0.08	0.38			
4.98	0.08	0.39			
5.14	0.08	0.40			
5.30	0.08	0.41			
5.46	0.08	0.42			
5.62	0.08	0.42			
5.78	0.08	0.43			
5.94	0.07	0.44			
6.10	0.07	0.44			
6.27	0.07	0.45			
6.43	0.07	0.45			
6.59	0.07	0.45			
6.75	0.07	0.45			
6.91	0.06	0.44			

Airfoil = NACA 4418, Number of Blade = 3, Blade Setting Angle, $\theta_p = 4^0$

Theoretical			Experimental		
Tip Speed Ratio (λ)	Torque Coefficient (C_Q)	Power Coefficient (Cp)	Tip Speed Ratio (λ)	Torque Coefficient (C_Q)	Power Coefficient (Cp)
0.08	.00e-3	2.00e-3	8.84	0.02	0.18
0.96	0.01	0.01	8.68	0.02	0.20
1.12	0.01	0.01	8.51	0.03	0.22
1.29	0.02	0.02	8.35	0.03	0.21
1.45	0.02	0.03	8.19	0.03	0.23
1.61	0.03	0.05	8.03	0.03	0.24
1.77	0.03	0.06	7.87	0.03	0.22
1.93	0.04	0.08	7.71	0.03	0.25
2.09	0.05	0.10	7.55	0.04	0.28
2.25	0.01	0.06	7.39	0.04	0.28
2.41	0.01	0.08	7.23	0.04	0.27
2.57	0.01	0.10	7.07	0.04	0.31
2.73	0.01	0.12	6.91	0.05	0.32
2.89	0.02	0.14	6.75	0.05	0.34
3.05	0.03	0.16	6.59	0.05	0.32
3.21	0.04	0.18	6.43	0.05	0.34
3.37	0.05	0.21	6.27	0.05	0.33
3.50	0.06	0.23	6.10	0.06	0.34
3.69	0.06	0.27	5.94	0.06	0.37
3.86	0.07	0.30	5.78	0.06	0.36
4.02	0.07	0.32	5.62	0.06	0.36
4.18	0.07	0.35	5.46	0.06	0.34
4.34	0.07	0.37	5.30	0.07	0.34
4.50	0.08	0.38	5.14	0.06	0.33
4.66	0.08	0.39	4.98	0.06	0.31
4.82	0.08	0.40	4.82	0.07	0.33
4.98	0.08	0.41	4.66	0.06	0.30
5.14	0.08	0.42	4.50	0.05	0.23
5.30	0.08	0.42	4.34	0.06	0.25
5.46	0.08	0.42	4.18	0.05	0.20
5.62	0.08	0.43	4.02	0.05	0.18
5.78	0.08	0.42	3.86	0.04	0.17
5.94	0.08	0.42	3.60		
6.10	0.07	0.42	3.50		
6.27	0.07	0.41			
6.43	0.07	0.41			
6.59	0.07	0.40			
6.75	0.07	0.39			
6.91	0.06	0.38			
7.07	0.06	0.37			

7.23	0.06	0.36			
7.39	0.06	0.35			
7.55	0.05	0.34			
7.71	0.05	0.33			
7.87	0.05	0.32			
8.03	0.05	0.31			
8.19	0.05	0.30			
8.35	0.04	0.29			
8.51	0.04	0.28			
8.68	0.04	0.27			
8.84	0.04	0.26			
9.00	0.04	0.25			
9.16	0.03	0.24			
9.32	0.03	0.23			
9.48	0.03	0.22			
9.64	0.03	0.21			
9.80	0.03	0.20			
9.96	0.02	0.19			
10.12	0.02	0.18			
10.28	0.03	0.14			
10.50	0.03	0.12			

Airfoil = NACA 4418, Number of Blade = 3, Blade Setting Angle, $\theta_p = 6^0$

Theoretical			Experimental		
Tip Speed Ratio (λ)	Torque Coefficient (C_Q)	Power Coefficient (Cp)	Tip Speed Ratio (λ)	Torque Coefficient (C_Q)	Power Coefficient (Cp)
0.8	0.005	0.004	9.5	0.020	0.19
0.96	0.01	0.009	9.2	0.025	0.229
1.12	0.015	0.017	9	0.026	0.23
1.29	0.021	0.026	8.5	0.028	0.24
1.45	0.026	0.038	8.03	0.031	0.245
1.61	0.033	0.052	7.71	0.033	0.255
1.77	0.039	0.069	7.55	0.035	0.268
1.93	0.046	0.088	7.39	0.038	0.284
2.09	0.053	0.11	7.23	0.039	0.28
2.25	0.06	0.134	7.07	0.041	0.289
2.41	0.066	0.159	6.91	0.043	0.295
2.57	0.072	0.186	6.75	0.047	0.32
2.73	0.077	0.211	6.59	0.046	0.3
2.89	0.082	0.237	6.43	0.048	0.31
3.05	0.085	0.259	6.27	0.052	0.325
3.21	0.087	0.279	6.1	0.054	0.329
3.37	0.088	0.297	5.94	0.057	0.34
3.53	0.089	0.314	5.78	0.058	0.335
3.69	0.089	0.329	5.62	0.061	0.345
3.86	0.089	0.342	5.46	0.063	0.345
4.02	0.088	0.353	5.3	0.064	0.339
4.18	0.087	0.363	5.14	0.061	0.315
4.34	0.086	0.372	4.98	0.062	0.31
4.5	0.084	0.379	4.82	0.061	0.294
4.66	0.083	0.386	4.66	0.064	0.3
4.82	0.081	0.392	4.5	0.061	0.275
4.98	0.08	0.397	4.34	0.061	0.264
5.14	0.078	0.401	4.18	0.056	0.235
5.3	0.076	0.405	4.02	0.058	0.235
5.46	0.075	0.407			
5.62	0.073	0.409			
5.78	0.071	0.411			
5.94	0.069	0.413			
6.1	0.068	0.414			
6.27	0.066	0.415			
6.43	0.065	0.415			
6.59	0.064	0.419			
6.75	0.062	0.419			
6.91	0.061	0.418			

7.07	0.059	0.417			
7.23	0.058	0.416			
7.39	0.056	0.415			
7.55	0.055	0.413			
7.71	0.053	0.411			
7.87	0.052	0.409			
8.03	0.051	0.406			
8.19	0.049	0.403			
8.35	0.048	0.4			
8.51	0.046	0.396			
8.68	0.045	0.392			
8.84	0.044	0.388			
9	0.043	0.383			
9.16	0.041	0.378			
9.32	0.04	0.372			
9.48	0.039	0.367			
9.64	0.037	0.361			
9.8	0.036	0.355			
9.96	0.035	0.348			
10.12	0.034	0.341			
10.28	0.032	0.333			

Airfoil = NACA 4418, Number of Blade = 3, Blade Setting Angle, $\theta_p = 8^0$

Theoretical			Experimental		
Tip Speed Ratio (λ)	Torque Coefficient (C_Q)	Power Coefficient (Cp)	Tip Speed Ratio (λ)	Torque Coefficient (C_Q)	Power Coefficient (Cp)
0.8	0.008	0.006	8.5	0.024	0.2
0.96	0.013	0.012	8.2	0.023	0.19
1.12	0.018	0.021	8	0.028	0.22
1.29	0.024	0.031	7.87	0.030	0.238
1.45	0.031	0.044	7.71	0.030	0.23
1.61	0.037	0.06	7.55	0.034	0.254
1.77	0.044	0.078	7.39	0.037	0.27
1.93	0.051	0.098	7.23	0.037	0.268
2.09	0.058	0.121	7.07	0.040	0.28
2.25	0.065	0.145	6.91	0.040	0.276
2.41	0.071	0.17	6.75	0.041	0.28
2.57	0.076	0.195	6.59	0.044	0.29
2.73	0.08	0.218	6.43	0.047	0.305
2.89	0.082	0.238	6.27	0.046	0.287
3.05	0.084	0.256	6.1	0.046	0.28
3.21	0.085	0.273	5.94	0.050	0.296
3.37	0.085	0.287	5.78	0.054	0.31
3.53	0.085	0.3	5.62	0.052	0.29
3.69	0.084	0.311	5.46	0.049	0.27
3.86	0.083	0.32	5.3	0.055	0.29
4.02	0.082	0.328	5.14	0.056	0.29
4.18	0.08	0.335	4.98	0.056	0.28
4.34	0.079	0.341	4.82	0.054	0.26
4.5	0.077	0.346	4.66	0.058	0.27
4.66	0.075	0.35	4.5	0.056	0.25
4.82	0.073	0.353	4.34	0.060	0.26
4.98	0.071	0.355	4.18	0.057	0.240
5.14	0.069	0.356	4.02	0.055	0.220
5.3	0.067	0.357	3.86	0.047	0.180
5.46	0.065	0.357	3.69	0.051	0.190
5.62	0.063	0.357	3.53	0.045	0.160
5.78	0.062	0.358			
5.94	0.06	0.357			
6.1	0.058	0.355			
6.27	0.056	0.353			
6.43	0.055	0.35			
6.59	0.053	0.347			
6.75	0.051	0.344			
6.91	0.049	0.34			
7.07	0.047	0.336			

7.23	0.046	0.331			
7.39	0.044	0.326			
7.55	0.042	0.32			
7.71	0.041	0.314			
7.87	0.039	0.307			
8.03	0.037	0.3			
8.19	0.036	0.292			
8.35	0.034	0.284			
8.51	0.032	0.276			
8.68	0.031	0.267			
8.84	0.029	0.257			
9	0.027	0.247			
9.16	0.026	0.237			
9.32	0.024	0.226			
9.48	0.023	0.214			
9.64	0.021	0.202			
9.8	0.019	0.189			
9.96	0.018	0.181			
10.12	0.017	0.167			
10.28	0.015	0.153			

Appendix-B_3: Experimental Data for 4-Blade HAWT Model

Airfoil = NACA 4418, Number of Blade = 4, Blade Setting Angle, $\theta_p = 0^0$

Theoretical			Experimental		
Tip Speed Ratio (λ)	Torque Coefficient (C_Q)	Power Coefficient (Cp)	Tip Speed Ratio (λ)	Torque Coefficient (C_Q)	Power Coefficient (Cp)
1.29	0.022	0.029	7.750	0.017	0.133
1.61	0.038	0.061	7.390	0.024	0.180
1.93	0.054	0.105	6.890	0.030	0.206
2.25	0.053	0.120	7.500	0.031	0.236
2.57	0.054	0.140	6.760	0.041	0.277
2.89	0.055	0.160	6.470	0.046	0.300
3.21	0.050	0.160	6.260	0.053	0.330
3.53	0.057	0.200	5.800	0.056	0.322
3.86	0.070	0.270	5.210	0.060	0.312
4.18	0.077	0.320	4.697	0.062	0.290
4.81	0.081	0.390	4.579	0.062	0.285
5.32	0.078	0.415	4.448	0.059	0.263
6.35	0.067	0.425	4.370	0.057	0.250
7.22	0.054	0.390	4.124	0.058	0.240
7.89	0.042	0.330	4.370	0.050	0.217
8.41	0.032	0.270	3.956	0.048	0.190
8.74	0.026	0.230			
9.15	0.020	0.180			
9.48	0.015	0.140			
10	0.008	0.080			
10.22	0.004	0.040			
10.55	0.002	0.020			

Airfoil = NACA 4418, Number of Blade = 4, Blade Setting Angle, $\theta_p = 2^0$

Theoretical			Experimental		
Tip Speed Ratio (λ)	Torque Coefficient (C_Q)	Power Coefficient (Cp)	Tip Speed Ratio (λ)	Torque Coefficient (C_Q)	Power Coefficient (Cp)
1.29	0.018	0.023	7.86	0.02	0.18
1.61	0.032	0.051	7.42	0.03	0.22
1.93	0.047	0.091	7.50	0.03	0.26
2.25	0.071	0.16	7.25	0.04	0.27
2.57	0.062	0.16	7.00	0.04	0.31
2.89	0.062	0.18	6.50	0.05	0.32
3.21	0.062	0.2	6.54	0.06	0.36
3.53	0.065	0.23	5.75	0.07	0.38
3.86	0.074	0.285	5.50	0.07	0.37
4.18	0.079	0.33	5.44	0.06	0.35
4.5	0.080	0.36	5.02	0.07	0.33
4.82	0.081	0.39	4.95	0.06	0.31
5.14	0.080	0.41	4.89	0.06	0.29
5.46	0.078	0.425	4.78	0.05	0.25
5.78	0.076	0.44	4.89	0.05	0.23
6.1	0.074	0.449	4.61	0.04	0.20
6.43	0.070	0.45	4.42	0.04	0.18
7	0.063	0.44	4.56	0.04	0.16
7.35	0.059	0.43	4.21	0.03	0.14
7.69	0.055	0.42	4.08	0.03	0.12
8.03	0.050	0.4	4.00	0.02	0.10
8.15	0.048	0.39	3.87	0.02	0.08
8.53	0.042	0.36			
8.68	0.039	0.34			
9	0.034	0.31			
9.32	0.030	0.28			
9.64	0.025	0.24			
9.96	0.020	0.2			
10.28	0.018	0.18			
10.6	0.013	0.14			
10.92	0.011	0.12			
11.25	0.009	0.1			
11.57	0.007	0.08			
11.89	0.005	0.06			
12.21	0.003	0.04			

Airfoil = NACA 4418, Number of Blade = 4, Blade Setting Angle, $\theta_p = 4^0$

Theoretical			Experimental		
Tip Speed Ratio (λ)	Torque Coefficient (C_Q)	Power Coefficient (Cp)	Tip Speed Ratio (λ)	Torque Coefficient (C_Q)	Power Coefficient (Cp)
1.29	0.022	0.029	7.35	0.021	0.152
1.61	0.038	0.061	7.39	0.023	0.172
1.93	0.054	0.105	6.89	0.029	0.203
2.25	0.072	0.162	6.81	0.035	0.236
2.57	0.054	0.14	6.76	0.041	0.277
2.89	0.052	0.15	6.47	0.046	0.300
3.21	0.050	0.16	6.26	0.053	0.330
3.53	0.065	0.23	5.80	0.057	0.332
3.86	0.075	0.29	5.21	0.062	0.322
4.18	0.081	0.34	4.70	0.064	0.302
4.81	0.083	0.4	4.60	0.064	0.295
5.32	0.079	0.42	4.40	0.062	0.273
6.35	0.068	0.43	4.30	0.060	0.260
7.22	0.054	0.39	4.20	0.059	0.246
7.89	0.043	0.34	4.10	0.055	0.227
8.41	0.034	0.29	4.00	0.051	0.203
8.74	0.029	0.25			
9.15	0.022	0.2			
9.48	0.017	0.16			
10	0.010	0.1			
10.22	0.008	0.08			
10.55	0.004	0.044			

Airfoil = NACA 4418, Number of Blade = 4, Blade Setting Angle, $\theta_p = 6^0$

Theoretical			Experimental		
Tip Speed Ratio (λ)	Torque Coefficient (C_Q)	Power Coefficient (Cp)	Tip Speed Ratio (λ)	Torque Coefficient (C_Q)	Power Coefficient (Cp)
1.29	0.027	0.035	7.39	0.032	0.240
1.61	0.043	0.07	6.97	0.039	0.270
1.93	0.061	0.118	6.64	0.047	0.310
2.25	0.053	0.12	6.26	0.048	0.300
2.57	0.054	0.14	6.06	0.055	0.332
2.89	0.055	0.16	5.84	0.053	0.310
3.21	0.056	0.18	5.50	0.058	0.320
3.53	0.068	0.24	5.55	0.061	0.340
3.86	0.083	0.32	5.08	0.069	0.350
4.18	0.090	0.375	4.47	0.074	0.330
4.5	0.089	0.4	4.41	0.068	0.301
4.82	0.086	0.415	4.30	0.071	0.307
5.14	0.083	0.425	4.24	0.067	0.283
5.46	0.079	0.43	4.11	0.065	0.266
5.78	0.074	0.427	4.02	0.060	0.240
6.1	0.068	0.415	4.24	0.052	0.221
6.43	0.062	0.4	4.06	0.049	0.198
6.75	0.058	0.39			
7.07	0.052	0.37			
7.39	0.049	0.36			
7.71	0.044	0.34			
8.03	0.040	0.32			
8.35	0.036	0.3			
8.68	0.032	0.28			
9	0.028	0.255			
9.32	0.025	0.23			
9.64	0.021	0.205			
9.96	0.018	0.18			
10.28	0.016	0.16			
10.6	0.013	0.14			
10.92	0.011	0.12			
11.25	0.009	0.1			
11.57	0.007	0.08			
11.89	0.005	0.065			
12.21	0.002	0.022			

Airfoil = NACA 4418, Number of Blade = 4, Blade Setting Angle, $\theta_p = 8^0$

Theoretical			Experimental		
Tip Speed Ratio (λ)	Torque Coefficient (C_Q)	Power Coefficient (Cp)	Tip Speed Ratio (λ)	Torque Coefficient (C_Q)	Power Coefficient (Cp)
1.29	0.033	0.042	8.02	0.021	0.165
1.61	0.049	0.079	7.44	0.025	0.184
1.93	0.068	0.131	7.36	0.032	0.238
2.25	0.005	0.012	6.90	0.033	0.226
2.57	0.047	0.120	6.53	0.042	0.274
2.89	0.048	0.140	5.82	0.057	0.331
3.21	0.050	0.160	5.38	0.061	0.327
3.53	0.065	0.230	4.90	0.062	0.306
3.86	0.078	0.300	4.79	0.055	0.264
4.18	0.081	0.340	4.24	0.063	0.265
4.5	0.082	0.37	4.37	0.056	0.246
4.82	0.081	0.390	4.13	0.059	0.242
5.14	0.079	0.405	4.12	0.055	0.225
5.46	0.075	0.41	4.20	0.048	0.203
5.78	0.072	0.415	4.10	0.039	0.160
6.1	0.067	0.41			
6.43	0.062	0.4			
6.75	0.056	0.38			
7.07	0.051	0.36			
7.39	0.045	0.33			
7.71	0.040	0.305			
8.03	0.035	0.28			
8.35	0.030	0.25			
8.68	0.026	0.23			
9	0.022	0.2			
9.32	0.018	0.17			
9.64	0.015	0.14			
9.96	0.012	0.12			
10.28	0.011	0.11			
10.6	0.009	0.1			
10.92	0.008	0.091			
11.25	0.004	0.047			

Appendix- C: Strain Gauge Calibration Graph